DOES EXPOSURE TO SIMULATED MICROGRAVITY AFFECT CRANIAL NEURAL CREST-DERIVED TISSUES IN *DANIO RERIO*?

By

Sara C. Edsall

Submitted in partial fulfilment of the requirements
for the degree of Master of Science

at

Dalhousie University
Halifax, Nova Scotia
August 2011

DALHOUSIE UNIVERSITY

DEPARTMENT OF ANATOMY AND NEUROBIOLOGY

The undersigned hereby certify that they have read and recommend to the Faculty of Graduate Studies for acceptance a t hesis entitled "Does Exposure to Simulated Microgravity Affect Cranial Neural Crest-Derived Tissues in *Danio rerio*?" by Sara C. Edsall in partial fulfilment of the requirements for the degree of Master of Science.

Dated: August 23, 2011

Supervisor: _____

Readers: _____

_____

_____

Departmental Representative: _____

DALHOUSIE UNIVERSITY

DATE: August 23, 2011

AUTHOR: Sara C. Edsall

TITLE: Does Exposure to Simulated Microgravity Affect Cranial Neural Crest-Derived Tissues in *Danio rerio*?

DEPARTMENT OR SCHOOL: Department of Anatomy and Neurobiology

DEGREE: MSc CONVOCATION: October YEAR: 2011

_____

Signature of Author

DEDICATION PAGE

I dedicate this thesis to my friends and family. Thank you for your continued guidance and support and your never-ending tolerance. I am who I am because of you.

Table of Contents

List of Tables

List of Figures

Abstract

To determine whether exposure to simulated microgravity (SMG) affects cranial neural crest (CNC)-derived tissues, zebrafish embryos were exposed to SMG starting at one of three developmental stages corresponding to CNC migration. Juvenile and adult fish were analyzed after exposure to SMG using statistics and geometric morphometrics for changes in melanophore surface area and number, and changes in skull morphology. Analyses reveal an initial increase in the surface area of melanophores present on the dorsal view of the juvenile skull and a decrease in melanophore number over the period of a week. Additionally, buckling is observed in CNC-derived frontal bones in juvenile fish after exposure. The effects on the melanophores are transient and the effects on CNC-derived bones are short-term. Surprisingly, severe long-term effects occurred in mesoderm-derived bones, such as the parasphenoid. In summary, exposure to SMG affects both CNC- and mesoderm-derived tissues in the juvenile and adult zebrafish head.

List of Abbreviations and Symbols Used

C+V, control with vibrations

CNV, control with no vibrations

dpf, days post-fertilization

EtOH, ethanol

hpf, hours post-fertilization

mpf, months post-fertilization

NBF, neutral-buffered formalin

PBS, phosphate-buffered saline

PFA, paraformaldehyde

RWV, rotating wall vessel

SL, standard length

SMG, simulated microgravity

Acknowledgements

My deepest and most sincere thanks go to my supervisor, Dr. Tamara Franz-Odendaal. Thank you for not only providing me with the opportunity to complete a MSc. degree, but for always pushing me to excel.

Thanks to my committee members, Dr. Kazue Semba, Dr. Frank Smith, and Dr. Boris Kablar for their continued guidance over the last two years.

I would like to acknowledge Matt Stoyek, who conducted the initial bioreactor experiments, as well as Dr. Moorman and Dr. Croll for the loan of the bioreactor.

I profusely thank both Dr. Gary Sneddon for aiding me with my statistical analysis (particularly with working out the linear regression model), and Megan Dufton, for her extensive morphometrics knowledge and help with the analyses.

I want to thank the Canadian Space Agency (CSA) and the Natural Sciences and Engineering Research Council of Canada (NSERC) for funding and the Canada Foundation for Innovation for providing the lab equipment. In addition, I wish to thank the Society for Comparative and Integrative Biology for a travel grant that provided me with the opportunity to present my research in Salt Lake City, UT.

Finally, I would like to thank my fellow lab mates for all their help in both the lab and the fish room, and in particular, Megan Dufton and Kellie Duench, for their eternal support and encouragement.

Chapter 1: Introduction

This chapter presents a detailed introduction to the thesis. Simulated gravity is the first topic covered, followed by a brief description of *Danio rerio* as a model organism for general development studies. This is followed by a section describing *Danio rerio* as a model for gravity-related studies, and a section on stress responses. These sections are followed by general descriptions of neural crest cells and bone development, and the chapter concludes with an objectives and significance section.

1.1 Simulated Microgravity

1.1.1 Introduction to Simulated Microgravity

Microgravity is a reduction in the magnitude of Earth's gravitational pull and is often referred to as zero-gravity and represented by the symbol μg. Microgravity is present beyond Earth's atmosphere, where the earth's gravitational pull is reduced (from 9.81 m/s^2 to 10 mm/s^2 when about 200 000 km away).

Simulated microgravity (SMG), on the other hand, is not true microgravity; SMG does not reduce the magnitude or direction of the Earth's gravitational pull, but creates a net force vector that is equal at all angles (Moorman et al., 1999) such that the organism/specimen being exposed is not pulled by Earth's gravity in any one direction. SMG is used as a ground-based method to expose organisms to microgravity, which otherwise can only be achieved by sending the organisms in space.

Ground-based SMG can be conducted on Earth by using one of a variety of devices. Clinostats (either 2D or 3D) are typically used for SMG studies involving plants. The device secures the specimen horizontally, and rotates along a single axis (2D) or multiple axes (3D) so that the gravitational pull is equally distributed across 360°.

In addition to the clinostats, SMG environments can be achieved by using a simple rotating device, a rotating wall vessel (RWV), otherwise known as a bioreactor. The bioreactor is the device used in this project, and is described below.

1.1.2 The Bioreactor Device

The bioreactor (Synthecon, Houston, TX), or RWV, consists of a hollow, transparent Lexan cylinder (about 10 cm in diameter), which surrounds a solid Teflon core (about 5 cm in diameter). The bioreactor cylinder, closed at both ends by Teflon caps, is a water-filled container in which zebrafish embryos can be placed (Figure 1.1). At one end, the Teflon cap has three small apertures through which water can be added or removed, and zebrafish embryos transferred. At the other end, the Teflon cap secures the bioreactor to a motorized base.

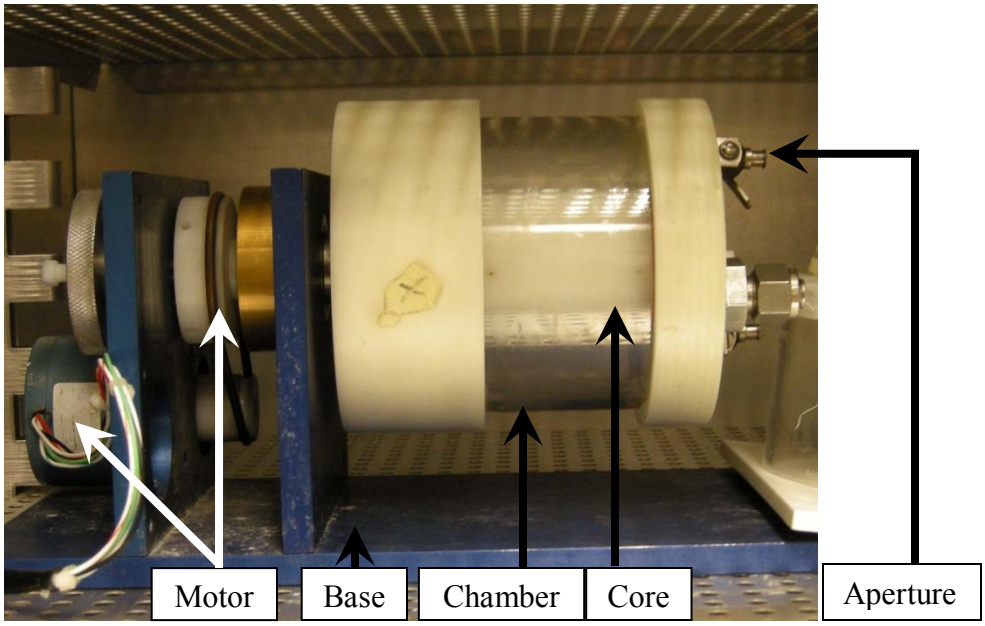

Figure 1.1: Lateral view of the RWV inside an incubator. The RWV attaches to a motorized base. When turned on, the chamber rotates, causing embryos to revolve around the central core.

Once the chamber is secured to the base, the motor is turned on, causing the bioreactor to rotate on the horizontal axis, at 18.5 rpm, a speed established originally by Moorman et al. (1999) and again by the Croll lab at Dalhousie University (Lindsey et al., 2011). At this speed, the fluid-filled chamber will cause the zebrafish embryos within it to orbit the central core. A circular orbit is indicative of SMG; if one particular force vector was stronger than the others, embryos would be pulled in that direction, and the orbit would be more elliptical in shape (Moorman et al., 1999; Moorman et al., 2002). For example, if the vessel were to turn too slowly, gravity would overcome the other forces, and the embryos would sit at the bottom of the bioreactor's chamber (Figure

1.2A). In contrast, if it were to turn too quickly, the embryos would be forced outward, simulating a centrifuge (Figure 1.2B).

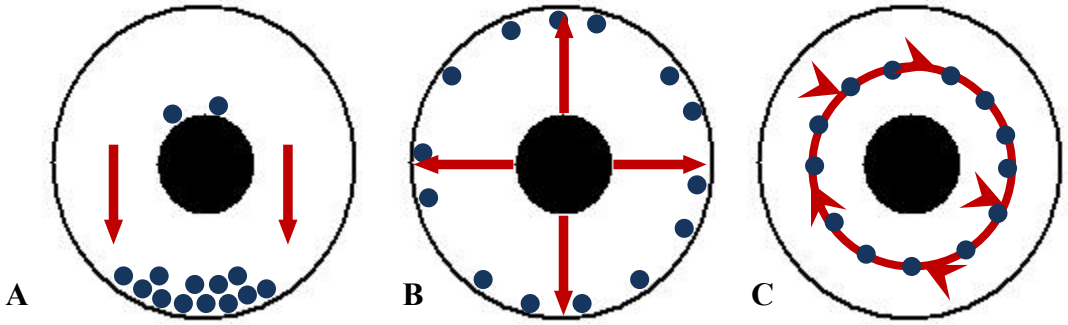

Figure 1.2: Three face-on views of the bioreactor with central core (solid black central circle) and embryos (small blue circles). A) Embryos settle on top of the core and at the bottom of the chamber when the bioreactor turns too slowly; gravity has overcome the other forces. B) Embryos are forced outward and against the outer chamber wall when the bioreactor turns too quickly. C) Embryos complete circular orbits when the speed of the bioreactor is such that they remain suspended midway between the core and the outer wall. Red arrows indicate directional movement of embryos. (Adapted from Moorman et al., 1999; Moorman et al., 2002).

Rotation of the bioreactor causes directional movement of the chamber, which causes directional movement of the fluid, which thus results in directional movement of the embryos. However, the fluid is continuously moving past the embryos, carrying them along in its "current". The net force vector acting on the embryos at every point of the rotation consists of a combination of the directional movement of the chamber, the gravitational vector, and the viscosity of the fluid (Moorman et al., 1999; Moorman et al., 2002). At the correct speed (i.e. 18.5 RPM), embryos are suspended midway between the core and the wall of the chamber, and a circular orbit occurs as a result of a net force vector that is the same magnitude at every point, but has an ever-changing direction. This is known as centripetal acceleration, where the velocity of the embryos through the fluid remains the same, but the direction of the vector is constantly changing, shifting the angle of the embryos as they orbit the core (Figure 1.3; Moorman et al., 2002). As a result, for every revolution around the central core, zebrafish embryos complete a full rotation (Figure 1.3).

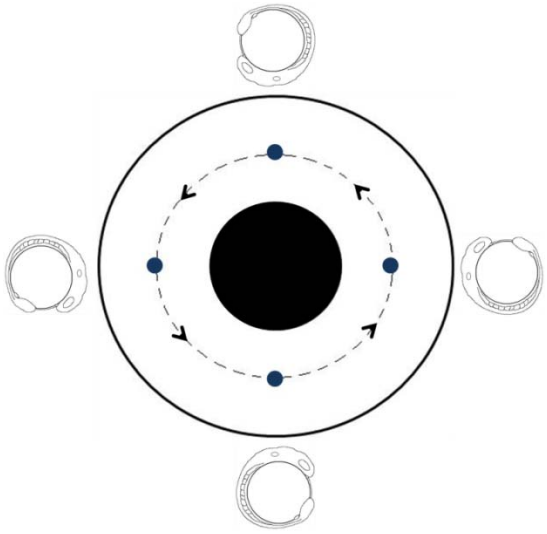

Figure 1.3. Schematic depicting the orientation of an embryo as it revolves around the central core of the bioreactor (front view). The constant turning of the embryo suggests that fluid forces act against the body axis of the embryos at a variety of angles, indicating that shearing forces are at play within the device. This may result in shear stress responses. Adapted from Moorman et al., (2002).

1.1.3 Microgravity Studies

Due to the popularity of space exploration and the possibility of space tourism, it is important to determine the effects SMG may have on humans undertaking space endeavours. As a result, many studies have been published, analyzing the effects of SMG on developing organisms (e.g. Serova et al., 1982; Neff et al., 1993; Gualandris-Parisot, 2001; Renn et al., 2006; Lindsey et al., 2011). These studies cover a vast array of organisms (e.g. tadpoles, rats, medaka, *in vitro* human cells) and a variety of tissue types (e.g. skeletal muscle, bone).

1.2 Zebrafish as a Model Organism

1.2.1. Zebrafish as a Model Organism for General Development Studies

During the last two decades, zebrafish (*Danio rerio*) have rapidly increased in popularity as a model vertebrate organism for developmental biology (Meyer et al., 1993; Cubbage and Mabee, 1996; Vascotto et al., 1997; Metscher and Ahlberg, 1999; Bradbury, 2004). They are easily manipulated, have a fully-sequenced genome and have multiple mutants readily available, making them an invaluable resource for genetic studies. They also are transparent and rapidly-developing as embryos; their short developmental time makes them a useful tool for studying embryogenesis and organogenesis. In addition, their skeletal properties, so similar to those of mammalian bone, make them an asset in studies examining bone development, growth, and

remodelling (i.e. Metscher and Ahlberg, 1999; Witten et al., 2001; Quarto and Longaker, 2005; Marí-Beffa et al., 2007; Witten and Huysseune, 2009).

1.2.2 Zebrafish in Microgravity Studies

Zebrafish, in addition to becoming an increasingly popular model organism in developmental biology, have become a popular model for gravitational studies (e.g. Moorman et al., 2002; Shimada et al., 2005; Renn et al., 2006; Muller et al, 2010; Lindsey et al., 2011). As the potential for life in space and extended space travel rapidly approaches, it is important to determine the effects exposure to gravitational changes has on living organisms. In particular, how will gravitational changes affect development of organisms that spend part of their key developmental stages in space, and what are the long-term effects? Scientists have begun to answer these questions using zebrafish.

Dr. Stephen J. Moorman (Robert Wood Johnson Medical School), a pioneer in the field of ground-based microgravity studies, has identified effects in the development of the vestibular system of zebrafish exposed to SMG (Moorman et al., 1999; Moorman et al., 2002). The vestibular system is responsible for equilibrium and orientation in response to gravitational direction. Exposure of zebrafish embryos to simulated microgravity (SMG) at particular developmental time points, resulted in defects in the otoliths, small structures belonging to the vestibular system, located in the inner ear (Moorman et al., 1999). In particular, a delay was observed in the development of the saccular otolith after exposure to 96 hours of simulated microgravity. In addition, defects were observed in zebrafish vestibulo-ocular reflexes (Moorman et al., 2002).

Another research group, Shimada et al. (2005), noted changes in β-actin gene expression in many parts of the embryos as a result of exposure to 24-48 hours of SMG starting at a variety of time points. Using GFP transgenic zebrafish, these researchers were able to identify upregulation of β-actin gene expression after exposure to SMG by measuring GFP intensity. β-actin, a ubiquitous cytoskeletal protein, is known to be upregulated under stressful conditions in the heart (mechanical damage to heart valves, volume overload; Tian et al., 1999). This was consistent with findings reported by Gillette-Ferguson et al. (2003), who determined that there was upregulation of β-actin in the heart of zebrafish after 24 hours of exposure to SMG.

In 2011, a study by Lindsey et al. examined the swim bladders of zebrafish exposed to SMG and compared them to those of fish raised under normal conditions. These researchers determined that even though there were initial effects (swim bladder inflation defects, abnormal swim bladder volumes and innervations) after 96 hours of exposure in the bioreactor, these effects were not maintained long-term. Forty-eight hours after exposure to SMG, the effects were no longer present (Lindsey et al., 2011).

The studies described above use zebrafish as a model for determining the effects of SMG on the developing vestibular system (i.e. Moorman et al., 1999; Moorman et al., 2002), on gene expression (i.e. Shimada et al., 2005; Shimada and Moorman, 2006), and on organ physiology (i.e. Lindsey et al., 2011). These studies, however, have all been conducted on embryonic zebrafish and only provide results for embryonic or juvenile fish. There are no published studies examining the full long-term effects of exposure to SMG on the morphology of adult zebrafish. It is important to know the possible long-term effects of exposure to SMG, no matter the length of the exposure, before sending humans to space. It is possible that initial effects may disappear, however there may be unknown long-term effects that could prove fatal. The goal of this study is to analyze the zebrafish skeleton after exposure, for both short- and long-term effects.

1.2.3 Stress and Zebrafish

Zebrafish have recently been identified as a valuable model for studies examining responses to stress since there is a high level of similarity between the stress-regulating systems of zebrafish and other, terrestrial, vertebrates (Steenbergen et al., 2010; Alsop and Vijayan, 2008). This similarity, in addition to the aforementioned benefits of the zebrafish as a model organism and model for SMG studies, makes zebrafish the ideal organism for determining whether or not animals are stressed by the environment in the bioreactor.

When considering biology and physics (i.e. the bioreactor), the general definition of stress is adjusted to incorporate the forces involved. Stress is thus defined as the physical deformation or change in physiology in response to forces acting on an object (i.e. a body). Stress occurs as the result of the force being distributed throughout the body, and may be mediated by stress hormone activity, which may in turn yield various

phenotypic changes (Harper and Wolf, 2009). Unfortunately, there is no single response to all stressors. Two types of stress are discussed here.

An environmental stress response is physiological, often cellular. It occurs when an organism attempts to adapt to a change in the environment, a change to which it is not accustomed (i.e. heat shock, high levels of chemicals in the water, changes in pH, etc.). Environmental stress often results in upregulation of levels of heat shock proteins (HSPs). In 2008, Connolly and Hall published a study examining the upregulation of HSP90 in response to heat shock. The researchers noted that heat shock at specific embryonic stages resulted in significant phenotypic changes in the trunk skeleton, and that these changes occurred within the expression boundaries of *hsp90* in the somites. In her doctoral dissertation (2008), Connolly suggested that the number of vertebrae was indirectly affected by the upregulation of HSP90. She concluded that the altered vertebrae number was a result of a "cascade of events" starting with increased HSP90 levels, ultimately affecting *fgf8* expression, which provides the cue for the formation of somite boundaries (Connolly, 2008). However, despite their name, HSPs are affected by multiple types of stressors, including mechanical stressors (Krone et al., 1997; Basu et al., 2002; Iwama et al., 2004; Connolly and Hall, 2008). Mechanical stress in fish is a response, often at the cellular level, to forces acting against the body of the fish (e.g. bites from predators, fluid flow). Both environmental and mechanical stress responses have been studied and described in fish, and in particular the zebrafish (e.g. Goto et al., 2003; Hallare et al., 2005; Yamamoto et al., 2005; Jiang et al., 2007; Connolly and Hall, 2008; Hierck et al., 2008; Schwartz and DeSimone, 2008; Harper and Wolf, 2009; Vasilyev and Drummond, 2010)

Within a fluid environment such as the bioreactor there are many known mechanical forces. One known fluid force that acts on submerged objects is "lift". Lift is caused by the flow of fluid past the object, and causes the object to move perpendicular to the direction of flow (Figure 1.4). In contrast, "drag", a second fluid force, acts in the opposite direction to the velocity of the object; slowing the movement of the object through the fluid (Figure 1.4; Pough et al., 2009). "Thrust", a third force, produced by the object, acts on the fluid so that the object may overcome drag. Fish, for example, use their fins and hydrodynamic body shapes to produce thrust, and propel themselves

through the water (Figure 1.4). Gravity, the ever-present downward pull on an object, is a fourth force present in fluid environments and acts on submerged bodies (Figure 1.4; Pough et al., 2009). Lift, drag, thrust, and gravity are consistently present in fluid environments no matter the direction of fluid flow, or the direction of movement of an object through a fluid. In contrast, the presence of a fifth force, "shear" force, depends on the angle of fluid flow to the long-axis of the submerged object (Figure 1.4). Simply put, shearing forces (a type of mechanical forces) are defined as any force exerted at an angle (tangential) to the long axis of the body, and are typical in laminar flow (Figure 1.4, red arrow; Pough et al., 2009). More specifically, shearing force refers to the mechanical forces exerted by a moving fluid on a still object. These forces can occur at the gross anatomical level, like strong currents flowing along a riverbed (van Rijn, 1984), or at the cellular level, such as interstitial fluid flowing past bone (Reich et al., 1990). Shearing stress is a product of the tangential forces that occur as a result of the velocity gradient between viscous fluid flow and still objects (Reich et al., 1990).

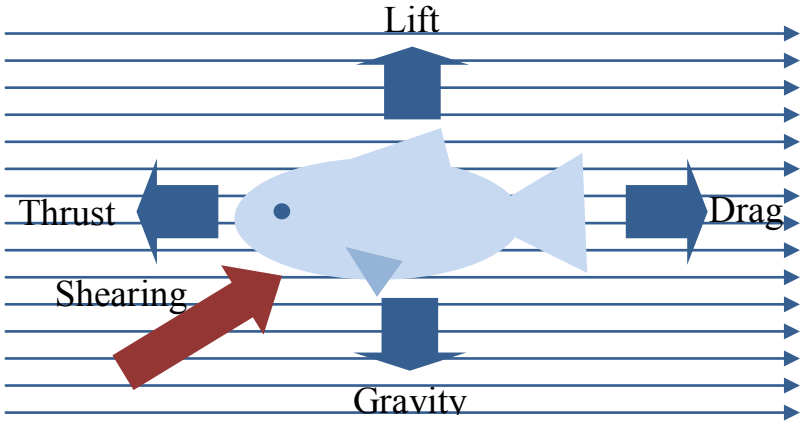

Figure 1.4: Schematic of the forces present in a fluid environment. Long, narrow blue arrows pointing to the right represent fluid flow direction.

It is important to determine if embryos are experiencing stress within the bioreactor so that effects due to SMG are not confounded by effects due to stress. In this particular case, any stress within the bioreactor is considered to be a mechanical stress. The environment has changed, which normally would suggest predominant environmental stressors, however the gravitational force is felt from all angles (discussed in Section 1.12) and mechanical forces (e.g. fluid flow), though minor in the bioreactor, may be acting on the embryos.

1.3 Neural Crest Cells

1.3.1 Introduction to Neural Crest

Neural crest cells (NCCs) are a multipotent population of cells unique to vertebrates that arise transiently along the length of the neural tube as it forms during embryogenesis (Figure 1.5). NCCs comprise the controversial fourth germ layer, and migrate throughout the body from the neural tube.

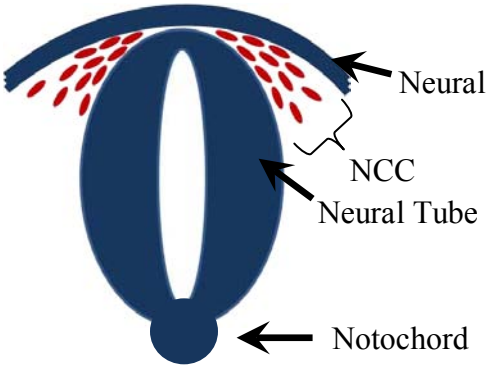

Figure 1.5: Schematic of the migration of NCC (red ellipses) during neurulation. Adapted from http://www.ratbehavior.org/images/NeuralCrestSmall.jpg

In zebrafish, the neural plate, a thickening of the head ectoderm is established through primary neurulation prior to the onset of the segmentation period of development (Kimmel et al., 1995). Epithelial infolding at the midline of the neural plate gives rise to a ventral, condensed structure known as the neural keel, at about 10 hours post fertilization (hpf). The neural keel then forms a round (still solid) rod, from which the neural tube forms through separation of the midline; this is referred to as secondary neurulation (Kimmel et al., 1995). A schematic is shown in Figure 1.6.

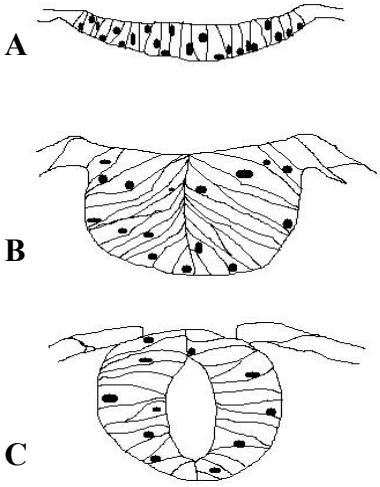

Figure 1.6: Schematic depicting primary and secondary neurulation in *Danio rerio*. A thickening of the dorsal head ectoderm gives rise to the neural plate (A) which then infolds at the midline, resulting in the formation of the neural keel (B). Separation along the midline of the neural keel yields a hollow neural tube (C). Adapted from Papan and Campos-Ortega (1994), and Kimmel et al., (1995).

Neural crest cells are divided into five different populations: vagal, sacral, cardiac, cranial, and trunk (Hall, 2009). The cells within these populations are capable of differentiating into a variety of tissue- and cell-types, such as pigment cells (i.e. melanophores and iridophores), neurons and glia of the autonomic nervous system, and cardiac tissues (i.e. smooth muscle and septa of the heart) (Hall, 1999; Vaglia and Hall, 2000; Lister et al., 2006; Sandell and Trainor, 2006; Hall, 2009). Cranial neural crest cells (CNCCs) differ from the other populations of NCCs in that they are naturally capable of also differentiating into bone and cartilage (Santagati and Rijli, 2003; Hall, 2005; Knight and Schilling, 2006; Hall, 2009). The CNCCs are the focus of this study and are discussed below.

1.3.2 Cranial Neural Crest Cells

Cranial neural crest cells (CNCCs) contribute to the ganglia of cranial nerves, ganglia of the parasympathetic nervous system, pigment cells, dental papillae, part of the mesencephalon, and the bones and cartilages in the cranial skeleton of vertebrates (Köntges and Lumsden, 1996; Santagati and Rijli, 2003). This is consistent across multiple vertebrate species (Gross and Hanken, 2008; Hall, 2009). It is the skeletogenic potential that distinguishes them from other NCCs, as mentioned above (Santagati and Rijli, 2003; Knight and Schilling, 2006; Gross and Hanken, 2008; Hall, 2009).

During neurulation in zebrafish, neural crest cells are induced at the lateral edges of the neural plate; they delaminate and migrate along specific pathways (Knight et al., 2003). *Hox* gene family members specify the anterior-posterior identities of the transverse hindbrain compartments known as rhombomeres (Santagati and Rijli, 2003). CNCC migration begins in the rhombomeres of the hindbrain (r2-r6); they travel down specific pathways to the branchial arches, where their segmental organization remains consistent with their rhombomeric origin (Schilling and Kimmel, 1994; Köntges and Lumsden, 1996). In general, migration of CNCCs consists of three phases (Kulesa et al., 2010).

Migration begins at the lateral plate border, where the non-neural ectoderm and mesoderm converge. Inductive signals initiate a change in cellular properties which ultimately results in an epithelial-to-mesenchymal transition (EMT) of the CNCCs (i.e.

cells become migratory) and their departure from the neural tube (Kulesa et al., 2010). Subsequently, the first phase of migration begins; acquisition of a dorsolateral migratory pathway; cell-cell communication and signals from the cells' microenvironment provide instruction on migration path and patterning. The second phase consists of controlled migration to the branchial arches; cells are capable of proliferating and remaining "on track". The third phase involves entry into the branchial arches; a variety of guidance cues are associated with successful invasion of the arches (Kulesa et al., 2010). Cells travel from the rhombomeres (divisions of the hindbrain) and the midbrain, to the branchial arches and the anterior portion of the skull, respectively (Figure 1.7).

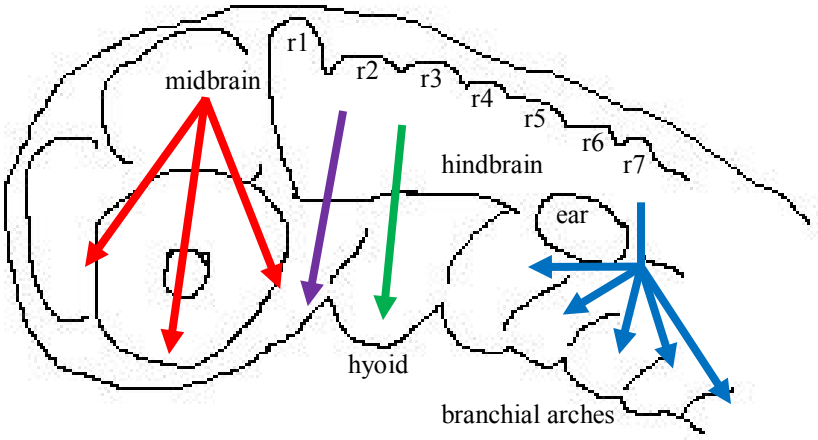

Figure 1.7 Schematic of an 24 hpf zebrafish showing CNCC migration from the hind- and midbrain regions. CNCCs migrating from the midbrain (red) migrate anteriorly and give rise to bones and cartilages of the face. CNCCs migrating from the hindbrain rhombomeres (r) enter the mandibular arch (purple arrow), the hyoid arch (green arrow), and the five branchial arches (blue arrows). They give rise to the mandible, hyoid arch, and branchial arches. Adapted from Knight and Schilling (2006).

Timing of migration of neural crest cells is crucial to this thesis. Onset of CNCC migration is an important factor in determining when embryos will be exposed to SMG (Figure 1.8) since I want to target this particular population of cells.

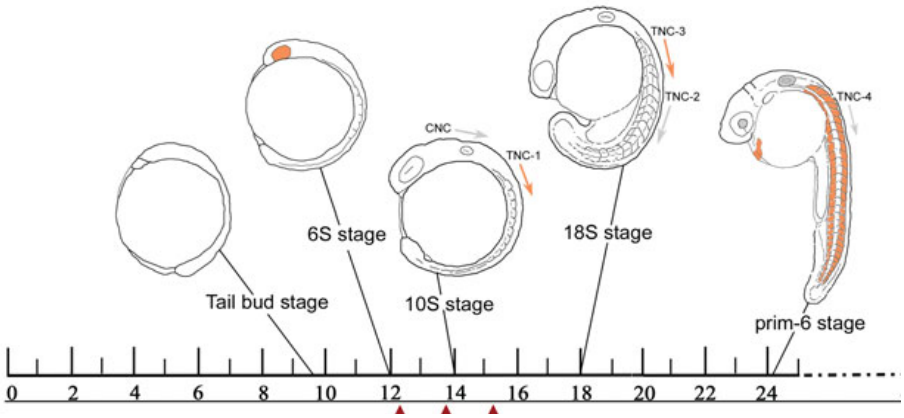

Figure 1.8: Schematic demonstrating the timing of neural crest cell migration. Scale below images indicates the age of the specimens (hpf).. CNCC migration begins just before 14 hpf. Adapted from Connolly and Hall (2008).

Fate maps have been developed in chicken and mouse to indicate which bones of the skull are CNCC-derived, and which are mesoderm-derived (e.g. Gross and Hanken, 2008). Fate maps are important to my study because I am determining the effects of SMG on cranial neural crest-derived tissues. Both cranial neural crest-derived tissues and fate maps are discussed in the sections below.

1.3.3 Pigmentation in Zebrafish

Zebrafish have three different types of pigment cells derived from neural crest cells (Figure 1.9). Xanthophores are yellow in colour and contain pteridine pigments; iridophores are iridescent and contain gold (or silver) reflecting platelets; melanophores are cells containing black melanin pigment (Johnson et al., 1995; Parichy, 2003; Kelsh, 2004; Quigley et al., 2004; Parichy et al., 2009). Chromatophores (xanthophores, iridophores, melanophores) are responsible for the characteristic striping patterns observed in the dermis of zebrafish (Quigley et al., 2004; Logan et al., 2006; Parichy, 2006). The pigment cells forming the stripes along the zebrafish abdomen are derived from trunk neural crest cells, and the pigment cells on the skull of the fish are cranial neural crest cell-derived (Kelsh et al., 1996; Vaglia and Hall, 2000; Parichy et al., 2003; Kelsh, 2004; Quigley et al., 2004; Budi et al., 2008; Donoghue et al., 2008).

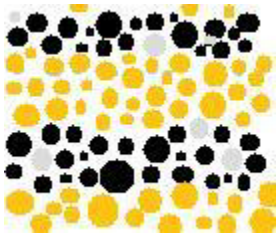

Figure 1.9: Schematic of the three pigment cell-types in a section of the lateral view of an adult zebrafish; the black melanophores, the yellow xanthophores, and the iridescent iridophores (silver). Adapted from Parichy (2003).

As embryos, zebrafish exhibit two distinct melanophore stripes, a dorsal stripe and a ventral stripe (Kelsh et al., 1996; Parichy, 2003; Quigley et al., 2004; Parichy et al., 2009). The melanophores in these stripes are derived from migratory (embryonic) neural crest whereas the adult pigmentation pattern arises as a result of differentiation of latent precursor cells (i.e. stem cells), also of cranial neural crest origin (Quigley et al., 2004). Xanthophores and iridophores develop later and are not part of the scope of this project; therefore, they will not be discussed further. Melanophores are highly-dynamic cells and melanin-transport within the cells is susceptible to light and dark environments (Figure 1.10; (Schliwa 1984; Thaler and Haimo, 1992; Rodionov et al., 1994; Brockerhoff, et al., 1995; Yamaguchi et al., 2007). Dispersal and aggregation of melanin has been determined to be regulated by cAMP levels (Logan et al., 2006). For example, epinephrine, which causes melanin granules to aggregate, functions by decreasing the levels of cAMP in the melanophores (Thaler and Haimo, 1992; Figure 1.10).

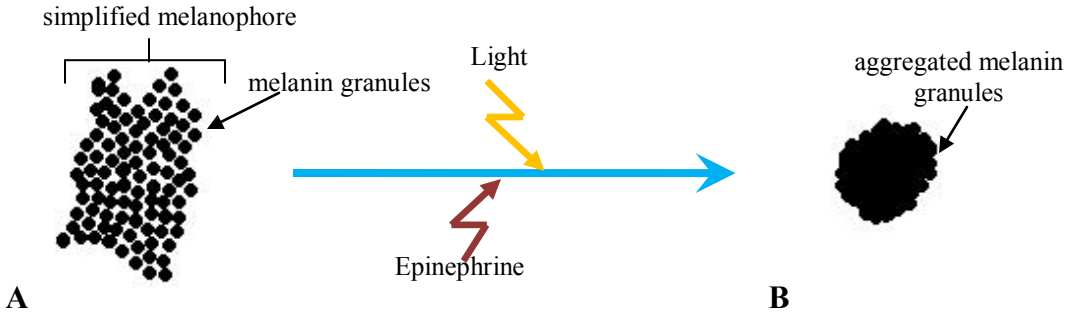

Figure 1.10: Schematic demonstrating dispersal and aggregation of melanin. (A) Simplified melanophore showing only the melanin granules dispersed. (B) Simplified melanophore, showing only the condensed aggregate of melanin granules after exposure to either light or epinephrine.

1.4 Skeletogenesis

There are four types of mineralized tissue: cartilage, bone, dentine, and enamel. Only cartilage and bone will be discussed here.

1.4.1 Cartilage and Bone

Mature cartilage, an avascular tissue, is composed of chondrocytes within an extracellular matrix (Hall, 2005). Cartilage forms via aggregation of cranial neural crest or mesodermal cells, and subsequent differentiation (Figure 1.11); it is deposited by chondroblasts, and resorbed by chondroclasts, and retains a supportive skeletal function.

In general, bone is comprised of osteocytes buried in a bone matrix (Hall, 2005; Franz-Odendaal et al., 2006); however, advanced teleosts have bone that lacks osteocytes and is thus acellular. The zebrafish, a more basal teleost, has cellular bone. Osteoblasts are cells that deposit bone, eventually burying themselves in the matrix and maturing into osteocytes. In contrast, osteoclasts are the bone-resorbing cells that aid in remodelling (Hall, 2005).

Bone forms by one of two broad methods (Figure 1.11). Intramembranous ossification occurs when bone forms directly from a mesenchymal condensation of neural crest- or mesoderm-origin. Endochondral ossification occurs when bone ossifies a cartilage template. Perichondral ossification occurs when bone ossifies the perichondrium of a cartilage precursor. There is debate as to whether this is a subtype of intramembranous or of endochondral ossification. The zebrafish cranium, as described by Cubbage and Mabee (1996) is composed of both endochondral and intramembranous bones, in addition to perichondral bones.

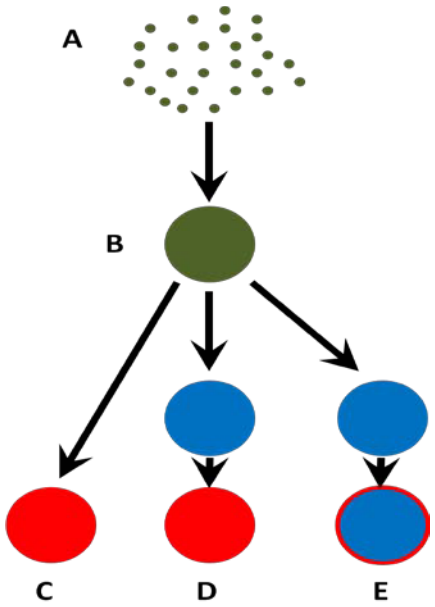

Figure 1.11: Schematic of the processes by which bone may be formed. Ossification begins with the migration and aggregation of precursor cells (A) which form a mesenchymal condensation (B). The condensation may then directly ossify (C), a process known as intramembranous ossification The condensation may also form a cartilage precursor , which is later replaced by bone (D), known as endochondral ossification. A third ossification type, perichondral ossification, also starts with a cartilage template, but ossification occurs in the perichondrium, the membrane surrounding the cartilage (E). It is debated as to whether perichondral ossification is intramembranous or endochondral.

1.4.2 Cranial Skeleton Development in Zebrafish

Development of the cranial skeleton in zebrafish was described by Cubbage and Mabee (1996). Ossification in the skull begins as early as 4 dpf (about 3 mm SL) in ceratobranchial 5, the notochord, and the operculum. Relevant to my study, the ossification for various regions of the skull are as follows. In the branchial arch region, ceratobranchial 5 is the first branchial arch to ossify. Branchials 1-4 ossify next, followed by ossification of the epibranchials, then the basibranchials and the hypobranchials. In the orbital region, the parasphenoid is the first to ossify, followed by the pterosphenoid, the first infraorbital, the orbitosphenoid, the frontal bones, the supraorbitals, the scleral ossicles, and then the remainder of the infraorbitals. The opercular region ossifies first in the operculum, and then in the interopercle, subopercle, and preopercle (Cubbage and Mabee, 1996). In Cubbage and Mabee (1996), details of each bone are given in terms of onset of ossification, contact with other elements, and whether they form via intramembranous or endochondral ossification. There is no description, however, of the origin of each element.

Due to the nature of this thesis, determining the effects of SMG on cranial neural crest-derived tissues, it is important to know the origin of the elements in the zebrafish skull, yet there is no published complete fate map for the cranial skeleton in zebrafish. There are, however, fate maps for both the chicken (Couley et al., 1993) and the mouse

(Chai et al., 2000) and there are some consistencies which are likely to apply across vertebrate groups; namely that the back of the skull is mesoderm-derived and the rest is neural crest-derived (Figure 1.12; Gross and Hanken, 2008). Therefore, in order to identify cranial neural crest- and mesoderm-derived bones in the zebrafish skull, I refer to published fate maps of other organisms.

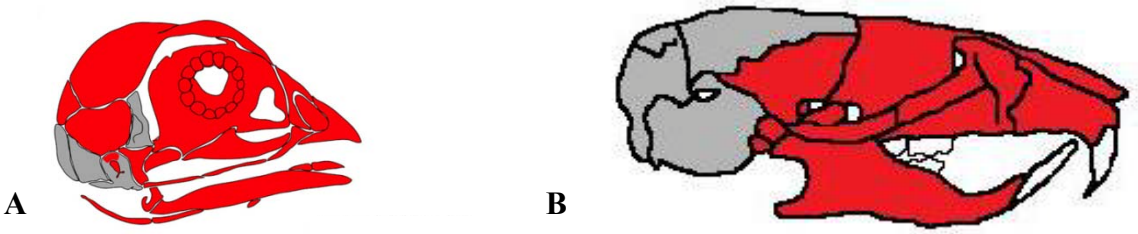

Figure 1.12: Vertebrate fate maps. (A) Chicken and (B) mouse. Bones in red are cranial neural crest-derived, bones in grey are mesoderm-derived. Adapted from Gross and Hanken (2008) and Santagati and Rijli (2003).

Partial maps for the zebrafish skull exist, and recently our lab has been working on a complete fate map of the zebrafish skull. Although unpublished to date, the similarities to mouse and chicken are present (Figure 1.13; Fisher and Franz-Odendaal, pers. comm.).

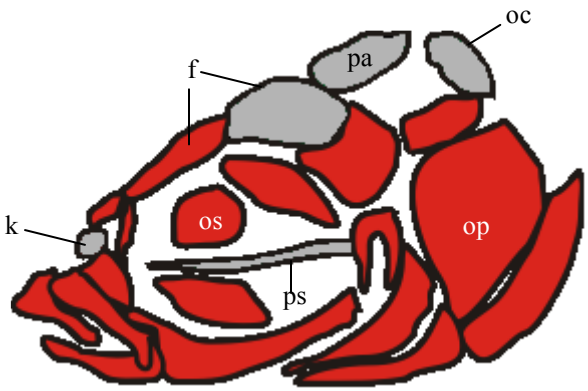

Figure 1.13: Fate map showing the cell-type origins of the bones in the cranial skeleton of the zebrafish. Grey elements are of mesoderm descent, and red bones are cranial neural crest-derived (Fisher and Franz-Odendaal, pers. comm). f, frontal; k, kinethmoid; oc, occipital region (exoccipital and supraoccipital); op, operculum; os, orbitosphenoid; pa, parietal; ps, parasphenoid; soc, supraoccipital.

1.5 Objectives

The primary objective of this MSc. thesis is to determine how exposure to SMG affects cranial neural crest-derived tissues in *Danio rerio*, with particular focus on the skull. To do this, I have broken the project down into three smaller objectives:

Objective 1: To determine whether or not shearing stress affects the skeleton in fish exposed to SMG as embryos. Are the changes seen in the skeleton (if any) a result of stress, exposure to SMG, or a combination of both?

Objective 2: To determine if exposure to SMG results in changes in the neural crest-derived melanophores on the dorsal skull.

Objective 3: Determine if exposure to SMG affects the cranial skeleton in larval and adult zebrafish.

1.6 Significance

The simulation of an environment lacking a gravitational stimulus denies zebrafish embryos their normal three-dimensional orientation system. The results will inform us as to whether or not cranial neural crest cells require gravity in order to give rise to the proper adult phenotype. Determining the effects of SMG on zebrafish cranial neural crest-derived tissues, in particular the melanophores and cranial skeleton will provide useful information in the context of 1) shear stress response, 2) abnormalities that arise due to defects in cranial neural crest cells, and 3) extended space flight and travel

- It is important to determine what effects are due to a shear stress response in the fish, and which effects are due to exposure to SMG. If we attribute shear stress effects as being a result of exposure to SMG or vice versa, we are misrepresenting the information, and thus misinforming future researchers.
- Cranial abnormalities/defects (syndromes, tumors, dysmorphologies) occurring as a result of defects in either cranial neural crest cell migration or differentiation are

referred to as neurocristopathies (Tobin et al., 2008; Hall, 2009). There are many birth defects that yield a variety of different phenotypes that can be traced back to problems with neural crest (i.e. Bardet-Biedl syndrome, Treacher-Collins syndrome, DiGeorge syndrome). These syndromes are characterized by abnormalities in the development of the craniofacial skeleton, often displaying defects in the formation of the cranial midline (Hall, 2009). By determining whether exposure to SMG affects the cranial skeleton, I will be able to contribute further information to the already widely-studied field of craniofacial dysmorphology. Knowing more about the development and behaviour of neural crest cells in space means we are better informed when attempting to correct it on Earth.

- Similarly, the effects of SMG on cranial neural crest-derived tissues will allow researchers to be better informed when the time comes to make decisions regarding extended travel and life in space. There are known effects on expression of some genes, and the development of the vestibular system (Moorman et al., 1999; Shimada et al., 2005; Shimada and Moorman, 2006) in addition to transient effects in the swim bladder of zebrafish (Lindsey et al., 2011). No studies, however, have determined the long-term effects that may be observed in adult specimens when exposed to SMG as embryos, nor have they considered the effects on the multipotent migratory population of cranial neural crest cells.

The results presented here will contribute to numerous fields of study (e.g. development, anatomy, space research) and will provide researchers with a foundation on which to pursue further microgravity studies.

Chapter 2: Materials and Methods

2.1 Fish Husbandry and Care

Stock wild-type (WT) AB zebrafish, *Danio rerio*, were obtained from the Zebrafish International Resource Centre (ZIRC; University of Oregon) through www.ZFin.org. Some male wild-type fish were also acquired from the Aquatron at Dalhousie University in 2009. Two strains of stock transgenic sox10*EGFP*crelox fish were obtained from Dr. Shannon Fisher, University of Pennsylvania, in 2010. Embryos from all stocks were obtained in the Mount Saint Vincent University fish facility. All fish were kept at 28.5°C on a 12-12 hour light cycle. Animal care protocols were submitted and approved annually by the SMU-MSVU Animal Care Committee, and guidelines set by the Canadian Council for Animal Care (CCAC) were followed.

2.2 The Bioreactor- Simulated Microgravity Experiments

After each successful spawning, embryos were staged according to Kimmel et al. (1995) and separated into one of three groups:

a) raised under normal conditions (control no vibrations, CNV);

b) exposed to vibrations (control with vibrations, C+V); and

c) exposed to simulated microgravity (SMG).

Fish from the CNV groups were raised in glass cups maintained at 28.5°C until they reached 4, 10, or 35 dpf at which point they were sacrificed and fixed. Fish to be raised to adulthood were raised in cups until they reached 3-4 weeks at which point they were transferred to an independent rack system and raised to four months. All fish were measured and the standard lengths (SL; length from tip of snout to base of caudal fin) were recorded upon fixation. Standard lengths were used as a proxy for age because there is significant variation in growth rates between individuals within a clutch and between clutches (Discussed in Chapter 3).

Embryos in group (c) above (i.e. those exposed to SMG) were placed in the bioreactor, a clear plastic chamber filled with zebrafish system water, attached to a motorized base, also referred to as a rotating wall vessel (RWV; Synthecon, Houston, TX; Figure 2.1). The bioreactor was kept in a glass-front incubator set at 28.5°C and

exposed to the regular light cycle. The bioreactor was turned on when embryos reached 10, 12, or 14 hpf (Figure 2.2), and was subsequently left on for 12, 24, 48, or 96 hours (Table 2.1). The full bioreactor protocol is in Appendix 1. The vessel turns at a rate of 18.5 RPM (previously optimized by Moorman et al., 1999) such that embryos are suspended in the water midway between the hollow core and the outer plastic edge of the chamber. At the end of the SMG exposure, embryos were removed from the bioreactor, placed in glass cups maintained at 28.5°C, and were raised under normal conditions until 4, 10, 35 dpf or to adulthood.

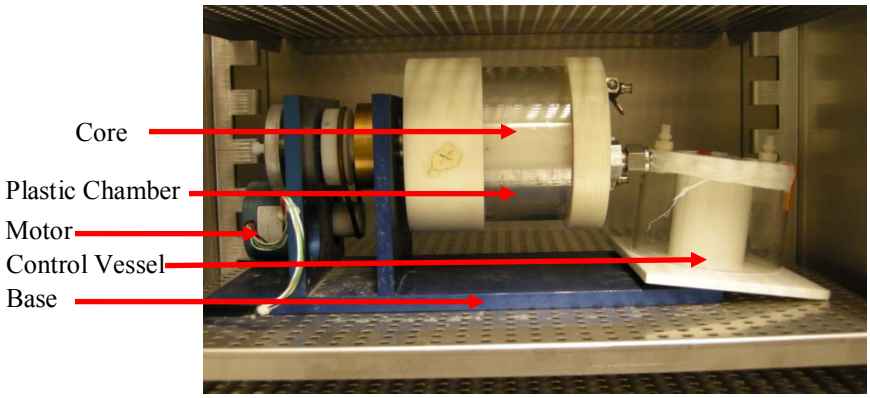

Figure 2.1: Image of the bioreactor (RWV) in the incubator. The control vessel is visible on the right-hand side. It is propped up on the base of the bioreactor, subjecting it to vibrations.

Fish exposed to vibrations (C+V) were placed in a water-filled plastic vessel with the same specifications as the bioreactor vessel (Figure 2.1) and positioned on the edge of the bioreactor base. This arrangement ensured that these fish were exposed to vibrations emitted by the bioreactor at the same time points described above for the SMG fish (Table 2.1). Upon completion of vibration exposure, fish were raised under normal conditions to 4, 10, 35 dpf or adulthood.

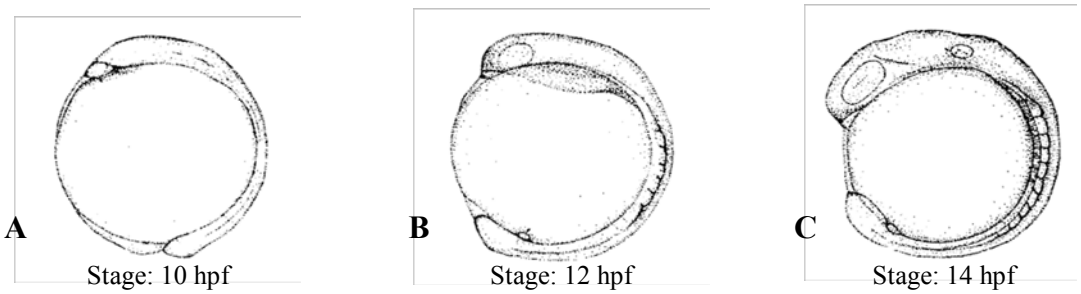

Figure 2.2: The embryonic stages at which zebrafish were put into either the bioreactor (SMG) or the control vessel (C+V). A) 10 hpf; B) 12 hpf; C) 14 hpf. Adapted from Kimmel et al. (1995).

Table 2.1: Notation used to indicate duration of exposure to SMG or vibrations (C+V) and the time of onset of the spin (stage).

Duration:	**12 hours**	**24 hours**	**48 hours**	**96 hours**
Stage				
10 hpf	12h SMG at 10 hpf/ 12h C+V at 10 hpf	24h SMG at 10 hpf/ 24h C+V at 10 hpf	48h SMG at 10 hpf/ 48h C+V at 10 hpf	96h SMG at 10 hpf/ 96h C+V at 10 hpf
12 hpf	12h SMG at 12 hpf/ 12h C+V at 12 hpf	24h SMG at 12 hpf/ 24h C+V at 12 hpf	48h SMG at 12 hpf/ 48h C+V at 12 hpf	96h SMG at 12 hpf/ 96h C+V at 12 hpf
14 hpf	12h SMG at 14 hpf/ 12h C+V at 14 hpf	24h SMG at 14 hpf/ 24h C+V at 14 hpf	48h SMG at 14 hpf/ 48h C+V at 14 hpf	96h SMG at 14 hpf/ 96h C+V at 14 hpf

2.3 Pigment Analysis

In order to determine the effects of SMG on pigmentation, the melanophores were analyzed. Embryos from the same clutch were divided into two groups; one group was exposed to SMG and the other to C+V for 96 hours starting at 10 hpf. These groups were chosen because I hypothesized that the longest exposure starting at the earliest time point would have the greatest effect on these cells. Upon removal from their respective vessels, six fish were randomly selected from each group and each fish was placed in its own individual well in a well-plate. These wells were kept in a glass-front incubator (exposed to normal light cycle) kept at 28.5°C, for a week. Care was taken to ensure that the lighting was the same for all fish.

Between 10 o'clock and 12 o'clock every day for seven days, the fish were anaesthetized through submergence in a non-lethal 0.01% dose of MS-222 (ethyl 3-aminobenzoate methanesulfonic acid salt, 98%; Sigma-Aldrich, E10521) in zebrafish system water. Fish were then moved to 2.4% Methyl-Cellulose (Sigma-Aldrich, M0387; Appendix 1) in system water, to ensure proper orientation and easy manipulation when photographing. The dorsal skull was photographed using a Nikon DXM1200C camera attached to a Nikon C-DSD115 stereomicroscope. Images of each individual were captured every day between 10 am and 12 pm (Figure 2.3A).

Pigment analyses were conducted on the surface area of the dorsal skull of the zebrafish. The total surface area of the dorsal skull was measured as the shortest distance between the eyes to the anterior-most edge of the swim bladder (Figure 2.3B). To assess pigment area, the surface area of individual regions of pigmentation on the dorsal skull was measured and summed for each fish on each day (Figure 2.3C). Surface areas were

calculated using NIS Elements 3.0 software. Using Microsoft Excel, the total pigmented area and the percentage of the dorsal head covered with pigment were calculated (e.g. Table 2.2).

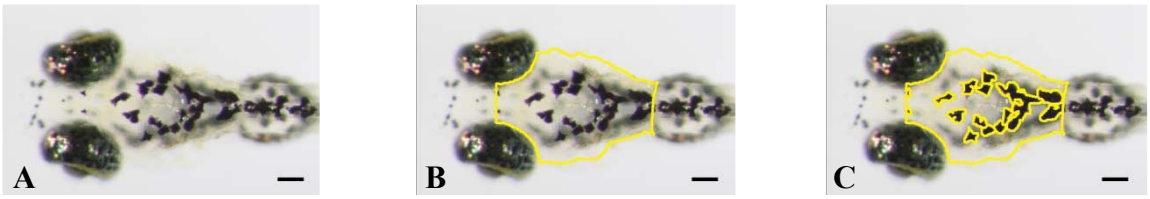

Figure 2.3: Three-step series of the same fish three days after removal from control vessel illustrating the protocol for measuring the percentage of the dorsal zebrafish head covered by melanophores. A) Dorsal view of the zebrafish head. B) Surface area of dorsal skull traced in yellow. C) Surface area of skull and groups of clustered melanophores traced in yellow. The fish shown is 3.8 mm SL and was exposed to vibrations for 96 hours starting at 10 hpf. Scale bars are 100 µm.

Table 2.2: Example of the data recorded and calculated when conducting analyses on the dorsal area of the skull and the surface area covered with pigment for the C+V group on the second day after exposure to vibrations for 96h starting at 10 hpf.

Fish Identity	Standard Length (mm)	Total surface area of dorsal head (mm^2)	Area covered by pigment (mm^2)	Percentage of head covered with pigment (%)
Control A	3.7	222.62	13.97	6.28
Control B	3.7	208.39	41.56	19.94
Control C	3.8	205.58	42.63	20.74
Control D	3.8	211.53	22.86	10.81
Control E	3.7	199.82	33.43	16.73
Control F	3.8	210.74	56.69	26.90
avg	**3.75**			**16.9 (± 7.4)**

The protocol outlined above was conducted four times with six fish per group, giving a total of 24 SMG fish and 24 C+V fish. The third and fourth time it was conducted, a melanophore count was included with the surface area measurements as follows. After each dorsal skull was photographed, 2-3 drops of a 1 mg/ml solution of epinephrine (Sigma-Aldrich, E1635) were added directly onto the fish in the 2.4% methyl-cellulose solution (e.g. Clark et al., 1986). Melanophores contracted within ten

minutes and individual melanophores were counted and recorded (Figure 2.4). The average number of melanophores was calculated in this way each day between 10 a.m. and 12 p.m., for a period of a week.

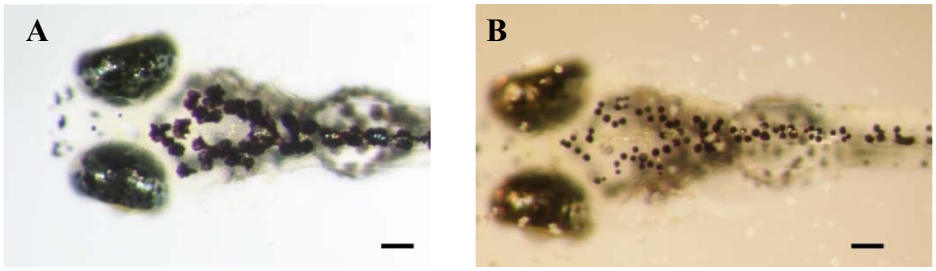

Figure 2.4: Fish from the C+V group (96h C+V at 10 hpf) photographed on the fourth day after removal from the control vessel, before (A) and after (B) treatment with epinephrine. The fish shown is 3.8 mm SL; scale bar: 100 µm.

Statistical analysis using Minitab (version 15.0) was conducted on the pigment data to determine whether the percentage of the surface area covered by melanophores in SMG samples differed significantly from the percentage covered in control fish. One-way ANOVA was used for both the surface area measurements and the melanophore counts (Appendix 4). In addition, a linear regression model was conducted on the trend-lines from the melanophore surface area measurements, and paired t-tests were conducted to compare values from the first day of measurement to values from the seventh day of measurement for both the surface area and number data.

2.4 Cartilage Stain

In order to assess whether or not exposure to SMG affected the morphology of the pharyngeal arches, larval zebrafish were stained for cartilage (adapted from Klymkowski and Hanken, 1991). Embryos were exposed to SMG (n=5), C+V (n=6), or CNV (n=6) for 96 hours starting at 10 hpf. At the end of 96 hours, fish were removed from their respective vessels and raised in normal conditions until 10 dpf, at which time they were euthanized in a lethal dose (0.1%) of MS-222. After euthanization, specimens were fixed overnight in 4% paraformaldehyde (PFA; Sigma-Aldrich, P6148) in 0.01M Phosphate-Buffered Saline (PBS, pH 7.4) at 4°C (see Appendix 1 for all recipes and full protocol).

Embryos were dehydrated the next day via an ethanol series to 70% ethanol and stored at 4°C.

Embryos were placed in a 0.015% alcian blue solution overnight for staining, and then rinsed in a 95% ethanol solution and placed in saturated borax (Sigma-Aldrich, B9876) solution overnight. The tissue was digested in a 2% borax/1% stock trypsin solution, and then bleached in 3% hydrogen peroxide (stock) in 1% potassium hydroxide (KOH; Sigma-Aldrich, P1767). The stained fish were then processed through a glycerol/KOH series to storage in 100% glycerol (Fischer Scientific G33-4). Full protocol details are in Appendix 1.

Images of the ventral view were taken of the pharyngeal arches of each specimen using a Nikon C-DSD115 stereo microscope and a Nikon DXM1200C camera**.** In order to quantify the shapes of the cartilaginous elements, morphometric analyses were conducted on the pharyngeal arches of the three groups (described in Section 2.8).

2.5 Bone Stain

Embryos were exposed to SMG, C+V, or CNV for 12, 24, 48, or 96 hours beginning at 10, 12, or 14 hpf (Table 2.1; Table 2.3). Embryos were then raised in normal conditions until adulthood. Fish were euthanized in a lethal dose of MS-222, and fixed overnight at room temperature in 10% Neutral-Buffered Formalin (NBF; Fisher Scientific, 72210). The following day, fish were either processed in an ethanol series for storage in 70% ethanol or placed in distilled water in preparation for the bone stain (Franz-Odendaal, 2007).

Fish stored in 70% ethanol were rehydrated and washed in distilled water. Specimens were bleached overnight, and subsequently rinsed in distilled water. The specimens spent the day in a saturated borax solution and were stained overnight in a 1 mg/ml alizarin red solution (in 1% KOH). The stained fish were rinsed in a 1% KOH solution, and tissue was digested in a 2% borax/1% trypsin solution for approximately three nights. They were then stored in 100% glycerol after going through a graded glycerol/1% KOH series. Full protocol details are in Appendix 1.

Images of dorsal and lateral views of each skull were taken using a Nikon DXM1200C camera hooked up to a Nikon C-DSD115 stereo microscope.

Morphometric analyses were conducted on the dorsal and lateral skull views in order to determine if dorsal and lateral skull morphology differed significantly between groups (described in Section 2.8).

Table 2.3: Sample numbers for bone-stained adults from different groups. These sample numbers are the same for the vertebrae analyses below.

Duration:	12h	24h	48h	96h
Stage:				
10 hpf	3 SMG; 1 C+V	3 SMG; 4 C+V	2 SMG; 2 C+V	6 SMG; 12 C+V
12 hpf	2 SMG; 6 C+V	12 SMG; 6 C+V	3 SMG; 2 C+V	4 SMG; 3 C+V
14 hpf	3 SMG; 4 C+V	4 SMG; 5 C+V	4 SMG; 2C+V	4 SMG; 3 C+V

2.6 Double-Stain

In order to determine if fish exposed to SMG and vibrations differed in skull morphology from fish raised under normal conditions at a juvenile stage, fish were stained at 4, 10, or 35 dpf using an acid-free double-stain for bone and cartilage (adapted from Walker and Kimmel, 2007). An acid-free stain is very important for juvenile fish because the acid used in a typical cartilage stain (Section 2.4) can decalcify the bone, thus giving incorrect bone stain results.

Embryos were exposed to SMG, C+V, or CNV for 12 hours beginning at 10 hpf, 24 hours beginning at 12 hpf, or for 96 hours beginning at 10 hpf. Embryos from each of these groups were then raised to 10 or 35 dpf in normal conditions. Fish were euthanized in a lethal dose of MS-222 and fixed overnight in 4% PFA in 0.01M PBS at 4°C. The acid-free double-stain for bone and cartilage (adapted from Walker and Kimmel, 2007) is described in Appendix 1. Samples were viewed on a Nikon C-DSD115 stereo microscope and left lateral images were taken using a Nikon DXM1200C (1500 SMZ) camera.

In order to determine if the morphology of bones in the lateral view was statistically significant between groups, morphometric analyses were conducted on the right opercula of 35 dpf samples (described in Section 2.8). The operculum is an easily

accessible intramembranous cranial neural crest-derived bone (Kimmel et al., 2010) for which morphometric landmarks have been previously established.

2.7 Evaluating the Potential Effects of Mechanical Stress

In order to determine if mechanical forces acting on the embryos within the bioreactor are causing a stress response, vertebrae counts were conducted on bone-stained adult fish exposed to SMG, vibrations alone, or raised under normal conditions. The reason the vertebrae were counted is because a previous study showing that heatshock of zebrafish embryos caused an upregulation in HSP levels, also showed significant differences in the vertebrae number of these fish as adults (Connolly, 2008). The standard length (SL) of specimens was measured and recorded as described. Precaudal and caudal vertebrae, as defined by Bird and Mabee (2003) as well as the total number of vertebrae were calculated (Figure 2.5; Table 2.4). All charts for vertebrae analysis can be found in Appendix 3.

Table 2.4: Example of the chart used for analyzing vertebrae. Precaudal and caudal vertebrae numbers are recorded alongside standard length (SL).

Fish Identity	Age (dpf)	SL (mm)	"Treatment"	Precaudal #	Caudal #	Total Vert #
ABAQ	120	20	96hr SMG at 10hpf	12	16	28
AB-21	122	18	96hr SMG at 10hpf	10	15	25
AB-22	107	21	96hr SMG at 10hpf	10	14	24
H2036.8xAB (a)	141	19	96hr SMG at 10hpf	10	16	26
H2036.8xAB (b)	141	20	96hr SMG at 10hpf	10	15	25

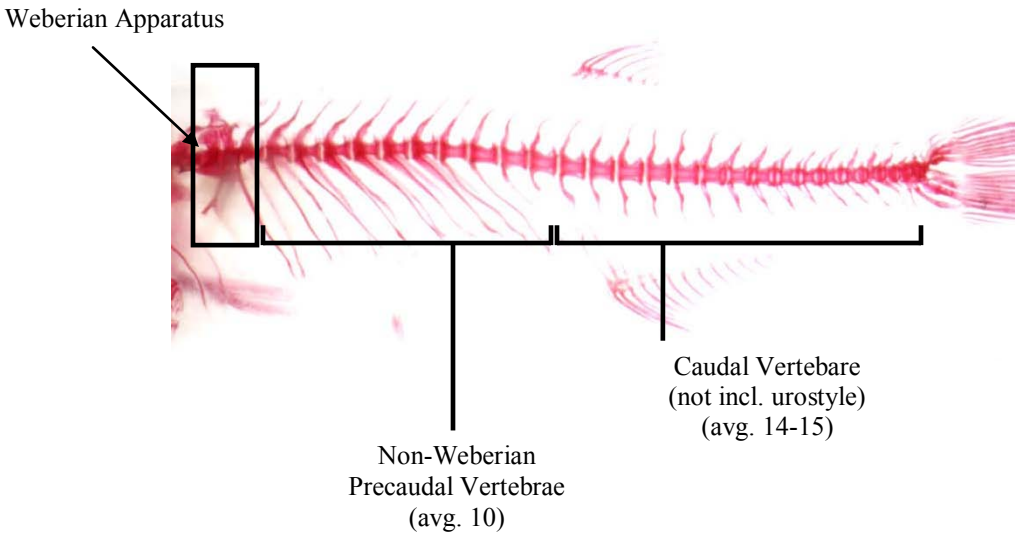

Figure. 2.5: Left lateral view of the trunk of a bone-stained adult zebrafish, indicating the precaudal (non-Weberian) and caudal (without urostyle) vertebrae.

Statistical analyses were conducted on precaudal, caudal, and total vertebrae numbers using Minitab (version 15.0). Specifically, non-parametric Kruskal-Wallis and Mann-Whitney U tests were used to determine whether the number of caudal and total vertebrae differed significantly between fish exposed to SMG, fish exposed to vibrations, and fish raised under normal conditions.

2.8 Morphometric Analyses

In order to determine if there were statistically significant differences between the pharyngeal arches and opercula of larval and juvenile specimens, and between the dorsal skull and opercula of adult specimens, morphometric analyses were conducted on:

a) the ventral view of the larval cartilaginous pharyngeal arches,
b) the dissected right opercula of 35 dpf fish,
c) the dorsal views of the adults, and
d) the dissected right opercula of adults.

In brief, two-dimensional configurations of the landmark coordinates were assigned and analyzed using tps software (F.James Rohlf; http://life.bio.sunysb.edu/morph/). Further analyses were conducted using IMP software, version 6a, (H. David Sheets, Canisius College;

http://www3.canisius.edu/~sheets/morphsoft.html), and Morphologika[2], version 2.5 (Paul O'Higgins, Hull York Medical School; https://sites.google.com/site/hymsfme/downloadmorphologica). Details of methods are described below but do not follow the order given in the following chapters.

2.8.1 Pharyngeal Arches

The ventral view pharyngeal arch images were uploaded as three separate groups of images (SMG, C+V, and CNV) to tpsUTIL (version 1.46) and converted to .tps file formats. The tps files for each group were opened one at a time in tpsDIG2 (version 2.16) and assigned 46 landmarks based on anatomical reference points (landmark descriptions are given in Appendix 2 and are shown in Figure 2.6A). As landmarks were applied, images were scaled to the same size using tpsDIG2, so that the morphology of the specimens is assessed accurately.

Landmarked images were then opened in tpsSUPER (version 1.14) and a "consensus", average, or "reference" morphology plot was generated for each group Figure 2.6B). Using tpsSPLIN (version 1.20) the consensus plot from the SMG group, was compared to both the CNV consensus, and C+V consensus in turn. The order in which these groups are compared does not affect the final result. The resulting thin plate splines graphically demonstrate where in the pharyngeal arches the greatest changes occurred when comparing each consensus. Splines comparing two consensuses will warp in regions where landmarks differ in location.

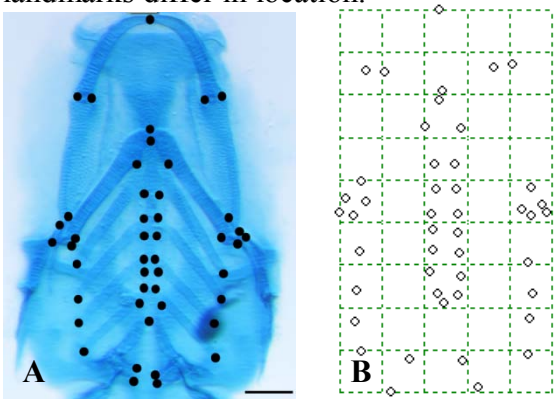

Figure 2.6: Images acquired using tpsDIG2 (A) and tpsSplin (B). A) Ventral view of the cartilage-stained pharyngeal arches of a SMG specimen (96h SMG at 10 hpf) showing the 46 landmarks. Fish shown is 4.0 mm SL. B) Consensus thin plate spline for the pharyngeal arch skeletons of the group of fish raised under normal conditions (CNV). Scale bar: 100µm.

In addition, in order to visually observe the morphological changes in the pharyngeal arch skeleton, Morphologika^2 (version 2.5) software was used to overlay the landmarks from all individuals within a group (SMG, C+V, CNV). Wireframe images for each specimen within the groups were generated by joining the landmarks (i.e. Figure 2.7). To do this, the original landmarked tps file from each group was opened in Morphologika and converted to a text (txt) file. These files were opened in notepad; at the bottom of the series of numbers listed, [wireframe] was typed on a new line. Below this, a list of landmark pairs was added. This resulted, when re-opened in Morphologika^2, in a line connecting the landmarks identified in each pairing.

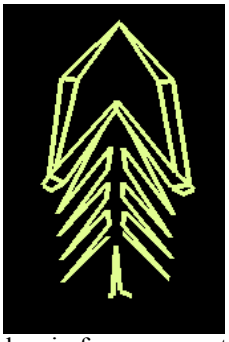

Figure 2.7: Example of a single wireframe computed using Morphologika^2, version 2.5, software, for a specimen exposed to SMG for 96 hours beginning at 10 hpf.

Finally, PCAGen6 and TwoGroup6h were used. PCAGen6 calculates the partial Procrustes distances and centroid size for the landmarks of each sample and conducts a principal components analysis on these distances. Principal components analysis shifts all the images so they overlay in a way that the landmarks line up as best as possible. As a result, the orientation of the images is not a factor. PCAGen6 converts the files to a format that can be analyzed by TwoGroup6h, and ensures that the statistical analysis conducted using TwoGroup6h is an accurate measure of the differences in morphology. TwoGroup6h is a statistical analysis of the differences in partial Procrustes distances between groups of fish. It completes pairwise comparisons (i.e. SMG vs. C+V) of the groups and indicates statistical significance in morphology by computing Goodall's F-test, and a *p*-value (analogous to the F- and p-values calculated using ANOVA).

2.8.2 Adult Opercula and Dorsal Skulls

In order to determine if statistically significant differences occurred in the morphology of adult skulls between different groups, morphometric analyses were conducted on the dorsal view of the skull and on the right opercula. The anterior-most frontals, in addition to the opercula, are cranial neural crest-derived bones. They are also all flat intramembranous bones, which makes it easier to assign 2-dimensional landmarks.

For the opercula analyses, the right opercula of adult zebrafish were dissected from the skulls and mounted in 100% glycerol on glass slides. Coverslips were applied and sealed with clear nail varnish. Images of both bone-stained right opercula and dorsal views of the adult skull were uploaded to tpsUTIL in groups (12h SMG and C+V at 10 hpf, 24h SMG and C+V at 12 hpf, and 96h SMG and C+V at 10 hpf) and converted to .tps file formats. Groups of images were then opened in tpsDIG2 and assigned landmarks according to anatomical reference points (Appendix 2). Dorsal images were assigned 15 landmarks initially, and then reduced to a set of 9 landmarks based on anatomical reference points which identify the frontal and parietal bones (described in Appendix 2 and shown in Figure 2.8A, B; Chapter 6). Right lateral opercula were assigned 5 landmarks based on anatomical reference points published by Albertson and Yelick, 2007 (Figure 2.8C). Vector analyses, which generate arrows indicating direction and magnitude of change in landmark location between experimental and control groups, in addition to splines, were created using a combination of tpsSUPER and tsp SPLIN. Wireframes were generated using Morphologika[2]. Further morphometric analyses were conducted on the dorsal skull and right opercula as described above using PCAGen6 and TwoGroup6h.

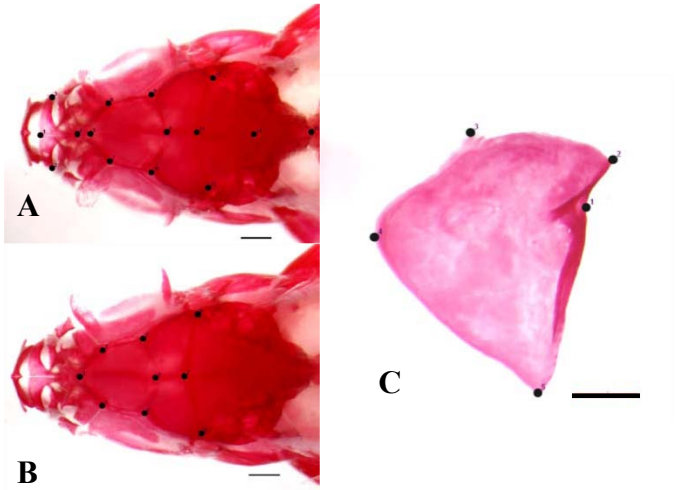

Figure 2.8: Dorsal view of two CNV adult skulls (A, B) and right lateral operculum from an adult bone-stained CNV zebrafish (C). A) The initial 15 landmarks chosen to analyze the frontal and parietal bones of the dorsal adult skull. B) The reduced set of 9 landmarks used to analyze the frontal bones only. C) The five landmarks assigned to the right opercula for morphometric analysis. Scale bars are 500 µm.

2.8.4 Juvenile Opercula

In order to determine whether significant differences occurred between the morphologies of juvenile skulls from different groups, morphometric analyses were conducted on the right opercula of 35 dpf double-stained zebrafish.

Acid-free double-stained right opercula were dissected from 35 dpf zebrafish and mounted flat on glass slides in 100% glycerol as previously described. Images of the right opercula from different groups (SMG, C+V, CNV) were uploaded to tpsUTIL and converted to .tps files. The tps files were then opened in tpsDIG2, where the same 5 landmarks described in Section 2.8.3 were applied to each individual (Figure 2.8). Vector analyses and splines were created using a combination of tpsSUPER and tpsSPLIN programs, wireframes were computed using Morphologika[2], and statistical significance was calculated using a combination of PCAGen6 and TwoGroup6h, as previously described.

Chapter 3: Zebrafish Growth Rates: An Analysis of Age (dpf) vs. Standard Length

3.1. Brief Introduction

Studies examining the zebrafish frequently identify the specimens with a standard length measurement (SL) in addition to, or instead of days post-fertilization (e.g. Eaton and Farley, 1974; Cubbage and Mabee, 1996; Ferreri et al., 2000; Franz-Odendaal et al., 2007; Parichy et al., 2009; Edsall and Franz-Odendaal, 2010). This occurs most often when the zebrafish have developed beyond the stages of development described by Kimmel et al. (1995) and when growth rates are influenced by stocking density, feeding, etc. (Nüsslein-Volhard and Dahm, 2002). Standard length is the distance from the snout of the fish to the base of the tail, or end of the vertebral column (Cubbage and Mabee, 1996).

A more precise method used in measuring larval zebrafish is notochord length (NL), a body length measurement used as a reference prior to notochord flexion. Often NL and SL are used together to describe a population of fish of varying lengths. There is no difference between the two measurements, however, when conducted prior to notochord flexion. For clarity, I will use SL for all ages discussed.

When using days post-fertilization (dpf) in addition to standard length (SL) it is important to investigate growth rates in each facility. To set the stage for the remainder of this thesis, and to enable comparison of this research to other published studies using standard length, age, or both, I have plotted the standard lengths of zebrafish that I raised in normal conditions in the Mount Saint Vincent University fish facility against their respective ages and compared these to published data sets (Figure 3.1).

3.2 Results

3.2.1 Fish Raised Under Normal Conditions

Zebrafish raised under normal conditions were fixed at 4 dpf (n=9), 10 dpf (n= 9), 35 dpf (n= 5), and adulthood (120 dpf; n= 15). Fish fixed at 4 and 10 dpf average 3.41 mm SL (± 0.16 and ± 0.12, respectively). Fish fixed at 35 dpf average 8.22 mm SL (±

2.1) and fish raised to adulthood (120 dpf) average 19.93 mm SL (± 1.58). These measurements (tabulated in Table 3.1) were plotted against the standard lengths of fish recorded by Cubbage and Mabee (1996), and Witten et al. (2001), and are shown in Figure 3.1. The Cubbage and Mabee (1996) values represent the best estimates for their data (represented as a chart in their Appendix). The Witten et al. (2001) measurements are taken directly from their Materials and Methods section. Although there may appear to be differences in the mean measurement values, when taking the measurement error (standard error, Table 3.1) into account, the differences in body standard lengths are neglible at each time point.

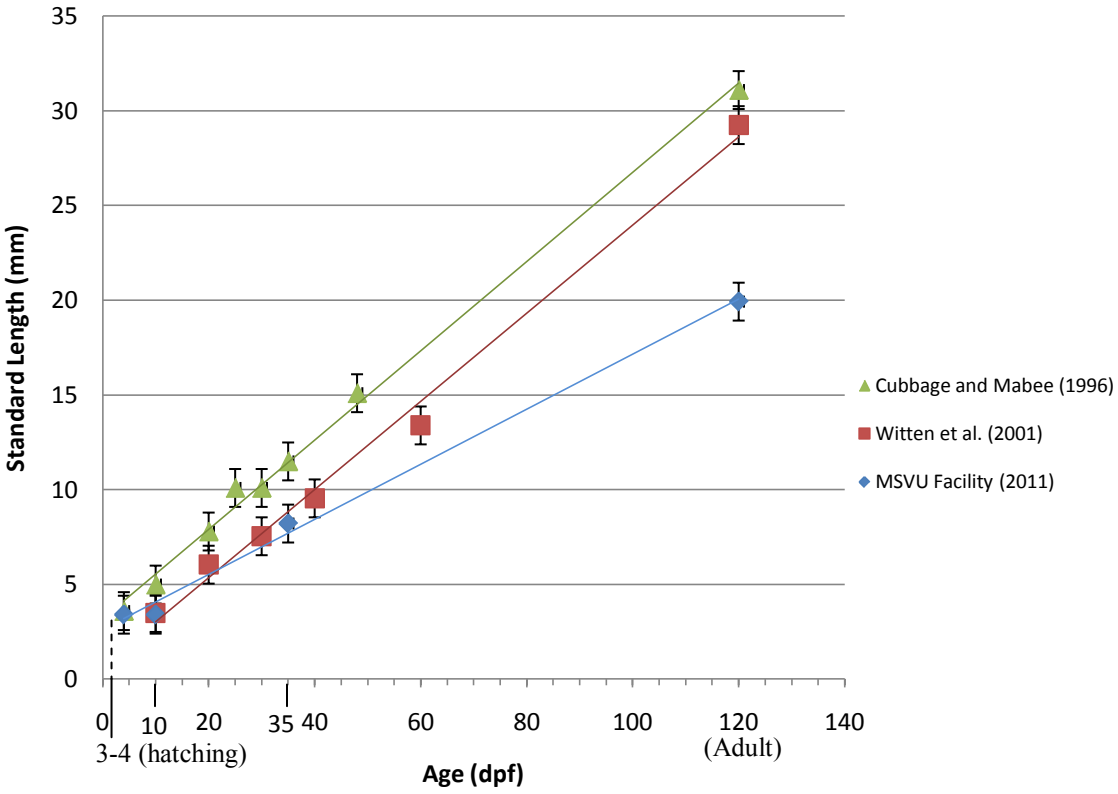

Figure 3.1: Growth rates of zebrafish raised under normal conditions in the fish facility at Mount Saint Vincent University, vs. fish lengths documented by Cubbage and Mabee (1996) and Witten et al. (2001). Trend lines illustrate a constant rate of growth throughout development.

The fish from all three facilities illustrated in Figure 3.1 demonstrate different hatching sizes and different growth rates, represented by their respective trend lines. The trend line for the fish in Cubbage and Mabee (1996) has an equation of y= 0.256x+ 2.564. Using this equation we know that when fish hatch (x= 4), they are approximately

3.6 mm SL and grow at a rate of 0.256 mm per day. The Witten et al. (2001) fish had a trend line with an equation of y= 0.2325x+ 0.7. Thus when fish hatch (x=4) they are approximately 1.63 mm SL; less than half the SL of the Cubbage and Mabee (1996) fish. The Witten et al. (2001) fish grow at a rate of 0.2325 mm per day; 0.0235 mm less than the Cubbage and Mabee (1996) fish. The MSVU Facility fish trend line has an equation of y= 0.145x+ 2.531. Using this equation, we calculate that at hatching (x= 4) fish are approximately 3.1 mm SL; 0.5 mm less than fish reared by Cubbage and Mabee (1996), but almost double the length of fish from Witten et al. (2001). In addition, the MSVU Facility fish grow at a rate of 0.145 mm per day. This growth rate is slower than both the Cubbage and Mabee (1996) and Witten et al. (2001) rates by 0.111 mm and 0.088 mm respectively.

The fish in Cubbage and Mabee (1996) are the largest at hatching (3.6 mm SL) and have the fastest growth rate (0.256 mm/day) compared to the Witten et al. (2001) and MSVU Facility fish (Figure 3.1). Witten et al. (2001) fish are almost half the length of Cubbage and Mabee (1996) and MSVU Facility fish at hatching (1.63 mm SL), but grow at a rate similar to the Cubbage and Mabee (1996) fish. MSVU fish are similar in length to the Cubbage and Mabee (1996) fish at hatching (3.1 mm SL), but grow at the slowest rate (0.145 mm/day). Though the rate of normal fish growth in our facility is lower than that observed by Cubbage and Mabee (1996) and Witten et al. (2001), it is the rate against which I compared the rate of growth of my experimental fish (Figure 3.2).

For this study, groups of fish were exposed to different durations of either simulated microgravity or vibrations starting at different developmental stages (Chapter 2.2). Fish were approximately the same size (SL) when added to either the bioreactor or the control vessel, and were then measured upon fixation at 4, 10, 35, and 120 dpf. The mean standard lengths were calculated and compared to the mean standard lengths of fish raised under normal conditions (Table 3.1; Figure 3.2). In addition, the SLs of the fish at hatching (4 dpf, or upon removal from the bioreactor for the 96h SMG and C+V at 10 hpf groups) were compared across all groups.

Table 3.1 Mean standard length of fish exposed to different environmental conditions, measured at 4, 10, 35, and 120 dpf. Conditions are:

a) Raised in normal conditions; no vibrations (CNV)
b) Exposure to vibrations for 12 hours starting at 10 hpf (12h C+V at 10 hpf)
c) Exposure to SMG for 12 hours starting at 10 hpf (12h SMG at 10 hpf)
d) Exposure to vibrations for 24 hours starting at 12 hpf (24h C+V at 12 hpf)
e) Exposure to SMG for 24 hours starting at 12 hpf (24h SMG at 12 hpf)
f) Exposure to vibrations for 96 hours starting at 10 hpf (96h C+V at 10 hpf)
g) Exposure to SMG for 96 hours starting at 10 hpf (96h SMG at 10 hpf)

Environment	Age (dpf)	Mean SL (mm)	Standard Error (mm)	n=	Trend line equation
CNV	4	3.41	± 0.16	9	y= 0.1453x+ 2.5314
	10	3.41	± 0.12	9	
	35	8.22	± 2.10	5	
	120	19.93	± 1.58	15	
12h C+V at 10 hpf	4	3.25	± 0.17	4	y= 0.1373x+ 2.5089
	10	3.68	± 0.26	5	
	120	19.00	n/a	1	
12h SMG at 10 hpf	4	3.28	± 0.22	8	y= 0.1091x+ 2.7328
	10	3.71	± 0.12	8	
	120	15.83	± 1.61	3	
24h C+V at 12 hpf	10	3.32	± 0.11	5	y= 0.119x+ 2.496
	35	7.13	± 1.67	15	
	120	16.67	± 1.63	6	
24h SMG at 12 hpf	10	3.22	± 0.16	5	y= 0.1055x+ 3.2433
	35	8.33	± 1.82	10	
	120	15.58	± 1.82	12	
96h C+V at 10 hpf	4	3.24	± 0.17	9	y= 0.1305x+ 2.6248
	10	3.40	± 0.18	4	
	35	7.75	± 0.78	11	
	120	18.17	± 1.41	12	
96h SMG at 10 hpf	4	3.32	± 0.13	13	y= 0.1434x+ 2.8172
	35	7.94	± 2.22	5	
	120	20.00	± 1.11	6	

3.2.2 Fish Exposed to Vibrations

The three different groups of fish exposed to vibrations (C+V; 12h at 10 hpf, 24h at 12 hpf, and 96h at 10 hpf) all have growth rates slightly lower than the fish raised under normal conditions (CNV; 0.1453 mm/day). Fish from the 12h C+V at 10 hpf group have a rate of 0.1373 mm/day; 0.008 mm less per day than the CNV rate (Table 3.1). Fish from the 24h C+V at 12 hpf group grow at a rate of 0.119 mm/day; 0.026 mm

less than the CNV rate. Fish from the 96h C+V at 10 hpf group grow at a rate of 0.1305 mm/day; 0.015 mm less than the CNV rate (Table 3.1). Of the three C+V groups, the 12h C+V at 10 hpf has the highest rate of growth, and the 24h C+V at 12 hpf has the lowest. The growth rates from all three C+V groups are within 0.03 mm/day of the CNV group rate of growth.

Similarly, the hatching size from each C+V group, calculated using their respective trend line equations (where x=4), differs only slightly from the CNV group (3.1 mm SL). Fish from the 12h C+V at 10 hpf group hatched at approximately 3.06 mm SL; 0.04 mm less than CNV fish (Table 3.1). Fish from the 24h C+V at 12 hpf group hatched at approximately 2.972 mm SL; 0.13 mm less than CNV fish at hatching. Fish from the 96h C+V at 10 hpf group hatched at approximately 3.15 mm SL; 0.05 mm larger than the CNV hatching size (Table 3.1). Of the three C+V groups, the 96h C+V at 10 hpf hatching length was the largest (3.15 mm) and the 24h C+V at 12 hpf was the smallest (2.972 mm; Table 3.1). Overall, the hatching SLs for all three C+V groups were within 0.13 mm of the CNV hatching SL.

In summary, the fish from the 24h C+V at 12 hpf have the slowest rate of growth and the smallest hatching SL of the three C+V groups compared to the CNV group. Fish from the 12h C+V at 10 hpf group have the highest rate of growth of the three C+V growths, and is closest to the CNV rate of growth. Fish from the 96h C+V at 10 hpf group have the largest hatching size of the three groups, and was closest to the hatching size of the CNV fish. Though differences exist between all three C+V groups, and between the C+V groups and the CNV group, the differences are minute, and thus the C+V groups are considered to be similar to the CNV group in both growth rate and hatching SL. This suggests that exposure to vibrations (C+V) does not greatly affect SL at hatching and overall growth rate. As a result, and for simplicity, the fish exposed to SMG will be compared to the fish from the CNV group for the remainder of the chapter.

3.2.3 Fish Exposed to SMG

The three groups of fish exposed to SMG (12h SMG at 10 hpf, 24h SMG at 12 hpf, and 96h SMG at 10 hpf) all have growth rates slower than the CNV rate (0.1453 mm/day). Fish from the 12h SMG at 10 hpf group have a growth rate of 0.1091 mm/day;

0.0362 mm/day less than the fish from the CNV group (Table 3.1). The 24h SMG at 12 hpf fish have a growth rate of 0.1055 mm/day; lower than both the 12h SMG at 10 hpf and CNV groups (0.0036 and 0.0398 mm/day respectively). Fish from the 96h SMG at 10 hpf group have a growth rate of 0.1434 mm/day; only 0.0019 mm/day less than the CNV growth rate, and greater than both the 12h SMG at 10 hpf and 24h SMG at 12 hpf growth rates (0.0343 and 0.0379 mm/day respectively; Table 3.1). The 12h SMG at 10 hpf and 24h SMG at 12 hpf are similar in growth rate (differ from each other by 0.0036 mm/day) and the 96h SMG at 10 hpf and CNV growth rates are similar (differ from each other by 0.0019 mm/day).

In contrast, whereas the growth rates of all SMG groups are lower than the CNV group, the approximate hatching size of each SMG group is larger than the CNV group. The hatching length for each SMG group was calculated from the trend line equation, where x= 4. The fish from the 12h SMG at 10 hpf group hatch at approximately 3.162 mm SL, and are thus 0.0692 mm larger than the CNV fish (Table 3.1). The fish from the 24h SMG at 12 hpf group hatch at approximately 3.6653 mm SL; 0.563 mm larger than the CNV group (Table 3.1). The 96h SMG at 10 hpf fish hatch at approximately 3.3908 mm SL; 0.2908 mm larger than the CNV group (Table 3.1). Of the three SMG groups, fish from the 12h SMG at 10 hpf hatch at the smallest SL and are most similar in SL compared to the CNV group. Fish from the 24h SMG at 12 hpf groups hatch at the largest SL overall.

In summary, the fish from the 12h SMG at 10 hpf group have the lowest hatching size, and the second lowest growth rate of all three SMG groups. The 24h SMG at 12 hpf fish are the largest at hatching, but have the smallest growth rate overall. The 96h SMG at 10 hpf fish hatch at a length that is about midway between the 24h SMG at 12 hpf hatching length and the CNV hatching length. The fish from the 96h SMG at 10 hpf group also have a growth rate that, of all three SMG groups, best resembles the CNV group.

3.2.4 Summary

The data suggests that exposure to vibrations for any period of time (12, 24, 96 hours) starting at either of the start points (10, 12 hpf) does not greatly affect the size of

the zebrafish at hatching, or their overall growth rates (Table 3.1; Figure 3.2). Fish from all C+V groups have hatching lengths smaller than those of the CNV and SMG groups. In contrast, the growth rates of fish from the C+V groups are generally larger than those of fish from the SMG groups, with the exception of the 96h SMG at 10 hpf group which has a growth rate that, of all groups (C+V and SMG alike), best resembles the CNV growth rate.

Overall, the largest hatching length was found in fish from the 24h SMG at 12 hpf group, suggesting that development is accelerated prior to hatching in this group, resulting in larger larval zebrafish. Despite the large hatching length, fish from this group had the lowest growth rate overall. Exposure to 24h SMG at 12 hpf may have accelerated growth of the embryos within the bioreactor, but upon hatching, resulted in a decreased growth rate when compared to all other groups. Thus, adults from this group are the smallest overall (Figure 3.2).

Compared to the 24h SMG at 12 hpf group, fish from the 12h SMG at 10 hpf group were more similar to the CNV group. The shorter exposure to SMG (12h) did not affect the size of the zebrafish at hatching compared to the hatching size of CNV fish, suggesting that the growth acceleration occurs after the 12^{th} hour of exposure (between the 12^{th} and 24^{th} hours). In addition, the growth rate, though lower than that of the CNV group, was not as low as the 24h SMG at 12 hpf growth rate. This suggests that the shorter exposure to SMG does not accelerate the growth of the embryos while they are in the bioreactor, but that the overall growth rate of this group is decreased compared to the CNV group, resulting in smaller adult SLs (Figure 3.2).

Fish from the 96h SMG at 10 hpf group hatch at a length that is midway between the length of the CNV fish and the length of the 24h SMG at 12 hpf (largest hatch length) fish. This indicates that growth acceleration is taking place during exposure, but not to the extent observed in the 24h SMG at 12 hpf group (again, perhaps only during the 12^{th} and 24^{th} hours of exposure). The 96h SMG at 10 hpf fish had the highest growth of all SMG and C+V fish; a growth rate that closely resembles the CNV rate. This indicates that the longer exposure time does not affect overall growth rate of the zebrafish, resulting in adults similar in size to the CNV adults (Figure 3.2).

Though there are differences in the hatching length of the fish when comparing all the groups, these differences are minute when considering the differences in the adult sizes, which vary greatly. This variation is a result of the varying growth rates. The effect of varying growth rates is most apparent in the 24h SMG at 12 hpf and 12h SMG at 10 hpf groups (Figure 3.2).

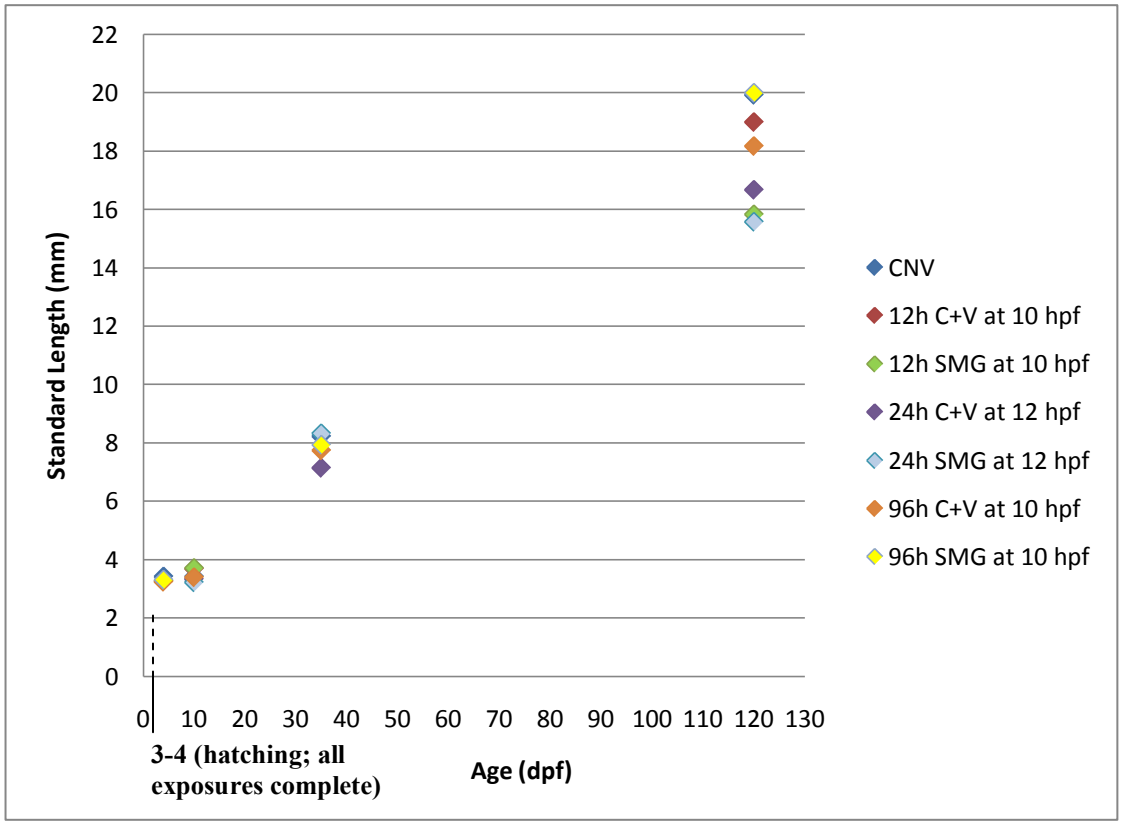

Figure 3.2: Mean standard lengths of fish exposed to different durations of either SMG or vibrations at 4, 10, 35, and 120 dpf, compared to the mean standard lengths of fish raised under normal conditions (CNV). For clarity, the seven trend lines and the standard error bars are not included in this figure.

3.3 Discussion

It appears that overall, the zebrafish raised by me under normal conditions in the Mount Saint Vincent University fish facility grow at a slower rate compared to Cubbage and Mabee, (1996) and Witten et al. (2001). It is possible that the strain of zebrafish I am using produces smaller adults in general. This information is critically important when analyzing the onset of ossification in the juvenile specimens documented in Chapter 7. It is also crucial to have this information because the skeletal data collected in Chapters 6

and 7 can now be easily compared to other published studies using SL references in addition to age.

Despite the slower rate of growth observed in my control fish (CNV) when compared to the two research groups, these fish have a faster rate of growth when compared to all fish exposed to either SMG or vibrations (C+V). The data indicate that exposure to vibrations affects neither the size of the zebrafish at hatching (4 dpf), nor ultimately their rate of growth, regardless of exposure duration or onset. Therefore, C+V fish are similar to CNV fish, and no effect is observed as a result of exposure to vibrations.

Despite the similarity between the C+V and SMG fish, differences exist between the SMG and CNV fish. The trend line equations for fish exposed to SMG suggest that exposure may accelerate growth of the embryos while in the bioreactor (between the 12^{th} and 24^{th} hour of exposure; larger sizes observed at hatching); however, no measurements are taken during exposure, so all that can be extrapolated is that 24h SMG at 12 hpf and 96h SMG at 10 hpf fish are larger at hatching. SMG growth rates after hatching (and after exposure) are ultimately lower than the CNV rates, resulting in smaller adult fish.

The SMG growth rates are lower than the CNV rates, with the exception of the 96h SMG at 10 hpf group of fish. These fish were second largest at 4 dpf and had the fastest rate of growth out of all the SMG and C+V fish. The 96h SMG at 10 hpf growth rate was the most similar to that of fish raised under normal conditions. This suggests that rate of growth may be higher while in the bioreactor, but that the fish from this group might be able to acclimatize to their environment within the 96 hours (4x longer than the 24h exposure). This possible acclimatization may be the reason why there is no overall change in their growth rate compared to the CNV group, which results in adults similar in size to the CNV adults. The large hatching size and low growth rate upon removal in the 24h SMG at 12 hpf group may be a result of the shorter exposure; the fish are not able to acclimatize, and thus their overall growth rate is lower.

In conclusion, exposure to vibrations does not affect the size of zebrafish at hatching (4 dpf), nor does it affect their overall growth rate. Exposure to SMG, however, results in zebrafish hatching at sizes larger than the hatching sizes of fish raised under

normal conditions. Furthermore, exposure to SMG appears to cause a decrease in overall growth rate, except when the embryos are exposed for 96 hours.

Chapter 4: Evaluating the Possible Effects of Stress

4.1 Brief Introduction

The bioreactor has been optimized to reduce shear stress present in the simulated microgravity environment (Moorman et al., 2002). It is possible, however that the flow of water in the bioreactor moves against the embryos, resulting in minor shearing forces acting on the fish (refer to Figure 1.4 in Chapter 1; Moorman et al., 2002). Shearing forces are a type of mechanical forces that act against the long-axis of the body (Reich et al., 1990). There are documented studies that have confirmed physiological responses to shearing stress in zebrafish (i.e. Reich et al., 1990; Yamomoto et al., 2005). It is therefore likely that embryos within the bioreactor will exhibit a stress response to these forces, if there is shear occurring in the bioreactor.

In response to environmental and mechanical stress in organisms, upregulation of heat shock proteins (HSPs) occurs (Sanders, 1993). Connolly and Hall (2008) determined that upregulation in response to heat shock occurred within the somitic boundaries in the zebrafish. In her doctoral dissertation (2008), Connolly showed that, in addition to abnormalities in the elements of the vertebral columns, there were significant changes in the number of vertebrae in adults who had been heat shocked as embryos. The variation in vertebrae number occurred primarily in fish exposed to the stressor during early stages of somitogenesis (10-16 hpf; Connolly, 2008; Kimmel et al., 1995).

In my thesis, embryos are exposed to either SMG or vibrations starting at 10 or 12 hpf, and enduring from 12-96 hours. These time points coincide with the key stages of somitogenesis that Connolly and Hall (2008) indicated were susceptible to (environmental) stress. Although in this thesis the stressors are mechanical, it is nevertheless still important to determine if shearing forces acting on the embryos result in a stress response so that I can eliminate stress as a confounding variable.

4.2 Results

In order to determine whether exposure to SMG and/or vibrations result in a similar stress response as reported by Connolly in her dissertation (2008),

immunohistochemistry was conducted to determine HSP90α levels in fish exposed to SMG. However, due to time constraints, the procedure could not be optimized, and thus a vertebral count of these fish as adults was conducted. This data is summarized in Table 4.1.

4.2.1 Precaudal Vertebrae

Connolly (2008) noted significant changes in the vertebral number in zebrafish heat shocked at the 12/13 somite stage (S; 15 hpf) and pec fin stage (60 hpf) when compared to her own control groups and to data published by Bird and Mabee (2003). Changes in vertebrae number were noted particularly in the caudal vertebrae (haemal arch-bearing vertebrae, excluding the caudal fin vertebrae), with the precaudal (rib-bearing) vertebrae displaying less variation in number (Connolly, 2008).

In my study, similar results were found when counting the precaudal vertebrae in fish exposed to SMG (Table 4.1). The natural range of precaudal vertebrae number is 9-11 (Bird and Mabee, 2003). The CNV group ranges from 10-11; however, only one of 15 fish has 11 precaudal vertebrae. Unfortunately, only one fish from the 12h C+V at 10 hpf group survived to adulthood; the precaudal vertebrae number for this fish falls within the natural range. Fish from the 12h SMG at 10 hpf group most frequently had 10 precaudal vertebrae; one individual had 12. The 24h C+V at 12 hpf and 24h SMG at 12 hpf groups both had fish with 10 precaudal vertebrae. Fish from the 96h C+V at 10 hpf group had precaudal vertebrae that ranged from 9-10 in number (only two individuals with 9 vertebrae). Fish from the 96h SMG at 10 hpf group had precaudal vertebrae that ranged from 10-12 in number (all but one individual had 10). The precaudal vertebrae appear to be robust (have little variation) with little to no variation in number. The majority of the individuals from all groups have precaudal vertebrae numbers within the natural range; only two individuals out of the overall 55 fish had 12 vertebrae and these may be outliers (Table 4.1).

In summary, most individuals have between 10 and 11 precaudal vertebrae. This falls within the published range of 9-11.

4.2.2 Caudal and Total Vertebrae

Connolly (2008) observed significant differences in the number of caudal vertebrae, and thus in the total number of vertebrae, in fish exposed to heat shock at 15 and 60 hpf. This data was compared to the data published by Bird and Mabee (2003). Bird and Mabee (2003) observed 15 caudal vertebrae (not including caudal fin vertebrae) in the zebrafish axial skeleton, but did not provide a range in this number. In my study, variation was observed in the number of caudal vertebrae (Table 4.1).

As a result of the caudal vertebrae variation, variation is also observed in the total number of vertebrae. The caudal vertebrae number ranges from 15-16 in the CNV group; the majority (10/15) of the fish have 15. The total vertebrae number thus varies from 25-27 (10 fish with 25, four fish with 26, and one fish with 27). The fish exposed to 12 hours of vibrations does not range in its' number of caudal vertebrae (14), or its' total vertebrae number (23) which are both below the numbers observed in the published literature. Fish from the 12h SMG at 10 hpf group are evenly distributed between having 13, 14, or 15 caudal vertebrae. The total vertebrae range in number from 24-25 only, with one individual displaying 24. Two individuals from the 24h C+V at 12 hpf group have 16 caudal vertebrae; these same two individuals have 26 total vertebrae. Three of the 24h SMG at 12 hpf fish have 16 caudal vertebrae (26 total), and two have 17 caudal vertebrae (27 total). Of the fish from the 96h C+V at 10 hpf group, five individuals have 16 vertebrae; only three have 26 total vertebrae. Fish from the 96h SMG at 10 hpf group were evenly distributed between having 14, 15, or 16 caudal vertebrae; one individual has 26 total vertebrae, and one individual has 28. The one individual with 28 total vertebrae had 12 precaudal and 16 caudal vertebrae; both of these values are outside the normal range observed in Bird and Mabee (2003), suggesting that this particular individual is an outlier.

In summary, variation occurs primarily in the number of caudal vertebrae for all experimental groups (except the 12h C+V at 10 hpf group) rather than in the number of precaudal vertebrae. The ranges are larger in the caudal vertebrae and there are more individuals displaying vertebrae numbers that differ from the published data. As a result, statistical analyses were conducted on the caudal vertebrae data, to determine if these variations are statistically significant.

Table 4.1: The modal number of vertebrae reported by Bird and Mabee (2003), MSVU fish raised in normal conditions (CNV), and MSVU fish exposed to 12, 24, or 96 hours of either vibrations (C+V) or SMG (Chapter 2). The range (minimum - maximum) of vertebrae is in parentheses.

Fish Treatment	Precaudal Vertebrae	Caudal Vertebrae*	Total Vertebrae**	n=
Data from Bird and Mabee (2003)	10 (9-11)	15	25	100
CNV	10 (10-11)	15 (15-16)	25 (25-27)	15
12h C+V at 10 hpf	9	14	23	1
12h SMG at 10 hpf	10 (10-12)	14*** (13-15)	25 (24-25)	3
24h C+V at 12 hpf	10	15 (15-16)	25 (25-26)	6
24h SMG at 12 hpf	10	15 (15-17)	25 (25-27)	12
96h C+V at 10 hpf	10 (9-10)	15 (15-16)	25 (25-26)	12
96h SMG at 10 hpf	10 (10-12)	15*** (15-16)	24, 25 (24-28)	6

*Number of caudal vertebrae, excluding the caudal fin vertebrae
**Total number of vertebrae, excluding the caudal fin vertebrae and the Weberian apparatus
*** Numbers represent the median for the group; the modal value was evenly distributed between three different numbers.

4.2.3 Statistical Analysis

Non-parametric statistics were conducted on the number of vertebrae for all fish used in this study, and shown in Table 4.1 (with the exception of the data for the single 12h C+V at 10 hpf fish). One-way ANOVA could not be conducted because the primary assumption, that the data is normally distributed, was not met. This was verified with Minitab (version 15.0) by determining that the shape displayed by a histogram of the residuals did not resemble a bell-curve and that the normal probability plot was not linear (not shown). As a result, two non-parametric tests were carried out: the Kruskal-Wallis, a one-way ANOVA of ranks, and the Mann-Whitney U test of significance. These tests were conducted on pairs of groups (listed under columns 1 and 2 in Tables 4.2 and 4.3), for both the caudal vertebrae and total vertebrae data (Tables 4.2 and 4.3 respectively).

These statistical tests show that overall there is no statistically significant difference between any of the groups when considering caudal vertebrae number (Table 4.2). The one exception is the comparison between the number of caudal vertebrae of the CNV group and the 12h SMG at 10 hpf group ($p = 0.038$). Connolly (2008) noted that the greatest difference in caudal vertebrae counts occurred in fish heat-shocked between 13 and 17 hpf ($p = 0.0018$); this coincides with the timing of the 12h SMG at 10 hpf exposure, which may explain why this group was the only group statistically different

from the CNV group (at the 5% level of significance). Connolly (2008), however, observed significant differences in fish heat shocked at other time points (in addition to the 13 and 17 hpf time points) compared to the control fish and published data, which is not the case in this study. The lack of statistical significance suggests that the caudal vertebrae number is not affected by exposure to either SMG or vibrations (C+V). The one exception (12h SMG at 10 hpf) may be an outlier, an effect of small sample numbers, or may be a result of the short exposure time.

Table 4.2: The p-values (significance) from the Kruskal-Wallis test (confirmed by Mann-Whitney U test) for comparisons of caudal vertebrae numbers between different groups (Group 1 vs. Group 2).

Caudal Vertebrae		
Group 1	**Group 2**	**p-value**
CNV	12h SMG at 10 hpf	0.038
CNV	24h SMG at 12 hpf	0.542
CNV	24h C+V at 12 hpf	1.000
24h C+V at 12 hpf	24h SMG at 12 hpf	0.640
CNV	96h SMG at 10 hpf	0.436
CNV	96h C+V at 10 hpf	0.714
96h C+V at 10 hpf	96h SMG at 10 hpf	0.349

No significant differences were observed in the number of total vertebrae when comparing different groups (Table 4.3). This is inconsistent with the observations made by Connolly (2008), who determined that total vertebrae number was statistically different in treatment groups compared to controls. This suggests that the total number of vertebrae is not affected by exposure to either SMG or vibrations (C+V).

Table 4.3: The p-values (significance) from the Kruskal-Wallis test (confirmed by Mann-Whitney U test) for comparisons of total vertebrae numbers between different groups (Group 1 vs. Group 2).

Total Vertebrae		
Group 1	**Group 2**	**p-value**
CNV	12h SMG at 10 hpf	0.374
CNV	24h SMG at 12 hpf	0.626
CNV	24h C+V at 12 hpf	0.938
24h C+V at 12 hpf	24h SMG at 12 hpf	0.640
CNV	96h SMG at 10 hpf	0.533
CNV	96h C+V at 10 hpf	0.661
96h C+V at 10 hpf	96h SMG at 10 hpf	0.673

In addition to differences in vertebrae number, Connolly (2008) noted skeletal defects present in the vertebral column. These include unfused arches, hemi-vertebrae, bifurcated ribs, and smaller-than-average centra in 28-71% of the heat-shocked fish. Similar skeletal defects were not observed in any of the groups exposed to either SMG or vibrations in this thesis.

4.3 Discussion

The purpose of analyzing the vertebral column in fish exposed to SMG and vibrations was to determine if shearing stress, a mechanical stress, might be a factor to consider when later analyzing the cranial skeleton (Chapters 6 and 7). HSP 90 (in addition to a variety of other heat-shock proteins) is known to be upregulated in zebrafish after exposure to either environmental or mechanical forces (Krone et al., 1997; Basu et al., 2002; Connolly, 2008; Connolly and Hall, 2008). Long-term effects of the upregulation of HSP90 propagate themselves in the vertebral column, resulting in a change in the number of vertebrae (Connolly, 2008). Connolly (2008) showed that heat shock, an environmental stressor, upregulates HSP90 levels, and that the upregulation in turn indirectly affects the number of caudal and total vertebrae. In my study, exposure to SMG and vibration, both mechanical stressors, did not yield significant differences in caudal and total vertebrae number overall. The count of vertebrae and their subsequent non-parametric statistical analyses revealed that, overall, there is no statistical difference between the number of vertebrae of fish exposed to SMG versus fish exposed only to vibrations (C+V) or fish raised under normal conditions (CNV).

One comparison did yield significant results however; the caudal vertebrae number of fish from the 12h SMG at 10 hpf group were statistically different than the caudal vertebrae of fish from the CNV group (p=0.038). This suggests that the shorter exposure to SMG might be more of a shock to the zebrafish unlike longer exposure times. This may be associated with the embryos not having enough time to acclimatize to their new environment within the bioreactor. It is also possible that the shock to the zebrafish results in effects that cannot be readjusted after removal, while being raised to adulthood.

Other HSPs have been investigated in the embryonic zebrafish, and in particular HSP70 (Sanders, 1993; Krone et al., 1997; Santacruz et al., 1997; Tawk et al., 2000; Basu

et al., 2002; Evans et al., 2005; Shimada and Moorman, 2006). Shimada and Moorman (2006) demonstrated that HSP70, a ubiquitous protein, is upregulated in the lens of zebrafish after exposure to SMG (24-48 hours of exposure starting as early as 6 hpf); however no phenotypic changes were observed in the lens or eye of the exposed embryos (Shimada and Moorman, 2006). Upregulation of the HSPs in general does not appear to have any documented long-term effects on cranial skeleton phenotype (e.g. Krone et al., 1997; Shimada and Moorman, 2006; Connolly and Hall, 2008).

If upregulation of HSP90 is occurring as a result of exposure to SMG, but has not manifested itself in changes to the vertebral column as seen in heat-shocked fish, it is possibly because a threshold has not been reached. This suggests that the fish are either only slightly stressed, or not stressed at all in the bioreactor. This is consistent with the bioreactor being optimized to reduce shear forces. If minor shear forces are present, they do not stress the embryos sufficiently to cause an upregulation of HSP90 that would lead to changes in vertebrae number. Therefore, the stress, in all likelihood, is not sufficient to affect the skeletal tissues examined in the remaining chapters of this thesis.

In summary, the HSPs can be upregulated by either environmental or mechanical stressors. Connolly (2008) determined that upregulation of HSP90 as a result of environmental stress acting on embryos indirectly caused variation in the caudal and total number of vertebrae of these fish upon reaching adulthood. Statistical analyses conducted on caudal and total vertebrae counts in adult fish exposed to either SMG or vibrations (mechanical stress) as embryos, determined that there are no effects overall. This suggests that the shearing (mechanical) forces of the fluid flow in the bioreactor do not cause a stress response in zebrafish, thereby eliminating stress as a factor contributing to abnormalities described in the following chapters.

Chapter 5: Analyzing Pigmentation Patterns

5.1 Brief Introduction

Cranial neural crest cells are capable of differentiating into a variety of different cells and tissues including, but not limited to, the glia of the autonomic nervous system, bones and cartilages of the cranial skeleton, cardiac tissues, and pigment cells (e.g. Hall, 1999, 2009). Of particular interest in zebrafish are the pigment cells; the yellow xanthophores, the iridescent iridophores, and the black melanophores. These three pigment cell types give rise to the larval pigment pattern and are all derived from cranial neural crest-cells (Quigley et al., 2004). The melanophores are the focus of this chapter.

The goal of this thesis is to determine the effects of SMG on cranial neural crest-derived tissues. To this end, analyses were conducted on the pigmentation pattern comprised of melanophores on the dorsal view of the larval zebrafish skull. Melanophores are an ideal pigment cell type to analyze as they are very easy to observe without staining.

5.2. Results

5.2.1 Melanophore Surface Area

As previously described in Chapter 2, only two groups were selected for pigment analyses: 96h C+V at 10 hpf and 96h SMG at 10 hpf (n= 24 each). Therefore, for the remainder of this chapter, the 96h C+V at 10 hpf group is referred to as the C+V group, and the 96h SMG at 10 hpf group is referred to as the SMG group. The average percentage of the dorsal view of the skull covered in melanophores was calculated for each group, each day, over the course of a week (Appendix 4), using measurements from individual fish. This experiment was conducted four times. The averages for each of the four experiments were combined as a single average for each day measurements were taken.

The data for the C+V group shows a decrease in the average dorsal surface area covered by melanophores over the course of a week. On Day 1 after exposure to vibrations, melanophores cover an average of 17.55% of the dorsal view of the C+V

skulls. This coverage decreases by 7.66% over a period of seven days, resulting in a final coverage of 9.89% on Day 7 (Figure 5.1), although this is not a significant decrease (p= 0.101). This suggests that a reduction in melanophore surface area occurs as the week progresses, or that there is either cell death or migration taking place, resulting in fewer melanophores.

Fish from the SMG group also showed a decrease in the average percent of the dorsal head covered in melanophores, although in this case the change from Day 1 to Day 7 was significant (p= 0.006; Figures 5.1 and 5.2). Melanophores covered, on average, 21.32% of the dorsal view of the skull on the Day 1 after exposure. This decreased by 10.11% over the course of a week, resulting in a final average coverage of 11.21% on Day 7 (Figure 5.1). This is a larger decrease than that observed in the C+V group (11.21% compared with 7.66%). This also suggests that either the melanophore surface areas are decreasing with each day after exposure, or that either cell death or migration is taking place, resulting in a lower number of melanophores. The standard error bars for the SMG group and the C+V group overlap every day except for Day 1 (Figure 5.1) suggesting that overall there is no significant difference between the two groups from Day 2-7.

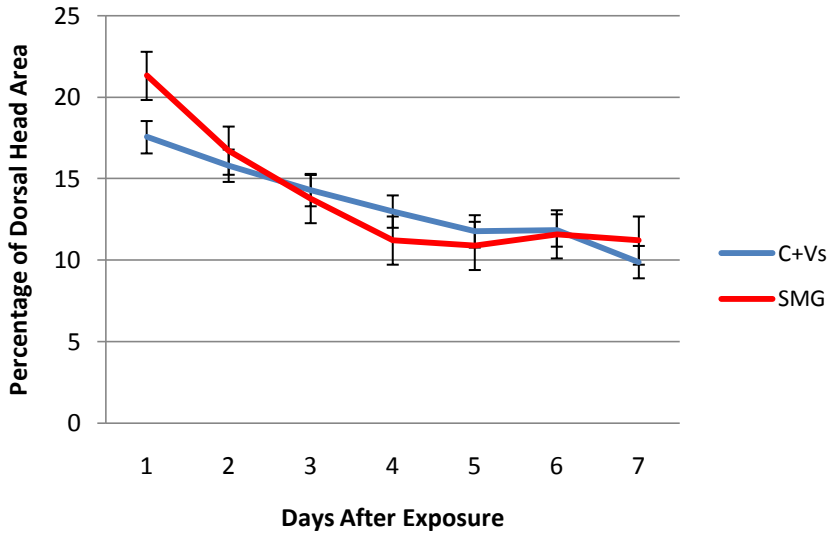

Figure 5.1: Average percentage of the dorsal skull area covered by melanophores for both C+V and SMG groups over the course of a week[1] (each data point represents 24 fish; six for each group, from four individual trials)

[1] Data are connected by lines to demonstrate the decreasing trend in the percentage of the surface area covered by melanophores.

Statistical analyses (below) were conducted on the data to determine if there are any statistically significant differences between the two groups, though the error bars suggest there is overall no significant difference between the two groups (overlap on every day but Day 1),. In addition, the two trend lines in Figure 5.1 appear to have three different slopes, one from Day 1 to 2, a second one from Day 3 to 5, and a third representing Days 6 and 7. Linear regression analyses (below) were conducted to determine if this was the case.

A one-way analysis of variance (ANOVA) comparing the average percentage of the dorsal skull covered by melanophores of the SMG and C+V groups confirmed that there was no significant difference between the two groups, $F(1, 12) = 0.04$, $p = 0.841$. In addition, although the standard error bars do not overlap on Day 1, a one-way ANOVA determined that there is no significant difference between the two groups on this day, $F(1, 46)= 1.54$, $p= 0.22$.

The trend lines in Figure 5.1 may have natural "breaks" in the slopes of the lines, with slight breaks occurring in both groups at Day 2 and again at around Days 5 and 6. As a result, a linear regression analysis was conducted on the trend lines of the data to determine if the data could be divided into three different slopes (Days 1-2, Days 3-5, and Days 6-7). The regression equation was determined (Equation 1) and was used to subsequently calculate the slopes of the three possible trend line sections for each group (SMG and C+V). This resulted in Equation 2 below.

$$\ln(y)= \beta_o+ \beta_1X_1+ \beta_2X_2+ \beta_3X_1X_2+ \beta_4(X_1-2)X_3+ \beta_5(X_1-5)X_4 \qquad \text{(EQ.1)}$$

The variables present in Equation 1 are as follows:

y= response variable (percentage of dorsal view covered with melanophores);

$\mathbf{X_1}$ = Day;

$\mathbf{X_2}$= 1, if SMG fish,

0, if Control fish;

$\mathbf{X_3}$= 1, if $2< X_1\leq 5$

0, if otherwise;

$\boldsymbol{\beta_4(X_1\text{-}2)X_3}$= Gives information about the data trend between Days 3-5.

$\boldsymbol{\beta_5(X_1\text{-}5)X_4}$= Gives information about the data trend from Day 6 to 7.

When both $\boldsymbol{\beta_4(X_1\text{-}2)X_3}$ and $\boldsymbol{\beta_5(X_1\text{-}5)X_4}$ are zero, the regression equation gives information about the data for Days 1 and 2.

The regression equation uses the natural logarithm of the response variable (y) in order to ensure that the regression assumptions are satisfied. More specifically, it ensures that the errors in the equation are normally distributed. Using the data for each individual fish from the four experiments, regression analyses, using Minitab (version 15.0), resulted in the following estimated values assigned to the β variables, yielding Equation 2. This equation describes the different slopes for the two trend lines in Figure 1.

$$\mathbf{ln(y)}= 2.89- 0.111\mathbf{X_1}+ 0.143\mathbf{X_2}- 0.0454\mathbf{X_1X_2}- 0.0041\mathbf{(X_1\text{-}2)X_3}+ 0.139\mathbf{(X_1\text{-}5)X_4} \quad \text{(EQ.2)}$$

Using Equation 2 and the variables as defined by Equation 1, we are able to test four hypotheses:

Hypothesis one: Does treatment (SMG or C+V) affect the percentage of the dorsal view of the skull covered with pigment? In other words, is there a significant difference between these two groups?

H_o: $\beta_2= 0$, $\beta_3= 0$

H_1: $\beta_2\neq 0$, $\beta_3= 0$; $\beta_2= 0$, $\beta_3\neq 0$; $\beta_2\neq 0$, $\beta_3\neq 0$

The null hypothesis (H_o) assumes that exposure, whether to SMG or vibrations, has no effect on the percentage of the surface area of the dorsal view covered with melanophores. According to the equation, the estimates of β_2 and β_3 are 0.1428 and 0.0454 respectively. The corresponding significance variables are $p= 0.239$ and $p= 0.115$ indicating that exposure to SMG or vibrations alone does not significantly affect the percentage of the dorsal view of the skull covered by melanophores. This suggests that the data for both groups can be represented by a single trend line and the alternative hypothesis (H_1) is therefore rejected.

Hypothesis two: Is there a break in the data at Day 2 that results in a different slope between Days 3 and 5?

H_o: $\beta_4 = 0$

H_1: $\beta_4 \neq 0$

The null hypothesis assumes that the data trend does not change at Day 2. According to the regression equation, the estimated β_4 value is -0.0041 and the corresponding p-value is $p = 0.943$, indicating that there is no significant change in the trend at Day 2. The alternative hypothesis is rejected again.

Hypothesis three: Is there a break in the data at Day 5 that results in a different slope between Days 6 and 7?

H_o: $\beta_5 = 0$

H_1: $\beta_5 \neq 0$

The null hypothesis assumes that the data trend does not change at Day 5. According to the regression analysis, the estimated β_5 value is 0.139, $p = 0.341$. This indicates that there is no significant change in the data trend at Day 5 and that the alternative hypothesis is rejected a third time.

Hypothesis four: Does the percentage of the dorsal view of the skull covered by melanophores depend on when during the week the measurement is taken (Day 1 vs. Day 6)?

H_o: $\beta_1 = 0$

H_1: $\beta_1 \neq 0$

The null hypothesis assumes that the day the measurement is taken does not affect the percentage of the dorsal view of the skull covered by melanophores. The estimated β_1 value, according to the regression equation, is -0.111. The p-value for β_1 is $p = 0.023$, indicating that the day the measurements are taken is significant at the 5% significance level. In this case, the null hypothesis (H_o) is rejected.

The linear regression model and the hypotheses show that there are no significant differences in the slopes of the trend lines from Days 1-2, Days 3-5, and Days 6-7, and

that both sets of data can be represented by a single trend line. The first three hypotheses were rejected, indicating that the data (either group) cannot be divided into three different sections of slope. The model accepts the fourth hypothesis, indicating that the only factor affecting the percentage of the dorsal view of the skull covered with melanophores is the day on which the measurement was taken. Therefore, all these statistics were conducted (including the one-way ANOVAs above), only to determine there are no statistical differences.

The difference between the melanophore coverage of the dorsal skull in the SMG group on Day 1 and Day 7 is illustrated in Figure 5.2. The larger surface area covered in 5.2 A appears to be a result of larger melanophores, whereas in B, the melanophores appear to be decreased in surface area. This observation lends to the hypothesis mentioned above that the overall decrease in the dorsal surface area of the head covered by melanophores is a result of decreasing melanophore surface area, and not a decrease in the number of individual melanophore cells. This can only be confirmed by conducting a count of the number of melanophores present within the dorsal region of the skull, which was conducted and is described in the next section.

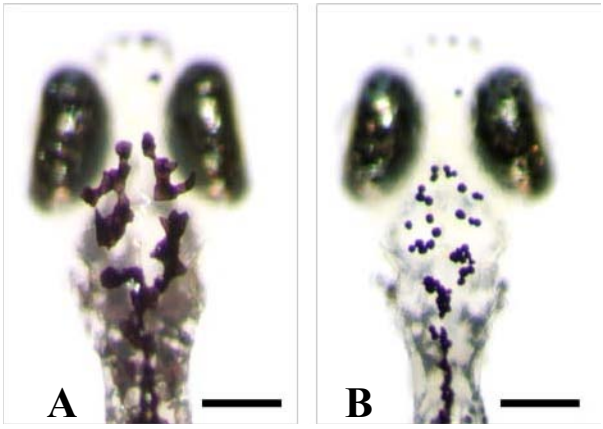

Figure 5.2: Comparison of the melanophore coverage on the dorsal view of the skull of a single fish on the first day after exposure (A) and the 7th day after exposure (B). Scale bars are 200 µm.

5.2.2 Melanophore Number

A count of the number of individual melanophore cells present on the dorsal view of the skull was conducted on individual fish from each group in the last two surface area experiments (n= 12 SMG fish; n=12 C+V fish). After dorsal view photographs were captured for surface area analysis (Section 5.2.1), fish were exposed to 2-3 drops of epinephrine which causes melanophores to instantly contract (see Chapter 2 for method).

The average number of melanophores in the dorsal view of the skull for each day after exposure was determined for both groups (SMG and C+V; Figure 5.3).

The average number of melanophores in the C+V group was 49.75 on Day 1. This number increased (not significantly, p=0.181) over the course of a week by 12.5, resulting in an average count of 62.25 melanophores on Day 7 (Figure 5.3). The overall increase in the number of melanophores, in addition to the decrease in surface area, suggests that as the cells increase in number throughout the week, they concurrently decrease in surface area.

Fish exposed to SMG also show an increase in the number of melanophores present in the dorsal view of the head over a week, although not a significant increase (p=0.186). On Day 1 the average number of melanophores on the dorsal view of the head was 40.58. This increased by 26.71 melanophores to yield an average number of 67.29 on Day 7 (Figure 5.3). This was more than double the increase observed in the C+V group. This suggests that the melanophores in the SMG group as well as the C+V group decrease in surface area, but increase in number as the week progresses.

The standard error bars in Figure 5.3 overlap on every day except for Day 1. This suggests that overall there is no significant differences between the two groups (again with the exception of Day 1). Regardless of this initial observation, statistical analyses were conducted.

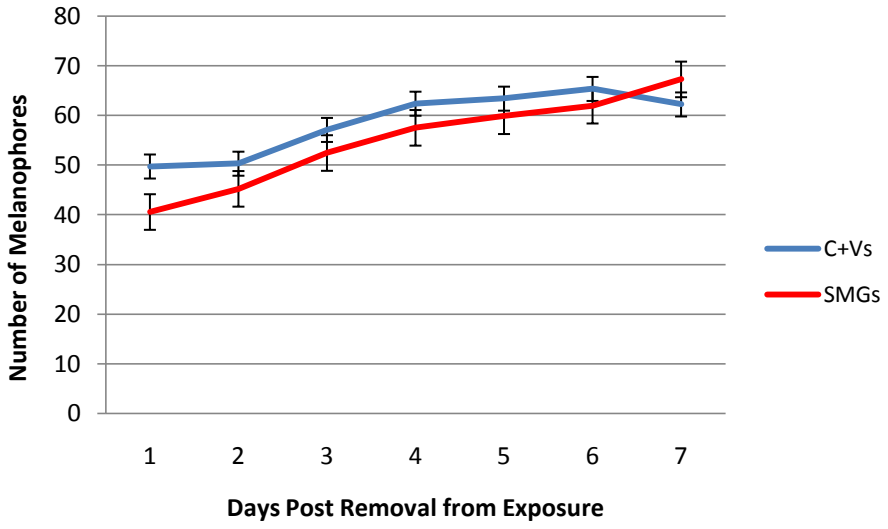

Figure 5.3: Average number of melanophores present on the dorsal view of the head in SMG and C+V groups over the period of a week.

One-way ANOVA conducted on the data from each group shows that there is no significant difference between the two groups overall, $F(1, 12)= 0.72$, $p= 0.414$, but that there is a statistically significant difference, to the 1% significance level, between the two groups on the first day after exposure, $F(1, 22)= 10.45$, $p= 0.004$. This significant difference on the first day suggests that the number of melanophores is affected by exposure to SMG immediately following exposure. The lack of statistically significant differences following the first day suggests that though the number of melanophores was affected initially, they are able to "catch up" to the C+V group from Day 2 after exposure onward.

5.2.3 Summary

Both groups demonstrate an overall decrease in melanophore surface area, and an overall increase in melanophore number, suggesting that melanophores are becoming smaller, and increasing in number as the week progresses. Both the decrease in surface area and the increase in melanophore number are greater in the SMG group than in the C+V group, suggesting that the initial surface area and number of melanophores after exposure may be more influenced by SMG than vibrations.

There is little to no difference between the two groups between Days 2 and 7 after exposure when considering both surface area and melanophore number, and overall there are no statistically significant differences. However, the data suggests that the differences between the two groups on Day 1 are larger than the slight differences between the two groups from Day 2 onward. This difference is statistically significant when considering only the number of melanophores, suggesting that melanophores in SMG fish are initially affected, but that they are able to recover and "catch up" to the C+V melanophores in both surface area and number by Day 7.

5.3 Discussion

Melanophores are a highly-dynamic population of melanin-containing cells (Rodionov et al., 1994; Yamaguchi et al., 2007) derived from neural crest (Kelsh et al.,

1996; Vaglia and Hall, 2000; Parichy et al., 2003; Kelsh, 2004; Quigley et al., 2004; Budi et al., 2008; Donoghue et al., 2008). In order to determine whether melanophores were affected by exposure to SMG, a comparison was conducted of both of the percentage of the dorsal view of the head covered with melanophores and the number of melanophores in the dorsal view of the head region between fish exposed to SMG and fish exposed to vibrations alone; each will be discussed separately.

5.3.1 Melanophore Surface Area

The surface area of the dorsal head covered by melanophores decreased over the course of a week in both groups. However, melanophores are capable of aggregating or dispersing their melanin in light and dark environments respectively. This ability to control their surface area in response to lighting may be the cause of the decrease observed. However, every measure was taken to ensure that lighting conditions were not a factor (e.g. consistent lighting conditions at time of analysis, proper orientation in glass-front incubator, etc.). Therefore, I do not think that lighting conditions are responsible for the observed decrease in melanophore surface area.

It is possible that the decrease in melanophore surface area over a period of a week is a natural occurrence. Though no published reports state this directly (e.g. Quigley et al., 2004; Parichy, 2007; Parichy et al., 2009), it is possible that decrease in pigment cell surface area is one way in which the larval melanophores prepare for upcoming metamorphosis, as metamorphic pigment cells have a smaller surface area than larval pigment cells. However, metamorphic pigment cells themselves do not start appearing until zebrafish have reached ~9 mm SL and metamorphosis does not take place until shortly after this. According to the trend line for growth of my MSVU fish in Chapter 3, metamorphosis will not occur until my fish have reached at least 23 dpf (~9 mm SL); almost two weeks after pigment analysis was conducted. For that reason, preparation for metamorphosis is highly unlikely to be the cause of the decrease in melanophore surface area. Published data confirms this by stating that the larval pigment pattern is fully established by 3 dpf, and remains constant for the next two weeks (Quigley et al., 2004). Therefore, some other factor, perhaps exposure to SMG, is affecting the surface area of the melanophores and could explain why the melanophores

in the SMG group, on the first day after exposure, had a greater surface area than those in the C+V group. It would also explain why the SMG group had an overall greater decrease in melanophore surface area than the C+V group.

5.3.2 Melanophore Number

An increase in the number of melanophores as zebrafish develop is natural (Quigley et al., 2004). As a result, the observed increase in melanophores over the course of a week after exposure (to SMG or vibrations) was not unexpected. However, as stated above, published data indicates that the larval pigment pattern is unchanging from 3 dpf to 17 dpf (Quigley et al., 2004). Therefore it is possible that some effect is taking place, especially when we consider that the SMG group, on the first day after exposure, had fewer melanophores than the C+V group, and ultimately gained more melanophores over the course of a week. Exposure to SMG may thus be playing a role in the increase in individual melanophore numbers.

5.3.3 Melanophore Surface Area and Number

When considering both melanophore surface area and melanophore number, there was a greater difference between the SMG and C+V groups on the first day after exposure than there was from Day 2 onward. This suggests, as mentioned above, that exposure to SMG may have an initial, transient effect on the melanophores. This effect (or perhaps these effects) is able to correct itself within 48 hours after removal (no significant difference between the two groups by Day 2 after exposure). The data suggests that exposure to SMG results in greater initial melanophore surface area, and a lower initial melanophore number than is observed in C+V fish.

The ability of the melanophores to adjust not only their melanin dispersal (surface area coverage), but the number of cells present on the dorsal view of the head in order to better resemble the phenotype observed in the C+V group suggests that there is a level of phenotypic plasticity at work within the population. These cells are able to adjust their surface area after being disrupted. In addition, they quickly increase in number after an initial lull. It may be that the melanophores have initially accommodated the change in their gravitational environment, which is indicated by the differences observed between

the two groups on the first day after exposure. Subsequently, the SMG melanophores seem to adjust and proceed with their normal development so that by Day 2, the surface area values and melanophore numbers in the SMG group approximate the data collected from the C+V group. This suggests that exposure to SMG does affect the cranial neural crest-derived melanophores, but that the effects are only present directly after exposure, and possibly during exposure (un-tested) and that exposure to SMG has no lasting effect on this pigment cell population.

Chapter 6: Analysis of the Adult Cranial Skeleton

6.1 Brief Introduction

The majority of the bones and cartilages in the cranial skeleton of zebrafish are cranial neural crest cell-derived (Schilling et al., 1996; Knight et al., 2004; Yu and Moens, 2005; Knight and Schilling, 2006) as in other vertebrates that have been studied (e.g. Gans and Northcutt, 1983; Couly et al., 1993; Hanken and Hall, 1993; Hall, 1999; Tobin et al., 2008; Hall, 2009). Therefore, to determine if exposure to SMG affects cranial neural crest-derived tissues, I examined the skulls of adult zebrafish that were exposed to either SMG or vibrations alone as embryos, and compared them to the adult skulls of individuals raised under normal conditions.

Fish were exposed to SMG or vibrations for 12, 24, 48, or 96 hours beginning at 10, 12, or 14 hpf (Table 2.1). Individuals were raised to adulthood, and then fixed and stained for bone.

6.1.1 Preliminary Data

Stress response observations (Chapter 4) suggested that the short exposure time (12h SMG at 10 hpf) was more of a shock to the zebrafish system. Initial observations of the cranial skeletons identified cranial abnormalities in this same group and in the 24h SMG at 12 hpf group. Fish from the 96h SMG at 10 hpf group did not exhibit any obvious cranial abnormalities, however this was the longest exposure time. These three sets of exposure time points were therefore investigated for adult cranial abnormalities and represent a "short" exposure (12h), a "medium" exposure (24h), and a "long" exposure (96h):

1) Exposure to SMG or vibrations for 12 hours beginning at 10 hpf (12h SMG at 10 hpf; 12h C+V at 10 hpf);

2) Exposure to SMG or vibrations for 24 hours beginning at 12 hpf (24h SMG at 12 hpf; 24h C+V at 12 hpf), and

3) Exposure to SMG or vibrations for 96 hours beginning at 10 hpf (96h SMG at 10 hpf; 96h C+V at 10 hpf).

6.2. Results

6.2.1 Left Lateral Adult Skull

6.2.1.1 Gross Morphology

There are no obvious morphological differences in the left lateral cranial view of fish belonging to the three C+V groups compared to the CNV group; for example, Figure 6.1 compares the 96h C+V at 10 hpf group to the CNV group. The shape of the skulls is similar, the SLs are similar (thus the size is similar), and there does not appear to be any major differences in the overall shape of individual bones (parasphenoid, operculum, frontals, parietals, orbitosphenoid). Therefore, for the remainder of this section, gross morphology comparisons are conducted between the SMG and CNV groups.

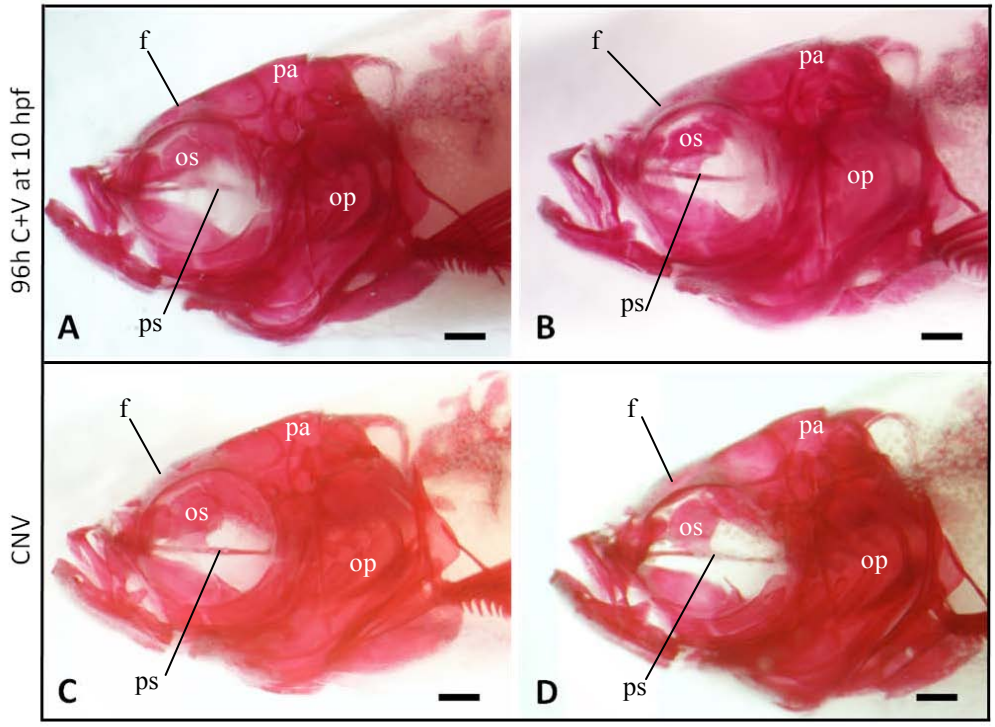

Figure 6.1. Left lateral cranial views of four bone-stained adult zebrafish.
(A, B) Representatives from the 96h C+V at 10 hpf group. (C, D) Representatives from the CNV group. A) 17.0 mm SL, B) 19.0 mm SL C) 20.0 mm SL, D) 19.0 mm SL.
f, frontals; op, operculum; os, orbitosphenoid; pa, parietal; ps, parasphenoid.
Scale bars are 500 μm.

The left lateral views of fish from the 96h SMG at 10 hpf group, like the C+V groups, greatly resemble the left lateral views of fish raised under normal conditions (Figure 6.2). There are no obvious differences in the shapes of the skulls when

comparing the 96h SMG at 10 hpf group to the CNV group, overall SL is similar (consistent with Chapter 3 results), and there are no obvious differences in individual bone morphology (e.g. parasphenoid, parietal, frontals, orbitosphenoid, and operculum). Thus the four representatives of the 96h SMG at 10 hpf groups skulls in Figure 6.2 greatly resemble the two CNV representatives in Figure 6.1. This suggests that 96h SMG at 10 hpf does not affect cranial morphology in the adult zebrafish.

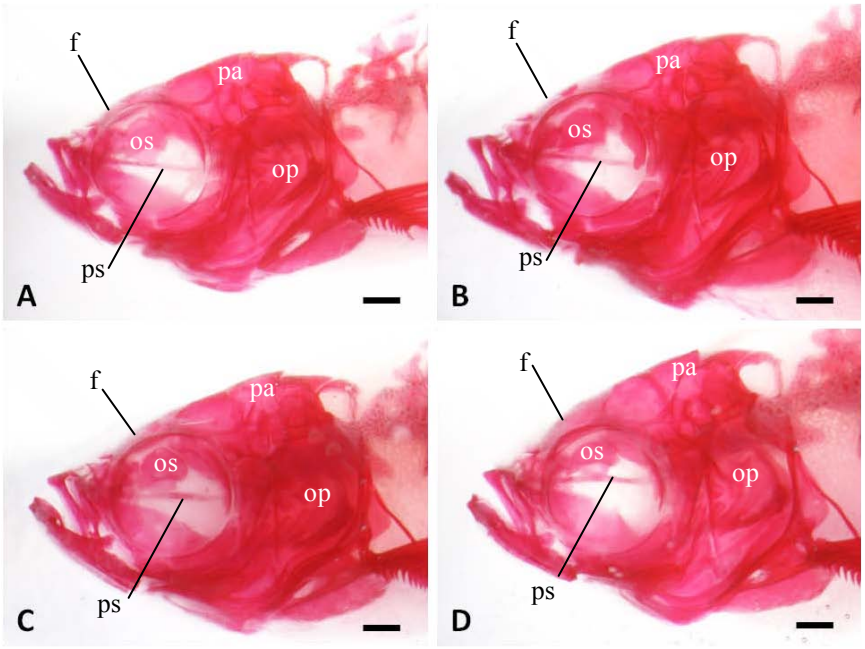

Figure 6.2: Left lateral views of the skulls of four bone-stained adult zebrafish that represent all the fish from the 96h SMG at 10 hpf group. A) 18.0 mm SL, B) 21.0 mm SL, C) 19 mm SL, D) 20.0 mm SL. f, frontals; op, operculum; os, orbitosphenoid; pa, parietal; ps, parasphenoid. Scale bars are 500 µm.

The lack of differences in left lateral skull morphology between the 96h SMG at 10 hpf group and the CNV is particularly obvious when considering the differences observed between the 24h SMG at 12 hpf group and the CNV group and the differences observed between the 12h SMG at 10 hpf and CNV groups (Figures 6.3, 6.4, and 6.5). The left lateral views of fish from the 24h SMG at 12 hpf group show variation in the shape of a few of the bones. Most notable were major changes to the parasphenoid, a mid-line bone which is between the eyes. The changes in parasphenoid morphology were categorized as mild, moderate, and severe (Figure 6.3). Slight thickenings of the parasphenoid ventral to its junction with the orbitosphenoid were classified as mild

morphological changes (Figure 6.3A). Buckles in the parasphenoid were classified as moderate morphological changes (Figure 6.3B). Buckles and holes in the parasphenoid were classified as severe morphological changes (Figure 6.3C). Three fish from the 24h SMG at 12 hpf group were chosen to represent each of the three parasphenoid categories in Figure 6.3.

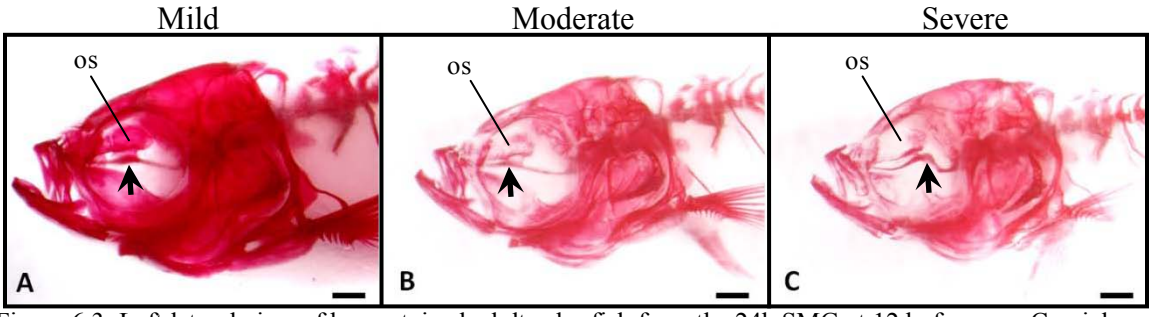

Figure 6.3: Left lateral view of bone-stained adult zebrafish from the 24h SMG at 12 hpf group. Cranial skeletal abnormalities ranged from mild in A (16.5 mm SL), to moderate in B (15 mm SL), to severe in C (14.5 mm SL). Especially noticeable were the changes in the morphology of the parasphenoid (black arrows). os, orbitosphenoid. Scale bars are 500 µm.

Four other representatives of the 24h SMG at 12 hpf group have abnormal parasphenoid morphologies (Figure 6.4). Enlarged images of the abnormal parasphenoids reveal holes in the posterior region of the parasphenoids (Figure 6.4B', C') thickening of the parasphenoids (Figure 6.4A', D') and buckling of the parasphenoids (Figure 6.4C', D'). Abnormal parasphenoids are present in 83% (10/12) of the specimens. Of the 83%, 70% (7/10) of the parasphenoids are classified as severe morphological changes.

In addition to abnormal parasphenoids, 24h SMG at 12 hpf fish showed delayed ossification of the orbitosphenoid (Figure 6.3 B and C), a general truncation of the skull evident by the rounding of the frontal and parietal bones, and variation in the size of the gap separating the supraoccipital and exoccipital bones compared to fish from the CNV group (e.g. Figure 6.4A, C, D, Figure 6.4C, D, and Figure 6.4A-D respectively). This suggests that exposure to 24h SMG affects the morphology of these particular bones. Further analyses are described in Section 6.2.1.2 below.

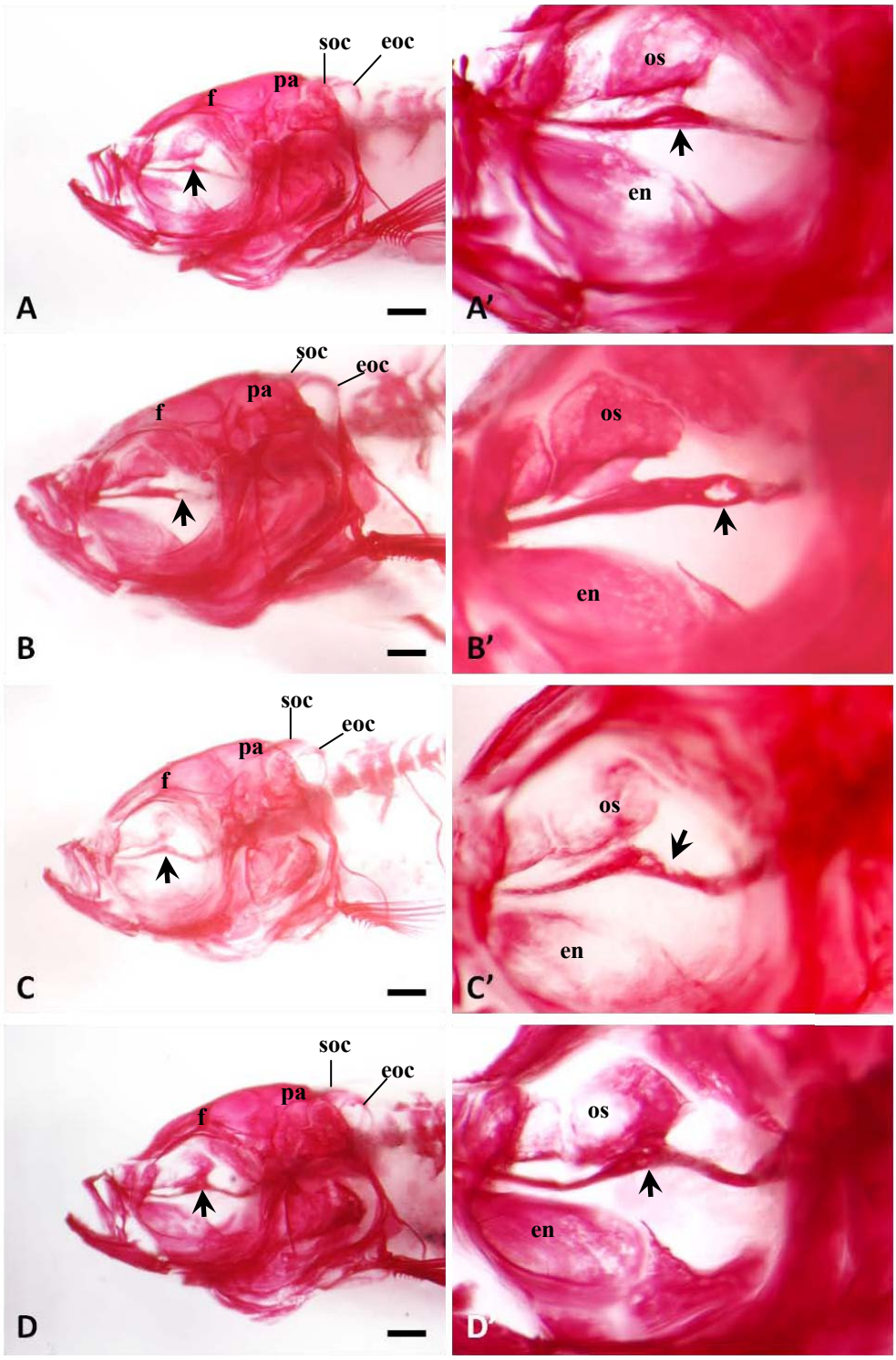

Figure 6.4: Bone-stained adult skulls of zebrafish from the 24h SMG at 12 hpf group. A' is magnified image of A; B' is magnified image of B; C' is magnified image of C; D' is magnified image of D. Left lateral views demonstrate parasphenoids (black arrows) with thickened regions (A, A', 14.0 mm SL), holes (B, B', 17.0 mm SL), buckling with holes (C, C', 15.0 mm SL), and buckling with thickened fusion to the orbitosphenoid (D, D', 14.0 mm SL). en, entopterygoid; eoc, exoccipital; f, frontal; os, orbitosphenoid; pa, parietal; soc, supraoccipital. Scale bars are 500 μm.

Fish from the 12h SMG at 10 hpf group demonstrate left lateral phenotypes similar to those seen in fish from the 24h SMG at 12 hpf group (Figure 6.5). Parasphenoids are either severely buckled or broken in all three of the specimens raised to adulthood (Figure 6.5). In addition to abnormal parasphenoids there is: a) variation in the size of the gap separating the supraoccipital and the exoccipital bones (Figure 6.5B and C); b) delayed ossification evident in the incompletely ossified orbitosphenoids and the opercula regions (Figure 6.5); c) skull truncation and thus rounding of the frontals and parietals in two out of the three specimens (Figure 6.5B and C).

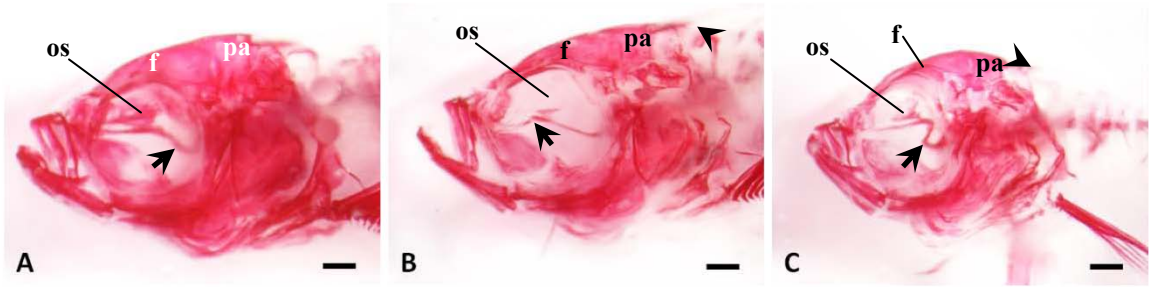

Figure 6.5: Left lateral views of the skulls of fish from the 12h SMG at 10 hpf group. Parasphenoids were greatly affected, which is evident in their buckling (A-C; black arrows). A) buckling in the posterior end of the parasphenoid; 17.0 mm SL. B) broken parasphenoid, and large gap between supra- and exoccipital (black arrowhead); 16.5 mm SL. C) Drastic buckling of the parasphenoid, rounding of the frontal and parietal bones, and fusion between the supra- and exoccipitals (black arrowhead); 14.0 mm SL. f, frontal; os, orbitosphenoid; op, operculum; pa, parietal.

In summary, fish from the C+V groups, and the 96h SMG at 10 hpf group do not display any noticeable morphological changes in the left lateral views of the skull compared to the CNV fish. This is surprising considering the long exposure time. Fish from the 24h SMG at 12 hpf and the 12h SMG at 10 hpf groups have the most significant changes in left lateral skull morphology compared to the skulls from the CNV group. Fish from these groups show striking differences in the morphology of the parasphenoid, the frontal and parietal bones, and the supra- and exoccipital bones. In addition, delayed ossification in the orbitosphenoid is observed (Figures 6.3, 6.4, and 6.5).

6.2.1.2 Morphometric Analysis

Morphometric analyses of the left lateral view of the adult skull of fish from the different exposure and control groups were conducted to statistically compare observed differences. It would be ideal to conduct morphometric analyses on the parasphenoid, the

bone displaying the highest amount of variation. However, this is technically challenging due to a lack of consistent anatomical reference points. The same is true for the left lateral view of the supra- and exoccipital bones. In addition, rounding of the frontals and parietals is a qualitative observation that is also difficult to quantify in lateral view. Because the parasphenoid morphology is so major, statistically proving that this is a significant change is not so critical to my evaluation of the effects of SMG on cranial neural crest-derived tissues. As a representative of an intramembranous cranial neural crest-derived bone, the operculum was selected for analyses of the left lateral view. Frontal and parietal bones are analyzed in the next section.

The location of the five anatomical reference points on the operculum of each specimen (Chapter 2, Appendix 2) were averaged to create a "consensus" morphology for the CNV group, and a consensus for each SMG and C+V group[2]. The vector plots are oriented the same way as shown in Figure 6.6 H. In Figure 6.6, each vector analysis (one analysis per box) compares the consensuses for two groups, with the reference (i.e. control) group indicated on the left hand side, and the experimental group indicated on the top. For example, Figure 6.6A compares the CNV consensus to the 96h C+V at 10 hpf consensus. The base of the arrows demonstrates where the reference landmarks are located, and the tip of the arrows shows where the same landmark from the experimental group is in comparison. Arrows indicate both the size and magnitude of the shift.

The vector analyses comparing the CNV group with the 96h C+V at 10 hpf group, the CNV group with the 96h SMG at 10 hpf group, and the 96h C+V at 10 hpf group with the 96h SMG at 10 hpf group all show very small changes in the location of most of the five landmarks. This suggests that neither 96h SMG at 10 hpf nor 96h C+V at 10 hpf affects the morphology of the operculum.

The vector plots comparing the CNV group with the 24h C+V at 12 hpf group, and the CNV group with the 24h SMG at 12 hpf group show changes in the morphology of the operculum for all landmarks. The arrows (vectors) are long and pointing towards the center of the plot (i.e. the center of the operculum), suggesting that the opercula of the 24h C+V at 12 hpf and 24h SMG at 12 hpf groups may be smaller in size than those of

[2] Morphometric analyses can only be conducted on groups with three or more individuals. For this reason a consensus could not be generated for the 12h C+V at 10 hpf group (n=1).

the CNV group. Direct observations, however, suggest that buckling/rippling of the opercula is occurring, resulting in a smaller surface area on the plot. The vector plot comparing the 24h C+V at 12 hpf group with its' SMG counterpart shows a similar inward (towards the center) shift of the landmarks. These vectors are not as long, however, suggesting that this shift is not as great as that observed when comparing either the 24h C+V or SMG at 10 hpf group to the CNV group.

The vector plot comparing the CNV group with the 12h SMG at 10 hpf group, shows a morphological change in the opercula of the SMG group. Long arrows pointing towards the center of the plot suggest that either smaller opercula are present in the 12h SMG at 10 hpf fish, or that buckling/rippling of the opercula is occurring causing a smaller 2D surface area. Statistical analyses were conducted on each set of comparisons in Figure 6.6 to determine whether the differences (if any) observed are statistically significant.

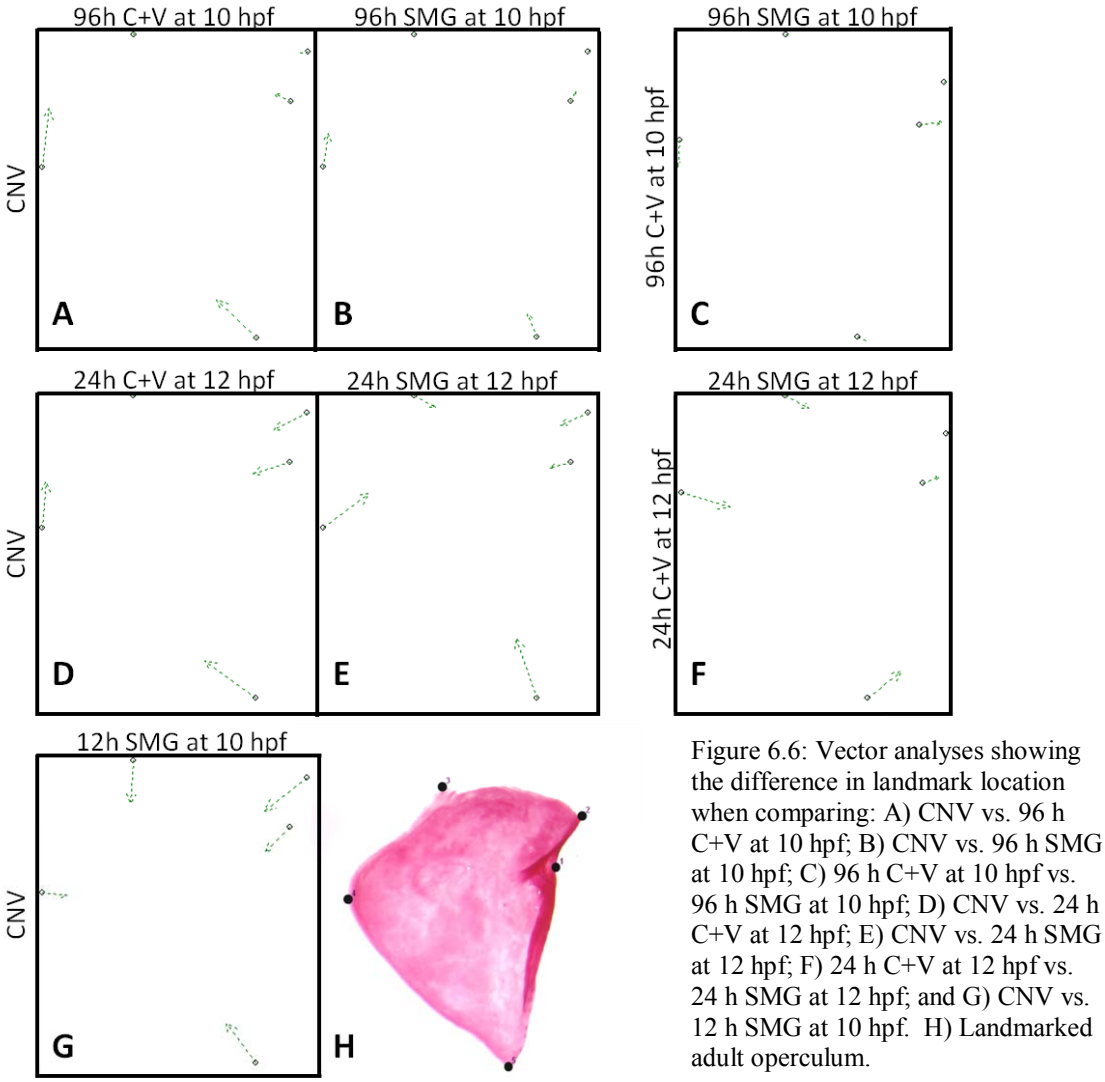

Figure 6.6: Vector analyses showing the difference in landmark location when comparing: A) CNV vs. 96 h C+V at 10 hpf; B) CNV vs. 96 h SMG at 10 hpf; C) 96 h C+V at 10 hpf vs. 96 h SMG at 10 hpf; D) CNV vs. 24 h C+V at 12 hpf; E) CNV vs. 24 h SMG at 12 hpf; F) 24 h C+V at 12 hpf vs. 24 h SMG at 12 hpf; and G) CNV vs. 12 h SMG at 10 hpf. H) Landmarked adult operculum.

Goodall's F-test (analogous to one-way ANOVA) was conducted on the pairs compared in the vector analyses (Table 6. 1). The analyses confirmed that there are no statistically significant differences ($p > 0.05$) between the opercula from the CNV group and the opercula of either the 96h SMG at 10 hpf or the 96h C+V at 10 hpf group. There are also no statistical differences between the opercula of the 96h SMG group at 10 hpf and the 96h C+V at 10 hpf group. This indicates that exposure to SMG, and vibrations alone, for 96 hours does not significantly affect the morphology of the operculum.

Table 6.1: Statistical analyses of the morphology of the bone-stained adult opercula.

Group 1	Group 2	Goodall's F-test	p-value	Significant
CNV	96hSMG at 10 hpf	0.86	0.52656	No
CNV	96hC+V at 10 hpf	1.89	0.0878	No
96hC+V at 10 hpf	96hSMG at 10 hpf	1.96	0.08166	No
CNV	24hSMG at 12 hpf	3.29	4.72E-03	Yes
CNV	24hC+V at 12 hpf	4.13	9.43E-04	Yes
24hC+V at 12 hpf	24hSMG at 12 hpf	0.80	0.57596	No
CNV	12hSMG at 10 hpf	2.20	0.05055	Yes

The statistical analyses, however, determined that there are highly significant differences between the opercula of the CNV group and the 24h SMG at 12 hpf group, and between the opercula of the CNV group and the 24h C+V at 12 hpf group ($p << 0.01$ for both). This indicates that both exposure to SMG and vibrations alone for 24 hours results in significant morphological variation in the opercula, unlike the 96h groups. When 24h SMG at 12 hpf and 24h C+V at 12 hpf are compared to each other, however, no significant differences are present. This indicates that the effects observed are a result of exposure to vibrations alone, and not a result of exposure to SMG.

Statistical analyses also determined that there is a significant difference (albeit less of a difference than above) between the opercula of the CNV group and the opercula of the 12h SMG at 10 hpf group ($p \approx 0.05$). This indicates that exposure to 12h SMG at 10 hpf has a small effect on operculum morphology, though it is unclear whether this effect is due to SMG or vibrations since I did not have enough samples in the C+V group.

6.2.2 Dorsal Adult Skull

6.2.2.1 Gross Morphology

Observations were made of the dorsal views of the adult skull. No obvious visible differences were detected when comparing the 12h C+V at 10 hpf, 24h C+V at 12

hpf, and 96h C+V at 10 hpf groups to the CNV group (not shown). Therefore, for the remainder of this section, the SMG groups will be compared to the CNV group (Figure 6.7).

The morphology of the dorsal view of fish from the 96h SMG at 10 hpf group greatly resembles the morphology of the CNV group (Figure 6.7A-F). Despite a difference in size, there are no obvious differences in the frontals and parietals, there is no observable delay in ossification (all bones are fully-formed), and adults from both groups are relatively the same size (consistent with Chapter 3 findings). This suggests that exposure to 96h SMG at 10 hpf does not affect the morphology of the dorsal view of the adult skull.

Fish from the 24h SMG at 12 hpf group show differences in skull morphology; skulls are narrower and truncated (consistent with smaller adult sizes reviewed in Chapter 3 results), with obvious changes in frontal and parietal bone morphology (Figure 6.7G-I). Additionally, there is delayed ossification (with very transparent frontals and parietals in these same specimens). These observations suggest that 24h SMG at 12 hpf affects the morphology of the dorsal bones of the skull.

Fish from the 12h SMG at 10 hpf group also show differences in morphology; skulls are either wider (Figure 6.7J) or narrower (Figure 6.8L) than CNV skulls, again with abnormal frontal and parietal morphology. In addition, there is delayed ossification (elements ventral to the frontal and parietal bones are visible through the bones) and skulls are overall smaller compared to CNV skulls (consistent with smaller adult sizes; Chapter 3). These gross observations suggest that exposure to 12h SMG at 10 hpf also affects the morphology of the dorsal bones of the skull.

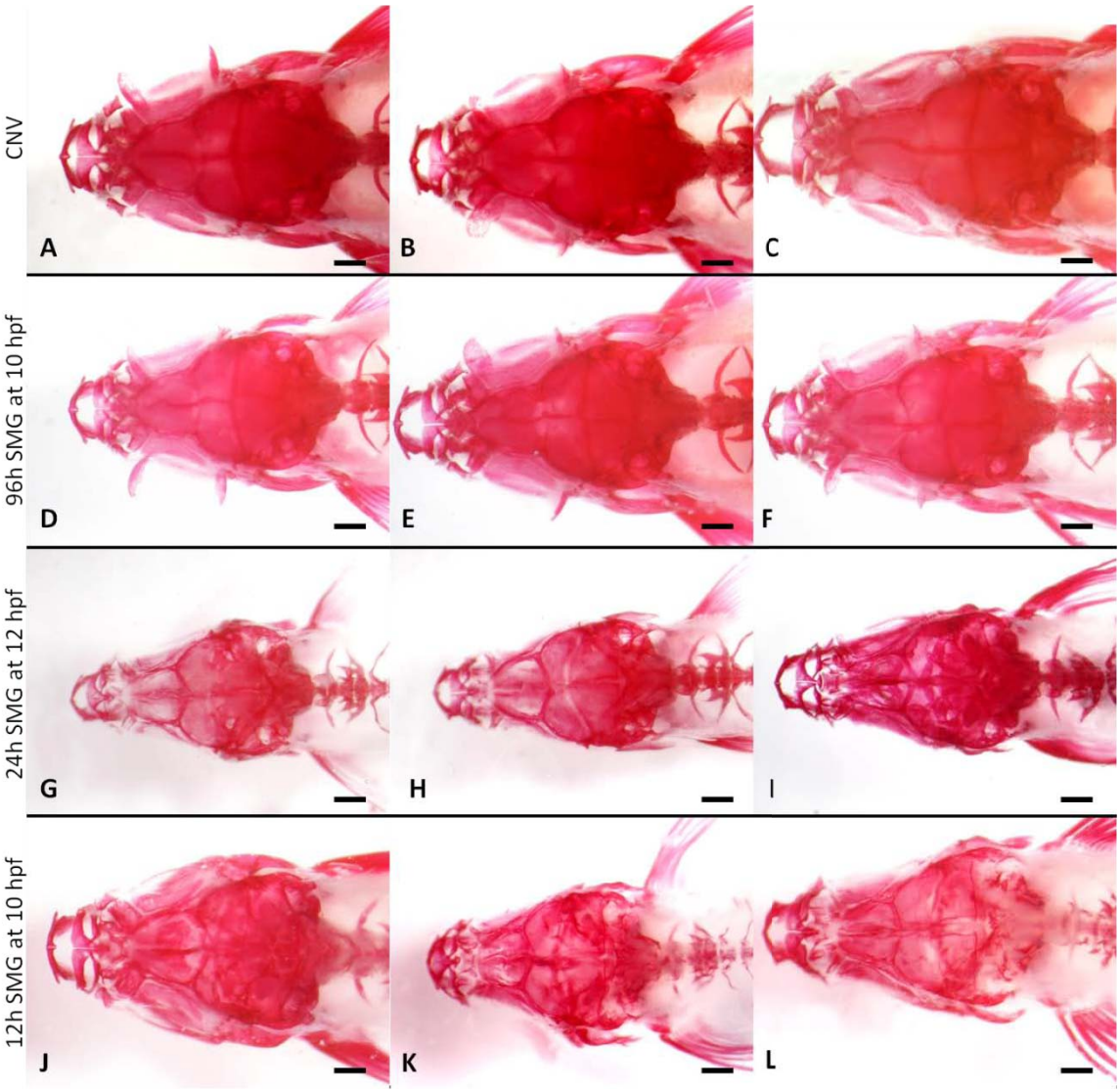

Figure 6.7: Dorsal views of the bone-stained adult skulls. A-C, are representatives of the CNV group measuring 19.0, 19.0, and 22.0 mm SL respectively; D-F, are representatives of the 96h SMG at 10 hpf group measuring 18.0, 21.0, and 19.0 mm SL respectively; G-I, are representatives of the 24h SMG at 12 hpf group measuring 14.5, 15.0, and 14.0 mm SL respectively; J-L, are representatives of the 12h SMG at 10 hpf group measuring 17.0, 14.0, and 16.5 mm SL respectively. Scale bars are 500 µm.

6.2.2.2 Morphometric Analysis

In order to determine if there were any quantitative changes to supplement the qualitative observations, morphometric analyses were conducted on the dorsal bones of the skull. Landmarks were assigned to 15 anatomical reference points and include the premaxilla, the kinethmoid, the frontals and parietals, and the basioccipital (Chapter 2; Appendix 2).

Thin-plate splines were generated in order to determine where the changes in morphology (if any) occur (Figure 6.8). Splines, like vector analyses, compare the consensuses of two groups. In Figure 6.8, the reference consensus for each spline is indicated on the left of the spline, and the experimental consensus is indicated above the spline. Landmarks are plotted on a grid and warping of the grid occurs when there is a difference in landmark location between the reference and experimental consensuses. The splines are orientated the same way as Figure 6.8H.

The thin plate splines show a slight warping in the anterior and lateral regions of all the splines, suggesting variation in the premaxilla, kinethmoid, and along the lateral edges of the frontals and parietals in all groups. The warping, however, is not drastic in any of the splines and there does not appear to be any changes in the posterior end of the dorsal part of the skull.

Statistical analyses (Goodall's F-test) were conducted on each set of comparisons in Figure 6.9 in order to determine whether or not the warping observed is statistically significant (Table 6.2). The analyses determined that statistically significant differences exist when comparing the 96h C+V at 10 hpf group to both the 96h SMG at 10 hpf and CNV groups ($p < 0.01$ for both; Figures 6.8A and C, respectively). The differences are also statistically significant when comparing both the 24h C+V at 12hpf and 24h SMG at 12 hpf groups to the CNV group ($p << 0.01$ and $p < 0.05$ respectively; Figures 6.8D and E, respectively), and when comparing the 12h SMG at 10 hpf group to the CNV group ($p < 0.05$; Figure 6.9G).

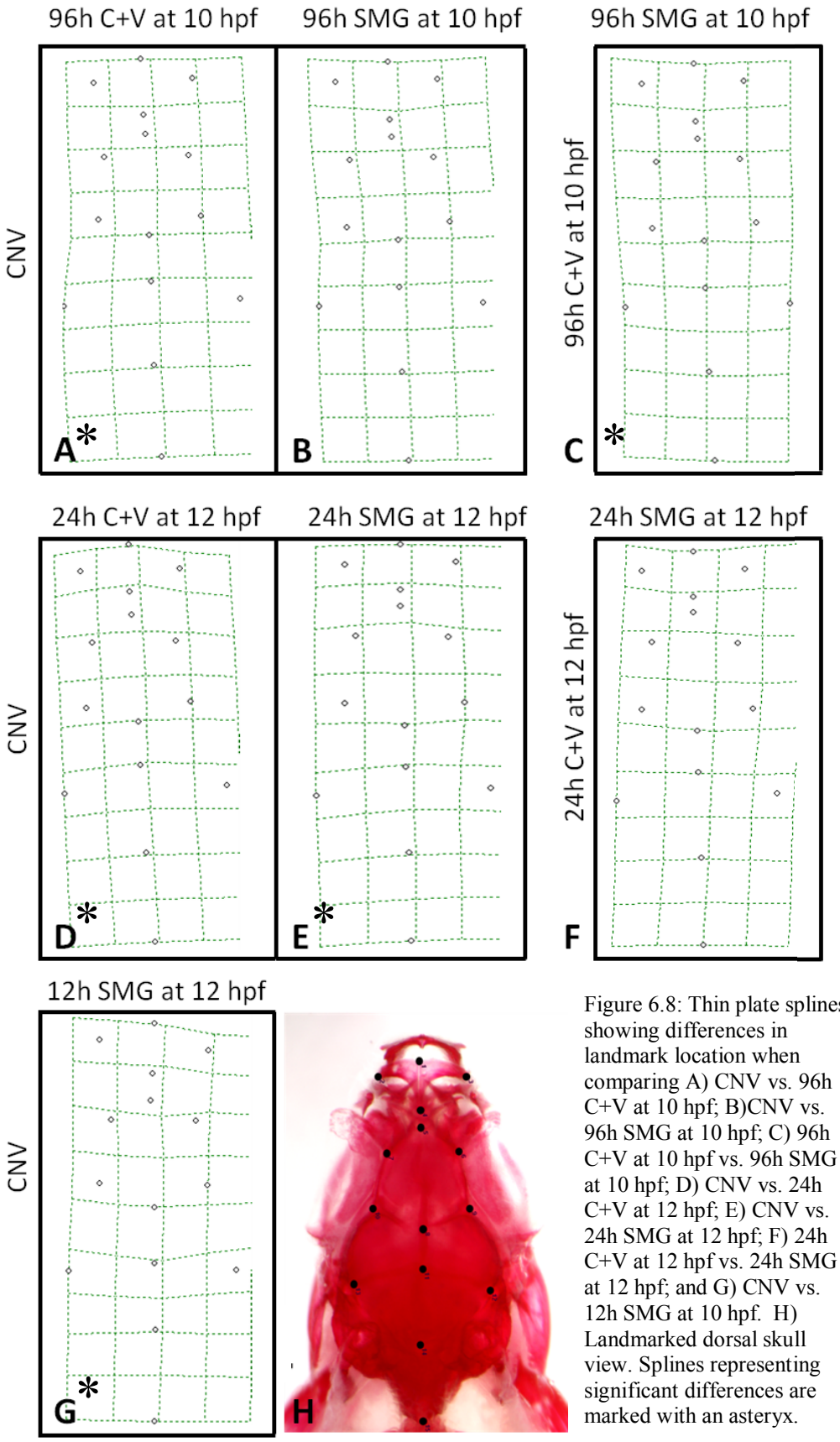

Figure 6.8: Thin plate splines showing differences in landmark location when comparing A) CNV vs. 96h C+V at 10 hpf; B)CNV vs. 96h SMG at 10 hpf; C) 96h C+V at 10 hpf vs. 96h SMG at 10 hpf; D) CNV vs. 24h C+V at 12 hpf; E) CNV vs. 24h SMG at 12 hpf; F) 24h C+V at 12 hpf vs. 24h SMG at 12 hpf; and G) CNV vs. 12h SMG at 10 hpf. H) Landmarked dorsal skull view. Splines representing significant differences are marked with an asteryx.

The statistical analyses results are strange in that they suggest overall that vibrations are responsible for the changes in morphology. The analyses conducted on the 96h C+V and SMG groups shows that the 96h SMG at 10 hpf data better resembles the CNV data, and that morphological differences were present primarily in the 96h C+V at 10 hpf group. This suggests that vibrations have a role, but that the vibrations did not affect the fish in the SMG group; it is possible that exposure to SMG cancelled out the effects of the vibrations.

The analyses conducted on the 24h C+V and SMG groups show that significant morphological differences are present in both groups when compared to the CNV group, but that the SMG and C+V groups do not differ from each other. This suggests that the vibrations are the source of the changes, and contrary to the 96h SMG at 10 hpf group, the SMG does not appear to cancel out the effects caused by vibrations. It is possible though that in the 24h SMG at 12hpf group, SMG has an effect on morphology on top of the effects caused by the vibrations, as the difference between the SMG and CNV groups was highly significant, while the difference between the C+V and CNV groups was less significant.

Table 6.2: Comparisons of the morphology of the dorsal view of the adult skull.

Group 1	Group 2	Goodall's F-test	P-value	Significant
CNV	96hSMG at 10 hpf	1.04	0.41394	No
CNV	96hC+V at 10 hpf	3.06	7.2043E-07	Yes
96hC+V at 10 hpf	96hSMG at 10 hpf	1.80	0.0099794	Yes
CNV	24hSMG at 10 hpf	4.06	1.4476E-10	Yes
CNV	24hC+V at 12 hpf	1.66	0.02307	Yes
24hC+V at 12 hpf	24hSMG at 10 hpf	1.40	0.093997	No
CNV	12hSMG at 10 hpf	1.61	0.031204	Yes

To ensure the data was completely accurate, I went back through the groups and examined every landmarked image looking for outliers; individuals that appear to be very

different from the others in their group. None were found. I decided to reduce the landmark data set and remove the landmarks from the basioccipital, premaxilla and kinethmoid, in case they were camouflaging changes in the frontals and parietals that were observed in the gross morphology in Sections 6.2.1 and 6.2.2 (Figure 6.9H; Appendix 2).

The thin-plate splines for this reduced dataset all have slight warping along the lateral edges, in the posterior region, and between the landmarks highlighted by the white square in Figure 6.10H. Although there is no severe warping, further analyses were conducted.

Statistical analyses (Goodall's F-test) were conducted on this reduced dataset and yielded slightly different results to the first analysis. Here, the 24h SMG at 12 hpf differs significantly from both the CNV and the 24h C+V at 12 hpf groups. This indicates that the 24h C+V at 12 hpf group is similar to the CNV group, and that exposure to 24 hours of SMG is responsible for the morphological changes observed in the frontals. The original analysis shows that the 12h SMG at 10 hpf group differs significantly from the CNV group. Interestingly, in the reduced dataset, this is no longer the case, indicating that the original effects observed were not in the frontal bones.

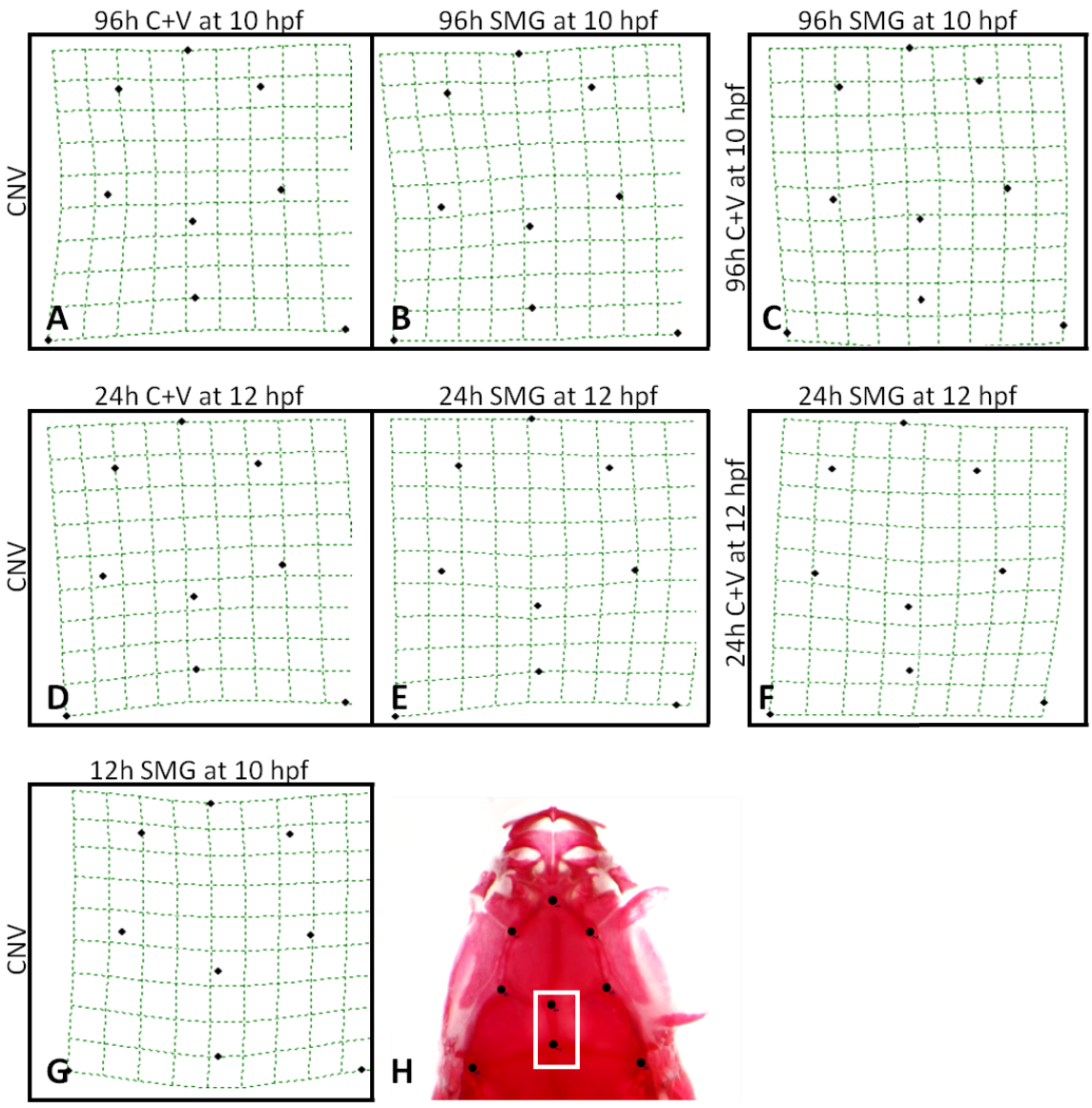

Figure 6.9: Thin plate splines showing differences in landmark location when comparing A) CNV vs. 96h C+V at 10 hpf; B) CNV vs. 96h SMG at 10 hpf; C) 96h C+V at 10 hpf vs. 96h SMG at 10 hpf; D) CNV vs. 24h C+V at 12 hpf; E) CNV vs. 24h SMG at 12 hpf; F) 24h C+V at 12 hpf vs. 24h SMG at 12 hpf; and G) CNV vs. 12h SMG at 10 hpf. H) Reduced dataset of nine landmarks with two landmarks (mid-point of overlapping frontals (top) and mid-point of the posterior-most edge of frontals (bottom)) within white square.

Table 6.3: Comparisons made of the revised adult dorsal skull morphometrics. Analysis conducted on the frontal bones in the dorsal view of adult cranial skeletons.

Group 1	Group 2	Goodall's F-test	P-value	Significant
CNV	96hSMG at 10 hpf	0.99	0.462	No
CNV	96hC+V at 10 hpf	4.29	5.10E-07	Yes
96hC+V at 10 hpf	96hSMG at 10 hpf	2.15	0.010484	Yes
CNV	24hSMG at 10 hpf	5.98	1.36E-10	Yes
CNV	24hC+V at 12 hpf	1.05	0.40271	No
24hC+V at 12 hpf	24hSMG at 10 hpf	1.94	2.38E-02	Yes
CNV	12hSMG at 10 hpf	1.38	0.16203	No

6.2.3 Summary

Overall, analysis of the adult cranial skeleton yielded a variety of results. The overall consistencies were that the group of fish exposed to 24 hours of SMG starting at 12 hpf was significantly different from the CNV group in all analyses conducted, and displayed mild to severe morphological abnormalities in several bones (parasphenoid, frontals, parietals, supra- and exoccipitals). In addition, fish exposed to 96 hours of SMG starting at 10 hpf were consistently not significant when compared to the CNV group in any of the analyses conducted.

6.3 Discussion

6.3.1 Left Lateral View Analyses

Gross observations of the left lateral view of the adult cranial skeleton revealed changes in the morphology of a variety of bones, in particular the parasphenoid. The parasphenoid is an endochondral/perichondral bone that attaches anteriorly to the vomer, posteriorly to the ethmoid, and dorsolaterally to the prootics (Cubbage and Mabee, 1996). There is, in addition, a small fusion dorsally with the orbitosphenoid. Interestingly, observations of the experimental fish with bent parasphenoids showed that the most

severe buckles occur towards the posterior end of the parasphenoid, away from its fusion to the orbitosphenoid. The orbitosphenoid is generally completely ossified when fish reach 8 mm SL; the observed delay in ossification may be a result of the slower growth rates observed in both groups (24h SMG at 12 hpf and 12h SMG at 10 hpf; Chapter 3) when compared to the onset of ossification. These groups were also the groups that showed abnormal parasphenoid morphologies.

There are few published studies documenting parasphenoid mutants. Often, abnormal parasphenoids occur as a result of changes in the size of the zebrafish skull due to mutation; however, researchers are more concerned with the effects the size change has on the jaw and branchial arches, as these elements are more vital to a properly functioning adult phenotype. Abnormal parasphenoids are present in an unresolved genetic mutant affecting the *tq235* allele described by Schilling et al. (1996), and a hammerhead mutant affecting the *ppt* gene described by Piotrowski et al. (1996). Neither mutant, however, displays a phenotype similar to the ones observed here (severe buckling, thickening, holes). This suggests that the changes observed in the morphology of the parasphenoid in this chapter are unique to fish that have been exposed to either 12 or 24 hours of SMG.

Less severe morphological changes were observed in the rounded shape of the dorsal skull bones (frontals and parietals) of a few specimens (Figures 6.3, 6.4, and 6.5), and in the smaller opercula sizes (Figure 6.7). In addition, delayed ossification was observed in the orbitosphenoid, particularly in specimens from the 24h SMG at 12 hpf and 12h SMG at 10 hpf groups (Figures 6.4 and 6.5 respectively).

Morphometric analyses conducted on the opercula from the different exposure groups demonstrated (with vector analysis and Goodall's F-test) that there was variation in the morphology of the opercula. The consensus for fish exposed to 24 hours SMG starting at 12 hpf compared to CNV fish is strongly significant. Vector analyses indicated a strong directional movement inward, indicating that either a smaller surface area is present, or buckling of the opercula is occurring, resulting in smaller 2D surface areas. The same inward shift in operculum landmarks was observed when comparing the consensus for fish exposed to 24 hours of vibrations starting at 12 hpf to the CNV consensus. However, the 24 hour SMG and 24 hour vibrations groups did not

significantly differ from each other. This result indicates that exposure (both to SMG and to vibrations alone) yields variation in the shape of the operculum, but that this variation is due to the vibrations, and not the simulated microgravity.

There are many published studies documenting changes in opercula morphology (e.g. Walker et al., 2007). In particular, Zugina et al. (2010) observed a decrease in opercula size in Jagged-Notch mutants, however the decrease only occurred in the width of the operculum, and not overall shape. The morphological change observed in this thesis was an overall decrease in opercula size from all edges. The operculum begins ossifying at 3 dpf, appearing as a small spur (Cubbage and Mabee, 1996; Kimmel et al., 2010). At 5 dpf, layers of bone are deposited at the base of the spur and resemble a veil (Kimmel et al., 2010). The only exposure groups that encompass any part of opercula ossification are the 96h SMG and C+V at 10 hpf groups. These groups, however, had the least amount of change in opercula morphology with no significant differences in size, and no observed buckling. The groups with significant differences, described above, were the shorter exposure times ending prior to the onset of opercula ossification. It is possible that the long exposure time is long enough for osteoblasts, CNC-derived cells responsible for depositing bone, to adapt to the different environment and proceed with normal deposition. It may be that the shorter exposure times are more of a shock, disrupting migration and/or proliferation of the osteoblasts, and possibly their ability to deposit bone. A smaller 2D surface area in general suggests that either a) fewer osteoblasts are present and less bone is deposited, or that b) osteoblast number is unaffected, but less deposition takes place. An alternative hypothesis based on observed buckling in the opercula in these SMG exposures is that, or c) the natural number of osteoblasts is present, and the normal amount of bone is deposited, but it is laid down incorrectly, resulting in buckling of the bone, which is not detected by geometric morphometrics and yields a smaller 2D surface area. Direct observations suggest that buckling of the opercula is occurring, which supports the hypothesis that the natural number of osteoblasts is present, and that bone is incorrectly laid down. Interestingly, vector analyses indicate that changes in opercula morphology occur in regions that ossify later, and the spur, the first to ossify, remains relatively unchanged.

6.3.2 Dorsal View Analyses

Dorsal view observations of the zebrafish cranial skeleton also showed changes in the skull. Delayed ossification was obvious in the dorsal view of the same fish in which it was observed in the left-lateral view (24 hour SMG and 12 hour SMG fish; Figure 6.8). Changes in morphology were not obvious; however, morphometric analyses determined that there are significant differences. The initial analysis of the dorsal skull (15 landmarks) was determined to be inaccurate (high variation in anterior elements camouflaging changes in frontal morphology) and thus analysis of the frontals alone (9 landmarks) was conducted. This reduced dataset determined that changes in morphology in fish from the long exposure groups (96h SMG at 10 hpf and 96h C+V at 10 hpf) is a result of vibrations. Contrary to this, changes in morphology observed in fish from the medium-length exposure groups (24h SMG at 12 hpf and 24h C+V at 12 hpf) are a result of simulated microgravity. The dorsal view morphology of fish from the short length exposure (12h SMG at 10 hpf) group were not affected by SMG.

There are very few known frontal or parietal mutant zebrafish. This is likely because these bones are part of the neurocranium and protect the brain. Phenotypic plasticity is responsible for ensuring the protection of the brain, preventing abnormal morphologies in these bones that may be fatal.

6.3.3 Overall Discussion

The initial observations of the gross anatomy of the cranial skeleton in adult zebrafish subjected to a variety of different SMG and vibration exposures as embryos indicate that there are skeletal abnormalities present when compared to CNV fish. These abnormalities are prominent in the parasphenoid and slightly in the operculum and frontal bones.

Fish from the 12 hour SMG group display severe changes in parasphenoid morphology, and yet do not differ significantly from the CNV group when the frontals are analyzed alone using morphometrics. The gross observations suggest that the short-term exposure to SMG has a large effect on morphology. However, without a substantial C+V group, morphometric analyses remain inconclusive.

Fish from the 24 hour SMG group, however, display significant changes in both left-lateral and dorsal view morphologies. The issue with this group, however, is that the morphometric analyses indicate that they do not differ significantly from their C+V counterpart, except when only considering the frontals. This indicates that the vibrations are the source of change, but that perhaps (when analyzing just the frontals) SMG causes effects in addition to the effects caused by exposure to vibrations.

According to a fate map generated using sox10 EGFP transgenic zebrafish, the kinethmoid, the supra- and exoccipitals, the parietals, the posterior half of the frontals, and the parasphenoid are mesoderm-derived bones. All other bones in the cranial skeleton are cranial neural crest-derived (Fisher and Franz-Odendaal, pers. comm). By referring to this fate map (Figure 1.13 Chapter 1), I determined that the majority of the bones in which morphological variation was observed throughout this chapter are not cranial neural crest-derived, but mesoderm-derived. Interestingly, the frontals have a dual origin; the anterior half of the frontals are cranial neural crest-derived, and the posterior half of the frontals are mesoderm-derived. Analyses, however, did not indicate whether the changes observed were in the anterior or posterior half of the frontals. The morphometric analyses conducted on the reduced set of frontal landmarks did not pinpoint where in the frontals the changes were occurring. Warping occurred primarily between the two halves. The goal of this thesis is to determine the effects of exposure to SMG on cranial neural crest-derived tissues, including the bones in the skull. The initial conclusion thus, is that neither exposure to SMG nor vibrations alone has affected cranial neural crest-derived bones in the adult. The most severe changes are present in the parasphenoid, a mesoderm-derived bone. There are two points to consider, however, before concluding that exposure to SMG has a major effect on mesoderm-derived bones in the skull.

The first point is that there are two sets of muscles originating at the parasphenoid, the adductor arcus palatini, and the adductor hyomandibula (Diogo et al., 2008). These muscles both insert at the medial sides of the hyomandibula, the adductor arcus palatini also inserting at the metapterygoid and entopterygoid (Diogo et al., 2008). This is relevant because the effects of microgravity and SMG on muscle in general are well documented (Hikida et al., 1989; Baldwin et al., 1990; Adams et al., 2000; Inobe et

al, 2002). The majority of these cases, however, study the effects on skeletal muscle in the calves of neonatal and adult rats (Baldwin et al., 1990; Adams et al., 2000; Inobe et al., 2002) and adult humans (Hikida et al., 1989) and it is established that exposure to microgravity results in loss of muscle mass in vertebrates (though no published studies describe effects of SMG on zebrafish muscle). In addition, the majority of the bones in the vertebrate skull are cranial neural crest-derived, as are the tendons and ligaments joining the mesoderm-derived muscles to the bones (Grenier et al., 2009). It has been demonstrated that there is a high level of interaction between the neural crest cells and the myogenic mesoderm (Grenier et al., 2009). Therefore, it is possible that exposure to SMG affects the integrity of the skeletal muscles in the skull directly, or indirectly by affecting the neural crest, which in turn affects the mesoderm-derived muscles through neural crest-mesodermal interactions. In particular, the muscles attaching to the parasphenoid may be affected. The abnormal shape of the parasphenoid in the adult specimens may be a result of changes in associated skeletal muscles, thus, this is a potential cause for the variation observed in the parasphenoid. In summary, it is possible that exposure to SMG affects the mesoderm derived skeletal muscle which translates into changes in the shape of this mesoderm-derived bone.

The second point to consider is that the parasphenoid is fused tothe orbitosphenoid, and the orbitosphenoid to the anterior half of the frontals (Cubbage and Mabee, 1996). The anterior half of the frontals are cranial neural crest-derived, while the posterior half of the frontals are mesoderm-derived (Fisher and Franz-Odendaal, pers. comm.). Cranial neural crest cells are documented to be highly plastic; they are capable of adapting to changes in their environment, resulting in an adapted adult phenotype (Anderson, 1997; Schilling et al., 2001; Yelick and Schilling, 2002). This is true for the skeletogenic cranial neural crest cells in zebrafish (Schilling et al., 2001). Schilling et al. (2001) determined using transplantation techniques, that cranial neural crest cells transplanted from one region to another would pattern the pharyngeal arches associated with the new region, and not the original one. With this in mind, it is possible that although the cranial neural crest-derived bones do not exhibit severe changes in morphology, the plasticity of cranial neural crest cells results in the formation of a relatively normal adult phenotype in bones derived from these cells. Furthermore, it is

also possible that changes exist in these elements early on in development, but that these changes are propagated through other bones. It may be that changes that started out in cranial neural crest-derived bones manifest in the adults as changes in other elements, such as the parasphenoid, that do not greatly affect the functionality of the developing zebrafish; a buckle in the parasphenoid is not as damaging as a buckle in the frontals. The potential for initial abnormalities in the frontals being manifested as abnormalities in the parasphenoid is supported by the fact that a SMG group presented here (24h SMG at 12 hpf) demonstrates slightly abnormal frontal morphology in the adult. This abnormal morphology may be evidence of a more severe morphology that may have been present in the frontals of juveniles (which is examined in Chapter 7).

These two points provide potential explanations for why the majority of the morphological changes in exposed fish are observed in the parasphenoid, a mesoderm-derived bone. The first point could be tested by conducting immunohistochemistry for skeletal muscle and analyzing the form and integrity of the muscles originating at the parasphenoid. If differences in the size and shape of the muscles attaching to the parasphenoid are present, it is likely that the changes in parasphenoid morphology are a result of this, rather than of direct effects from SMG.

Regardless of where the effects initially occur, or where they are propagated, the results presented in this chapter suggest that exposure to either SMG or vibrations alone result in changes in the morphology of various bones in the zebrafish cranial skeleton. This is particularly true for fish from the 24h SMG at 12 hpf and 24h C+V at 12 hpf groups, suggesting the medium-length exposure has the greatest effect. This information is important because it suggests that the C+V groups do not always best resemble the CNV group; that vibrations play a greater role than was originally thought. It also suggests that one particular exposure duration (24h) has overall a greater effect on morphology than the other durations (in particular the 96h), and that surprisingly, the shortest duration (12h) has a great effect on particular elements (e.g. parasphenoid).

Chapter 7: Juvenile Skeleton

7.1 Brief Introduction

The second point discussed in Section 6.3.3 (hypothesis that initial effects are present in cranial neural crest-derived bones in juvenile specimens, but cranial neural crest cell plasticity results in normal adult phenotypes in these bones) is tested in this chapter. Examining the cranial skeleton at various larval/juvenile ages in exposed fish will determine the morphology of the cranial neural crest- and mesoderm-derived bones. My hypothesis: if the parasphenoid is buckled at these stages, then SMG likely directly affects the parasphenoid (assuming the muscles do not play a role). If the parasphenoid is not buckled or bent at the earlier stages, the effects are likely indirect, originating elsewhere such as in the skeletal muscle or in cranial neural crest-derived bones (e.g. frontals and parietals), and propagating themselves through the parasphenoid upon reaching adulthood. An effect originating in the frontals or parietals would be confirmed if juvenile phenotypes display abnormal frontal/parietal morphologies.

Severe abnormalities were observed in the parasphenoid, a mesoderm-derived bone, and more minor effects in the frontal bones, a dual-origin bone, of fish exposed to SMG. In order to determine if this is a result of initial effects of SMG on cranial neural crest-derived bones, larval/juvenile fish from each of the groups discussed in Chapters 3-6 were double-stained for bone and cartilage using an acid-free whole-mount stain to maintain bone integrity (Walker and Kimmel, 2007). Gross anatomical observations were made of the left-lateral views of the skulls at 4, 10 and 35 dpf (for 4 dpf analyses, fish exposed to either 96h SMG at 10 hpf or 96h C+V at 10 hpf were fixed upon removal).

7.2 Results

7.2.1 Gross Observations

Overall, fish stained at 4 dpf do not exhibit abnormal skull morphologies (Figure 7.1). Ossification is present to the same degree in the parasphenoid of all fish within the CNV, C+V (not shown) and SMG groups. In addition, no abnormalities are observed in the shape of the calvariae. Fish from the CNV group (n= 9; Figure 7.1A, B) only display

bone-staining in the posterior-most region of the parasphenoid (arrows), indicating that this bone has started to ossify. This was also true for specimens exposed to 12 hours of SMG starting at 10 hpf (n= 8; Figure 7.1C, D), and specimens exposed to 96 hours of SMG starting at 10 hpf (n= 13; Figure 7.1E). Fish exposed to either 24h SMG at 12 hpf or 24h C+V at 12 hpf did not maintain their integrity throughout the staining procedure and could not be used for analysis. These fish are only 3-4 mm in SL.

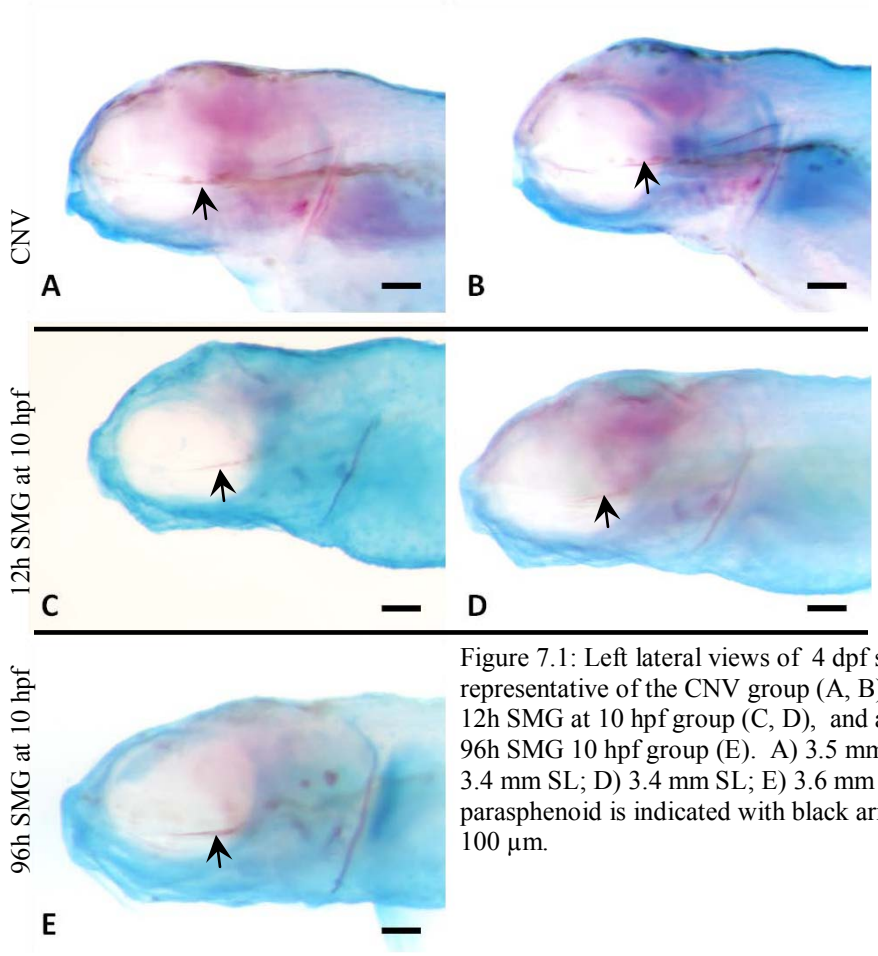

Figure 7.1: Left lateral views of 4 dpf specimens representative of the CNV group (A, B), representatives of the 12h SMG at 10 hpf group (C, D), and a representative of the 96h SMG 10 hpf group (E). A) 3.5 mm SL; B) 3.5 mm SL; C) 3.4 mm SL; D) 3.4 mm SL; E) 3.6 mm SL. Ossification of the parasphenoid is indicated with black arrows. Scale bars are 100 µm.

Interestingly, fish stained at 10 dpf yielded different results compared to the fish stained at 4 dpf (Figure 7.2). At 10 dpf, ossification has begun in the notochord, ceratobranchial 5 (CB5), the opercula, and the entopterygoids in addition to further ossification of the parasphenoid in CNV fish. Fish from the CNV group (n= 9) were further ossified than all other groups (Figure 7.2A, B). Fish from the 12h SMG at 10 hpf group (n= 8) show similar progress in ossification of the parasphenoid, notochord, and

CB5 as the CNV fish. Some 12h SMG at 10 hpf samples (28%) are delayed in the ossification of the opercula and entopterygoids (Figure 7.2C).

Fish from the 24h SMG at 12 hpf group demonstrate highly abnormal shaping in the frontal and parietal region, with severe buckling occurring where the anterior part of the frontals overlaps with the posterior part (Figure 7.2E, F). This was present in 100% of the specimens (n=5). There was also a delay in ossification in all the elements mentioned above, with CB5 appearing to be the only element with any degree of ossification. Fish from the 96h SMG at 10 hpf and 96h C+V at 10 hpf groups did not maintain their integrity throughout the staining process and thus could not be used for analysis. Fish from all the C+V groups (not shown) resembled the fish from the CNV group in both morphology and progression of ossification.

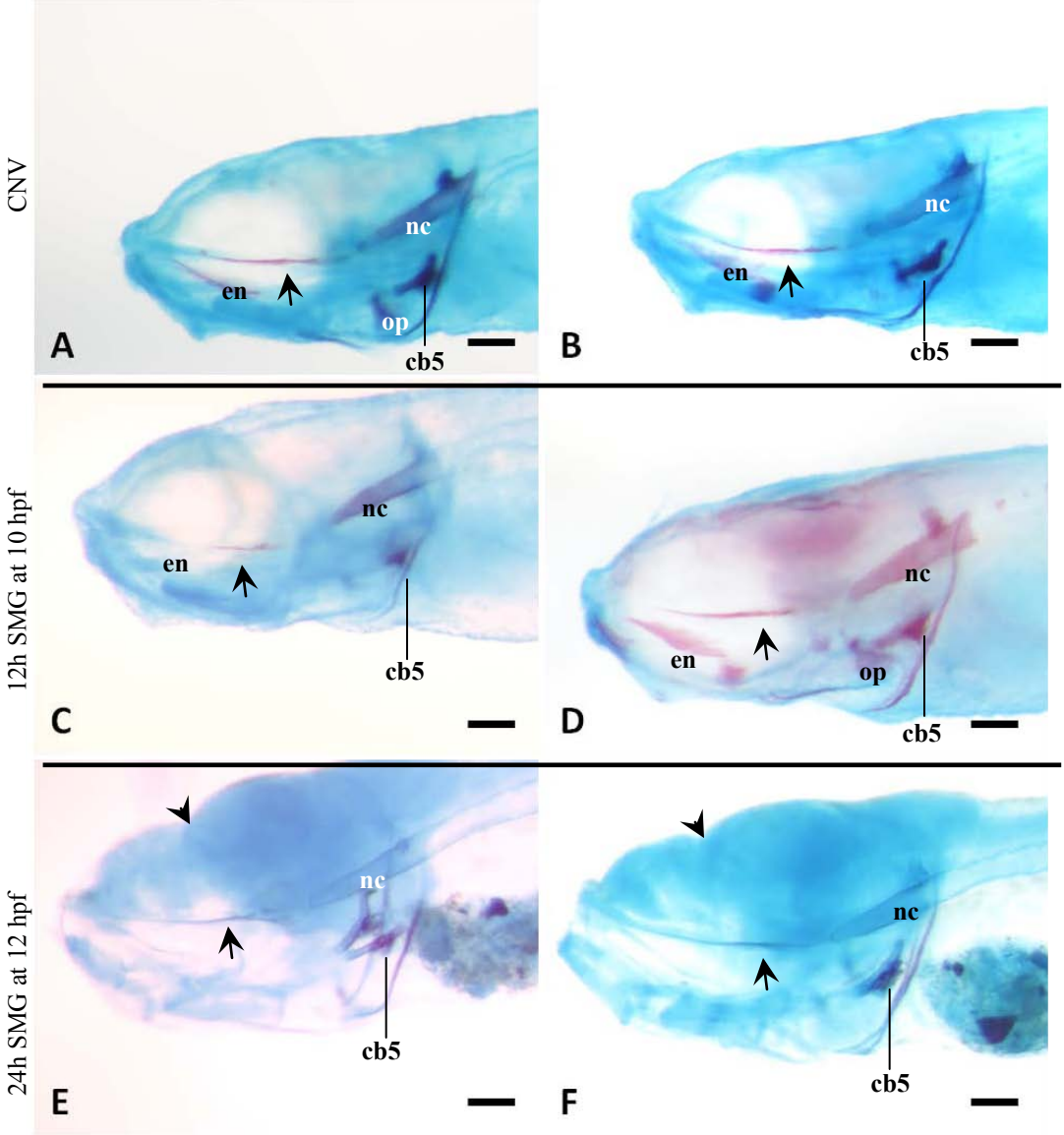

Figure 7.2: Left lateral views of 10 dpf double-stained fish representative of the CNV group (A, B), representative of the 12h SMG at 10 hpf group (C, D) and representative of the 24h SMG at 12 hpf group (E, F). A) 3.5 mm SL and B) 3.6 mm SL show ossification in the parasphenoid (black arrows), the operculum, the entopterygoid, and the notochord at this view. C) Delayed ossification, 3.6 mm SL; D) Ossification in the parasphenoid, entopterygoid, notochord, operculum, and ceratobranchial 5; 3.5 mm SL. E) 3.3. mm SL and F) 3.3 mm SL both are delayed in ossification and have distinct buckles in the junction between the anterior and posterior frontals (black arrowhead). cb5, ceratobranchial 5; en, entopterygoid; nc, notochord; op, operculum. Scale bars are 100 μm.

In 35 dpf stained samples, there is no apparent change in the morphology of the cranial skeleton in any of the fish exposed to SMG in this chapter (Figure 7.3; fish exposed for 12 hours were not raised to 35 dpf due to sample numbers and time constraints), despite changes observed at 10 dpf and at adulthood (parasphenoid, operculum, etc.). Fish from the CNV group (n= 5) have a fully ossified, normal parasphenoid and orbitosphenoids at varying stages of ossification (Figure 7.3A, B). There are no observable abnormalities in the frontal and parietal bones, and the skull appears normal.

Fish from the 24h SMG at 12 hpf group (n= 10) did not demonstrate abnormal parasphenoids at 35 dpf, unlike the adults (Chapter 6). In addition, the severe buckling of the frontals that was observed in this group at 10 dpf is now absent (Figure 7.3C, D).

At 35 dpf, fish from the 96h SMG at 10 hpf group (n= 5) show similar results to their 4 dpf counterparts; there are no apparent changes in overall morphology of the skull, and there does not appear to be any delay in ossification when compared to the CNV group; the parasphenoid is fully ossified, and the orbitosphenoids are at varying stages of ossification (Figure 7.3E, F).

The skull morphology of fish from the groups exposed to vibrations, both the 24h C+V at 12 hpf (n= 15) and the 96h C+V at 10 hpf (n= 11) groups, greatly resemble the skull morphology of the CNV fish; no morphological changes are observed overall. In addition, ossification does not appear to be delayed (not shown).

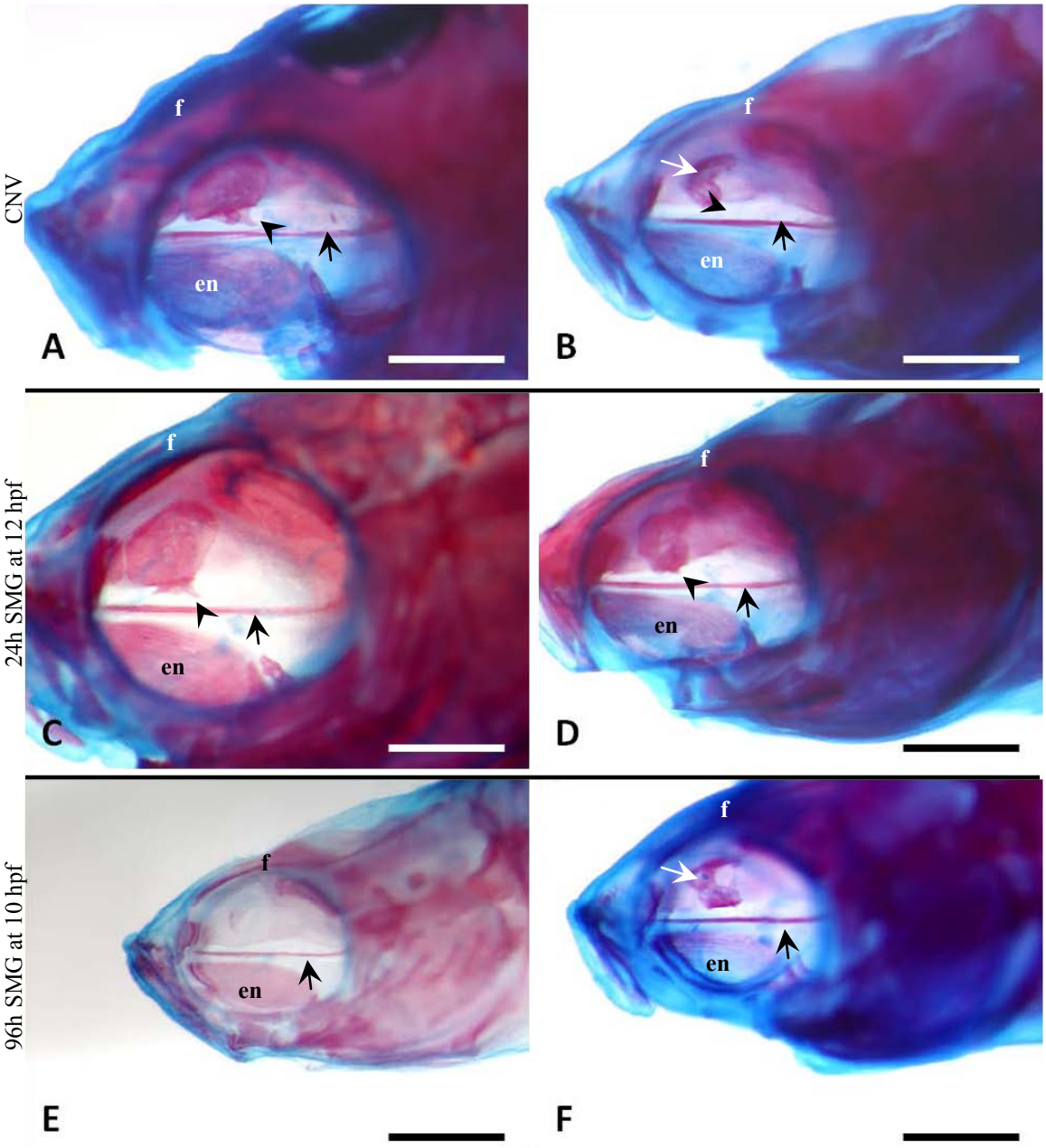

Figure 7.3: Left lateral view of the double-stained skulls of 35 dpf fish representative of the CNV group (A, B), representative of the 24h SMG at 12 hpf group (C, D) and representative of the 96h SMG at 10 hpf group. A) 9.6 mm SL, and B) 8.1 mm SL, have completely ossified parasphenoids (black arrows). The orbitosphenoid has not fused to the parasphenoid at this point (black arrowhead). B) Orbitosphenoid is incompletely ossified (white arrow). C) 10.4 mm SL and D) 8.0 mm SL have completely ossified parasphenoids with no attachment to the orbitosphenoids (black arrows and arrowheads, respectively). E) 8.0 mm SL and F) 7.5 mm SL have fully ossified parasphenoids (black arrows). The orbitosphenoid has only just begun ossification in (E), and ossification is not yet complete in (F; white arrow). en, entopterygoid; f, frontals. Scale bars are 500 µm. Mandibles have been removed from all specimens.

7.1.2 Morphometric Analyses

In order to determine if effects are present in a cranial neural crest-derived bone at a juvenile stage, morphometric analyses were conducted on the right opercula of 35 dpf specimens from all groups. Significance values are recorded in Table 7.1. Landmarks were assigned to the same five anatomical reference points as in Chapter 6 (Appendix 2; Table 7.1).

Morphometric analyses (Goodall's F-test) determined that there are no significant differences between the morphology of opercula from the 96h SMG at 10 hpf and 96h C+V at 10 hpf groups when compared to the opercula from the CNV group ($p > 0.05$ for both comparisons). However, the 96h SMG at 10 hpf opercula differed significantly from the 96h C+V at 10 hpf opercula ($p < 0.05$; Table 2.1).

The opercula of fish from the 24h SMG at 12 hpf and 24h C+V at 12 hpf groups do not significantly differ in morphology from the CNV opercula ($p > 0.05$ for both comparisons). The opercula from the 24h SMG at 12 hpf group did, however, differ significantly from the opercula from the 24h C+V at 12 hpf group ($p < 0.05$). Thus the fish from the 24h SMG and C+V groups displayed similar results as those observed in the 96h SMG and C+V groups. This suggests that SMG and vibrations (either for 24h starting at 12 hpf or for 96h starting at 10 hpf) are causing opposite effects, which results in the two groups being significantly different from each other, but not different from the CNV group.

Table 7.1: Pairwise comparisons made using Goodall's F-test. Each row represents an analysis of the two samples indicated, with F- and p-values noted in columns four and five.

Group 1	Group 2	Goodall's F-test	p-value	Significant
CNV	96hSMG at 10 hpf	1.83	0.10812	No
CNV	96hC+V at 10 hpf	1.88	0.1005	No
96hC+V at 10 hpf	96hSMG at 10 hpf	2.73	0.020548	Yes
CNV	24hSMG at 12 hpf	2.20	0.0596	Borderline
CNV	24hC+V at 12 hpf	2.07	0.0722	No
24hC+V at 12 hpf	24hSMG at 12 hpf	2.23	0.04834	Yes

Vector analyses of the juvenile opercula demonstrate strong directional movements of the landmarks when comparing either the 96h SMG at 10 hpf group or the

96h C+V at 10 hpf group to the CNV group (Figure 7. 4A and B respectively). Overall, both analyses show movement of the landmarks up and to the right. The vectors comparing the 96h SMG at 10 hpf group to the 96h C+V at 10 hpf group, however, show strong downward movements of the landmarks.

Directional magnitude was not as severe as described above when comparing the 24h SMG at 12 hpf and the 24h C+V at 12 hpf groups to the CNV group (Figure 7.4D and E respectively). The vectors shift upwards and to the right. The changes were less drastic when comparing the two groups to each other (Figure 7.4F).

An overall shift upwards and to the right is present in the vector analyses for all comparisons, except the analysis comparing the 96h SMG at 10 hpf group to the 96h C+V at 10 hpf group (Figure 7.4C). It is possible that, because the operculum has not fully developed at this point (Cubbage and Mabee, 1996; Kimmel et al., 2010), the shape is highly variable and still subject to SL.

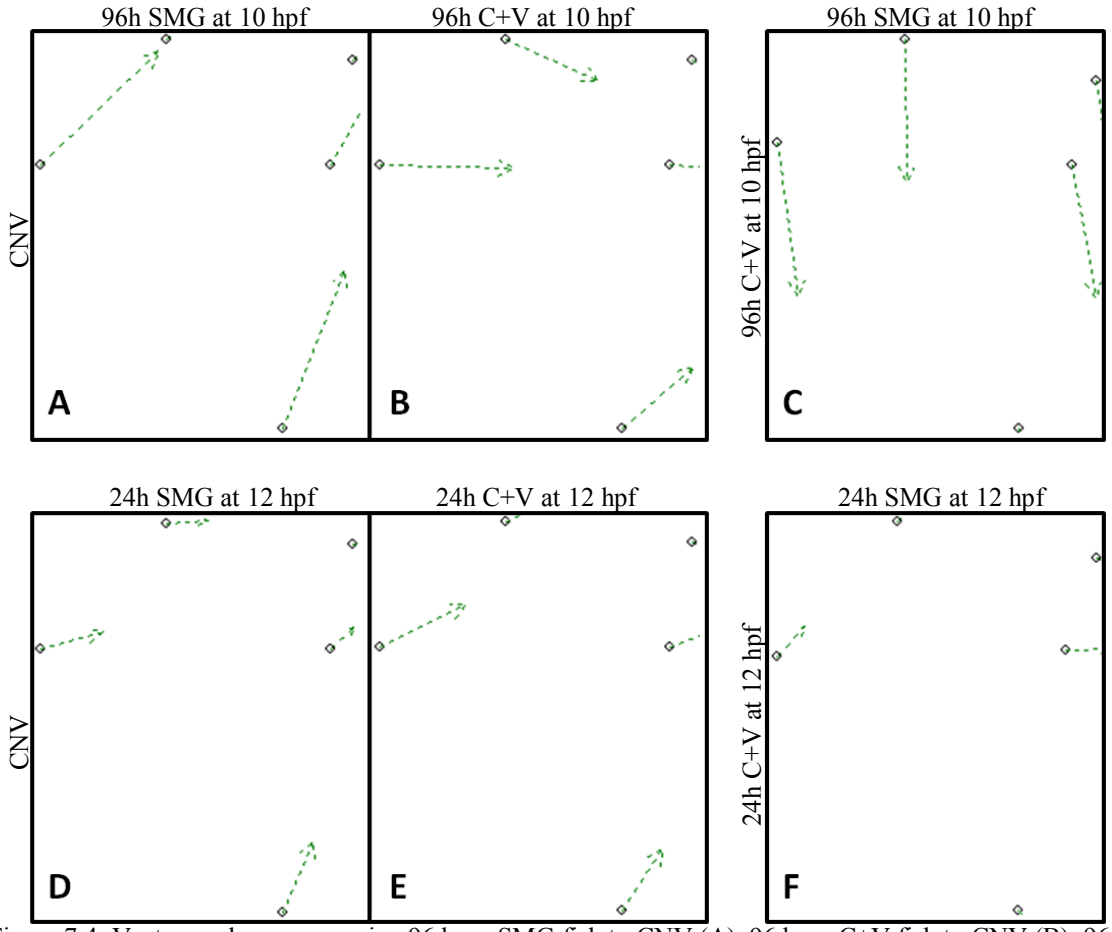

Figure 7.4: Vector analyses comparing 96 hour SMG fish to CNV (A), 96 hour C+V fish to CNV (B), 96 hour SMG fish to 96 hour C+V fish (C), 24 hour SMG fish to CNV (D), 24 hour C+V fish to CNV (E), and 24 hour SMG fish to 24 hour C+V fish (F).

7.1.3 Pharyngeal Skeleton

In order to determine if exposure to SMG affects the pharyngeal skeleton which is cranial neural crest-derived, zebrafish were divided into three groups: 96h SMG at 10 hpf, 96h C+V at 10 hpf, and CNV. Morphometric analyses were conducted on landmarks assigned to 46 anatomical reference points (Figure 2.6A, Chapter 2; Appendix 2).

Wireframes show variation within each group, which is indicated by the partial overlapping of the wireframes (Figure 7.5). Observationally, all three groups of wireframes show variation in the anterior end of the skull (mandible; top portion of the image), along the midline, and in the posterior-most (and lateral-most) region of the mandible. Variation within the arches is highly evident in the 96h C+V at 10 hpf and 96h SMG at 10 hpf groups (Figure 7.5B and C respectively).

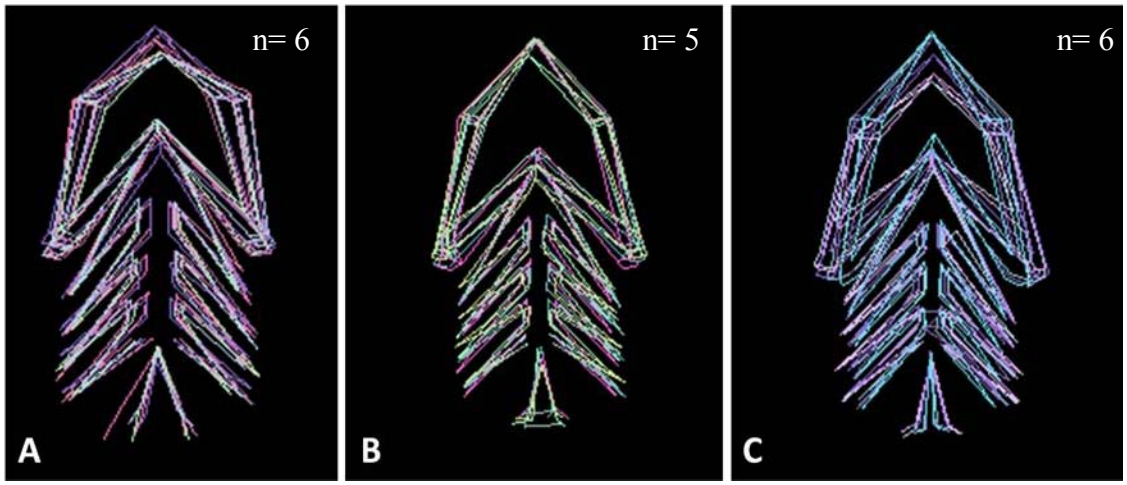

Figure 7.5: Wireframes showing variation within the CNV group (A), the 96h C+V at 10 hpf group (B), and the 96h SMG at 10 hpf group (C).

Goodall's F-test was conducted to determine the level of statistical significance between the pharyngeal arch morphologies of the SMG and CNV groups, the C+V and CNV groups, and the C+V and SMG groups (Table 7.2). The tests determined that all three groups differ significantly from each other ($p <<<< 0.01$ for all three comparisons).

Table 7.2: Pairwise comparisons of the pharyngeal arches in 10 dpf cartilage-stained CNV, SMG , and C+V zebrafish.

Group 1	Group 2	Goodall's F-test	p-value	Significant
CNV	96hSMG	4.68	0.00000	Yes
CNV	96hC+V	3.26	0.00000	Yes
96hC+V	96hSMG	2.42	1.31E-11	Yes

Thin-plate splines comparing the C+V group to the CNV group, the SMG group to the CNV group, and the SMG group to the C+V group showed warping along the lateral and posterior edges, with more pronounced warping along the medial line (Figure 7.6). This was true for all splines.

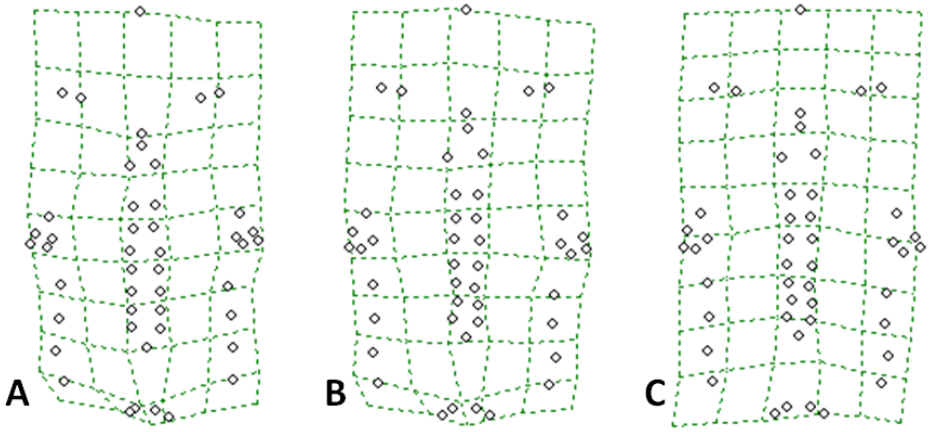

Figure 7.6: Thin plate splines comparing A) 96h C+V at 10 hpf to CNV; B) 96h SMG at 10 hpf to CNV, and C) 96h SMG at 10 hpf to 96h C+V at 10 hpf. Anterior is at the top.

These splines, coupled with the statistical analysis, suggest that the morphology of the pharyngeal arches, a set of neural crest-derived endochondral bones, are affected by both vibrations and SMG. However, they also suggest that exposure to SMG causes morphological changes in addition to that caused by exposure to vibrations.

Overall, the morphological effects observed in the juvenile cranial skeleton were limited to severe buckling between the anterior (cranial neural crest-derived) and posterior (mesoderm-derived) halves of the frontals of 10 dpf specimens from the 24h SMG at 12 hpf group, slight variation in the shape of the opercula in the 96h SMG at 10 hpf and 96h C+V at 10 hpf groups (when compared to CNV fish and each other), and statistically significant variation in the morphology of the pharyngeal arches of fish from the 96h SMG at 10 hpf and 96h C+V at 10 hpf groups when compared to the CNV group

and each other. In summary, these results for the juvenile cranial skeleton suggest that SMG has an effect on the morphology of the frontals, the opercula and the arches, but that vibrations also have an effect.

7.3 Discussion

Cranial neural crest-derived bones, and some mesoderm-derived bones, appear to be affected by exposure to SMG, when observed at juvenile stages. Not only are the pharyngeal arch morphologies significantly different in SMG fish (96h SMG at 10 hpf), but exposure to 24 hours of SMG starting at 12 hpf (24h SMG at 12 hpf) resulted in severe changes in the morphology of the frontal bones, a characteristic not observed in the adult skulls in Chapter 6. In addition, the drastic buckleing observed in the mesoderm-derived parasphenoids of the adults (Chapter 6) was not observed in the juveniles. This contributes to the hypothesis that the adaptability of the cranial neural crest cell population results in the relatively normal adult phenotypes observed in cranial neural crest-derived bones. Changes are present in the cranial neural crest-derived bones of juveniles which is evident at 10 dpf, but not at 4 dpf (above). These changes, however, disappear by the time the fish reach 35 dpf. In the adults (Chapter 6), no obvious abnormalities were present in the frontals; however, severe buckling is present in the parasphenoid, a mesoderm-derived bone that is not affected in the juveniles. This suggests that the effects seen in the cranial neural crest-derived elements (i.e. frontals) at juvenile stages might be propagated during development and manifest in the mesoderm-derived midline bone (i.e. parasphenoid) by adulthood.

The anterior half of the frontals are cranial neural crest-derived, whereas the posterior half of the frontals, in addition to the parietals, are mesoderm-derived (Franz-Odendaal, pers. comm.). There is a suture present between the posterior half of the frontals and the parietal bones, known as the coronal suture. It is analogous to the posterior frontal suture in mice and the metopic suture in humans (Quarto and Longaker, 2005; Sahar et al., 2005). In most vertebrates (e.g. chicken, mouse, human), this suture is known to be neural crest-derived and is present at a neural crest-mesoderm interface (Jiang et al., 2002). It interacts posteriorly with the mesoderm-derived parietal bones, where they meet the neural crest-derived posterior-most frontals (e.g. Sahar et al., 2005).

In contrast to these other vertebrates, the posterior-most frontals in zebrafish are mesoderm-derived (Franz-Odendaal, pers. comm.) and therefore the suture (unknown origin in zebrafish) would be present at a mesoderm-mesoderm interface. Ossification of the mesoderm-derived parietals in mammals requires interaction with the neural crest-derived suture, and thus it is possible that this interaction is required by both the parietals and the posterior-most frontals in zebrafish. It may be that this suture is affected by SMG and/or vibrations, resulting in changes in the frontal and parietal bones, or effects due to SMG and/or vibrations in the frontal and parietal bones result in changes to the suture. In addition, the mesoderm origin of the posterior half of the frontals in zebrafish results in a neural crest-mesoderm interface within this elemenet that is not present in other vertebrates, and therefore it is possible that this new interface is also affected. Regardless, it is possible that neural crest-mesoderm interactions may be involved in the effects observed in the zebrafish cranial morphology.

The results of both the opercula and pharyngeal arch analyses suggest that a causal effect other than, or in addition to SMG is occurring. Both sets of data suggest that exposure to vibrations may affect morphology (opercula and pharyngeal arches). The opercula are highly variable in size and shape at this stage, however, and therefore may be unreliable for morphometric analysis (Kimmel et al., 2010). The pharyngeal arch analyses suggest that SMG and vibrations both greatly affect the morphology of the pharyngeal arches. Many arch mutants are known (e.g. Piotrowski et al., 1996; Schilling et al., 1996), and it is therefore possible that the morphological changes observed in the pharyngeal arches in this thesis resemble a phenotype characteristic of a known arch mutant; however, it is unclear exactly what morphological changes are significant in the present study. Warping was observed in several regions (i.e. lateral and posterior edges, medial line), but it is not obvious whether or not changes in size or changes in overall shape caused the three groups to differ significantly from each other.

Alhough the opercula analyses may be unreliable due to high natural variation, and the pharyngeal arch analyses suggest that vibrations, in addition to SMG, affect morphology, the results from this chapter are important. It is very useful to know that an element that provides a reliable morphometric analysis in adults (the operculum) may not be useful in juveniles. When comparing two different age groups, it is important to

choose an element that can be reliably analyzed at both ages, so comparisons can be more easily conducted. Furthermore, it is important to know that exposure to vibrations results in changes to the pharyngeal arch morphology in addition to effects from SMG exposure. This shows that vibrations play a greater role than anticipated (also shown in Chapter 6), and indicates that researchers should employ the appropriate control groups in future studies, to ensure that effects from vibrations are not associated with exposure to SMG. In addition, abnormalities in the 24h SMG at 12 hpf juvenile (10 dpf) frontal bones that are not present in the adult frontal bones indicates that cranial neural crest cell adaptability is at work. The adaptability of the cranial neural crest cells is ensuring that the adult phenotype is not fatally deformed, by propagating the abnormalities to the parasphenoid, a mesoderm-derived bone that is severely buckled in adult specimens, but not in juveniles. This demonstration of the adaptability of cranial neural crest-cells contributes to the growing knowledge of this population of cells, and shows that exposure to SMG is not enough to prevent these cells from forming a normal adult craniofacial phenotype.

Chapter 8: Discussion

8.1 Discussion on whether exposure to SMG affects Cranial Neural Crest-Derived Tissues

Preliminary observations of the adult skeleton and pigment cells provided insight to the possible effects of stress and SMG on the developing zebrafish. Analysis of the trunk skeleton suggests that stress is not a long-term factor in the overall skeletal phenotype (Chapter 4). If a stress response occurred, it did not manifest itself through the vertebral column of the adult skeleton as in the response to heat shock (Connolly, 2008). Furthermore, the initial observations of both the pigment and adult skull results suggested that neither exposure to SMG nor vibrations alone affected tissues derived from cranial neural crest cells, however mesoderm-derived bones were affected. There were no overall significant differences between SMG and C+V groups when comparing melanophore surface area and number after exposure (Chapter 5) and there appeared to only be changes in mesoderm-derived bones in the adult skull (e.g. parasphenoid; Chapter 6).

Further investigations, however, did not confirm the initial observations, but revealed specific details that lead me to believe that cranial neural crest-derived tissues are affected by SMG. Statistical analyses identified an initial, transient difference in the melanophore surface area and number between the SMG and C+V groups after exposure (Chapter 5). Morphometric analyses confirmed significant differences in the morphology of the adult operculum, a cranial neural crest-derived bone (Chapter 6). Observations made of the juvenile skulls demonstrated morphological differences in cranial neural crest-derived bones (e.g. frontals), and not in mesoderm-derived bones (e.g. parasphenoid). In addition, morphometric analyses show significant differences in the morphology of the juvenile opercula and pharyngeal arches (both of neural crest origin; Chapter 7).

Overall, Chapters 5 through 7 support my hypothesis that cranial neural crest-derived tissues (i.e. pigment, cranial bones) are affected by exposure to SMG and/or vibrations alone. Morphological changes appear to be more severe in the 24h SMG at 12 hpf group. This group has severe changes in the frontal bone morphology within the

juvenile skull (10 dpf). The abnormal frontal morphologies, however, are no longer evident by 35 dpf. As adults, morphological abnormalities are more noticeable in the operculum, and particularly the parasphenoid, than in the frontals (which are no longer buckled, but appear slightly rounded). This suggests an initial effect in cranial neural crest-derived bones that is not observed long-term, but manifests in the morphology of the adult parasphenoid. This is consistent with the initial, transient effect observed in the size and number of melanophores in 96h SMG at 10 hpf individuals in Chapter 5.

Abnormal morphologies were present in juvenile cranial-neural crest derived bones that comprise part of the neurocranium and protect the brain. The same abnormal morphologies were not present in the adult skulls, illustrating adaptability of this cell population. This is also evident in the pigment analyses; changes are present initially, but the resulting phenotype remains unchanged. Cranial neural crest cells are known to be plastic; accommodating various changes in the environment without affecting the final phenotype (Schilling et al., 2001; Trainor et al., 2003; Le Douarin et al., 2004; Sandell and Trainor, 2006). The results observed in this thesis support these previous findings. In addition, neural crest cells are known to interact with mesoderm (e.g. Grenier et al., 2009), which may partly explain how the changes were propagated to the mesoderm-derived parasphenoid.

The results presented here are consistent with other documented transient effects observed in zebrafish after exposure to SMG. A study conducted by Shimada et al. (2005), demonstrated that various durations of exposure (18-60 hours) to SMG starting at varying time points (8-56 hpf) affected gene expression in various zebrafish organ systems, but that these systems recovered within 80 hours of being removed from exposure. Though these researchers did not rear the fish to adulthood, the observed recovery at the gene level of the affected organ systems allows us to assume that a relatively normal phenotype of these systems would have been present. Research conducted by Lindsey et al. (2011) determined that significant differences in zebrafish swim bladder development existed between a SMG group and a control with vibrations (C+V) group after removal from exposure. This was observed in addition to a decrease in standard length (SL) and abnormal swimming behaviours in the SMG fish. These effects, however, were no longer visible by three weeks after exposure, indicating that the

effects are transient, and fish are able to resume normal growth and development (Lindsey et al., 2011). Moorman et al. (1999), as discussed in Chapter 1, observed defects in the developing otoliths of zebrafish 24 hours after exposure to 72h of SMG when compared to fish exposed to vibrations and/or fish raised under normal conditions. The researchers, however, did not raise the animals beyond 96 hpf and thus it is unclear whether or not the fish in this study would have compensated for these defects and resumed normal development as was observed in the other studies described above.

My SMG study is unique in that the fish exposed to SMG and C+V were raised to adulthood. Therefore, after determining that exposure to SMG causes effects in pigment and skull morphology, I was able to determine how the initial effects manifest themselves long-term. It is possible that fish in the studies described above would have had adult phenotypes different to those present in the juveniles they reported.

Ultimately, my study suggests that SMG does have an effect on cranial tissues, regardless of origin or mode of ossification (endochondral/perichondral parasphenoid, intramembranous operculum). It also suggests that effects in the CNC-derived tissues is transient, and does not cause severe defects in CNC-derived parts of the adult zebrafish craniofacial skeleton. This is significant because exposure to microgravity environments during space travel may have initial effects that manifest themselves differently long-term. The bent frontals present in the juvenile fish were capable of regaining a normal adult phenotype by propagating their changes through to the parasphenoid, resulting in a buckling of the parasphenoids in adults.

It is not clear exactly how the effects are propagated; there are numerous possibilities. For example, it is possible that the change is mechanical; as the frontals adjust they may "pull" on the orbitosphenoid which in turn may "pull" on the parasphenoid, causing it to buckle (parasphenoid is fused anteriorly and posteriorly, and so the effects are limited to its middle region). It is also possible that exposure to SMG directly affects bone deposition and resorption, as well as neural crest-mesodermal interactions which in turn affect the bones. Changes in bone deposition may accommodate for the buckling in the frontal bones, resulting in a more rounded morphology as well as a "rippled" morphology in the opercula. In addition, abnormal bone resorption may be responsible for the holes observed in adult parasphenoids.

Interactions between the CNCCs present in the cranial sutures and the mesoderm-derived frontals and parietals may play a part in the initial buckling observed in the frontals. These interactions may also contribute to the buckling of the parasphenoid due to the mesoderm origin of the muscles and bone, and the cranial neural crest origin of the tendons. There are many different possibilities, mechanisms, and cell-types that may be affected by exposure to SMG that may cause the morphological changes observed in this study. Therefore, "how" the changes occur remains unknown. As for "why" the changes are propagated from the frontals to other bones (e.g. parasphenoid, operculum), it is possible that these other bones are not as important. It may be that the parasphenoids and opercula are less vital to the survival of adult zebrafish than the frontals, which, as part of the neurocranium, protects the brain. It would therefore be interesting to determine which elements would display the long-term effects in mammals (e.g. humans), where no parasphenoid or operculum exist. I predict that long-term effects of exposure to SMG may be more detrimental to mammals than fish because these bones are lacking and my data show that there are initial effects that will be propagated to the rest of the skull.

8.2 Conclusion

In conclusion, this study provides valuable information on the effects of SMG on developing cranial neural crest-derived tissues. The plasticity of the cranial neural crest cells buffers the final phenotype from being critically affected by propagating the effects through other skeletal elements that are not as vital to the organism. Thus, effects due to SMG or vibrations observed upon removal and shortly thereafter, are not observed in adults. This information is vital to space travel and long-term SMG exposure studies. Though initial effects as a result of exposure may or may not be observed, it is important to raise the experimental organisms for as long as possible to determine the long-term effects that may not be visible initially.

Furthermore, exposure to vibrations had a greater effect than anticipated, and some results (morphology of the adult operculum) cannot be attributed solely to exposure to SMG. Thus, future experiments examining SMG effects must ensure that proper control groups are employed; otherwise, effects that are a result of vibrations produced by the SMG device may be inaccurately attributed to SMG exposure.

Finally, no cranial abnormalities comparable to known neurocristopathies were observed. This information, therefore, would not be overly useful for cranial neural crest studies examining neurocristopathies. The information gleaned from this thesis, however, provides interesting insight into the type of environmental changes that can affect cranial neural crest cells and how these cells cope and adapt. It is particularly interesting that not even a change in gravity can prevent this remarkable population of cells from fulfilling its developmental destiny.

8.3 Future Directions

Future studies should first attempt to eliminate vibrations as a confounding variable. Using the control vessel exposed to vibrations showed that vibrations play a role in some of the changes observed, thus, a bioreactor, or a similar device, that produces little to no vibrations would be ideal for future studies. In the meantime, all future SMG studies should ensure that they use the proper controls.

This thesis opens up a variety of possibilities for future studies. I have listed the two that I believe would be of the greatest value.

1) Muscle. A study examining the effects SMG has on development of muscle would be of great value. There are multitudes of muscles present in the cranial skeleton of the zebrafish, originating and inserting at both cranial neural crest- and mesoderm-derived bones, resulting in multitudinous musculo-skeletal interactions. It would be important to determine how these muscles are affected, and whether or not it is an effect in the muscles that is causing the changes observed in the cranial morphology. In addition, muscle is mesoderm-derived, like the parasphenoid.
2) Bone deposition and resorption. Fish from the same time points as the above thesis, but stained for bone deposition and resorption would indicate whether or not these processes are affected by exposure to SMG. Balancing deposition and resorption is important to the overall skeletal homeostasis in the developing fish and may provide further insight into how SMG affects the bones of the skull and how compensation has happened.

References

Adams, G.R., McCue, S.A., Bodell, P.W., Zeng, M., and Baldwin, K.M. 2000. Effects of spaceflight and thyroid deficiency on hindlimb development. I. Muscle mass and IGF-I expression. Journal of Applied Physiology 88(3): 894-903.

Albertson, R.C., and Yelick, P.C. 2007. *Fgf8* haploinsufficiency results in distinct craniofacial defects in adult zebrafish. Developmental Biology 306: 505-515.

Alsop, D., and Vijayan, M.M. 2008. Development of the corticosteroid stress axis and receptor expression in zebrafish. American Journal of Physiology: Regulatory, Integrative and Comparative Physiology 294: R711-R719.

Anderson, D. 1997. Cellular and molecular biology of neural crest cell lineage determination. Trends in Genetics 13(7): 276-280.

Baldwin, K.M., Herrick, R.E., Ilyina-Kakueva, E., and Oganov, V.S. 1990. Effects of zero gravity on myofibril content and isomyosin distribution in rodent skeletal muscle. The FASEB Journal 4: 79-83.

Basu, N., Todgham, A.E., Ackerman, P.A., Bibeau, M.R., Nakano, K., Schulte, P.M., and Iwama, G.K. 2002. Heat shock protein genes and their functional significance in fish. Gene 295: 173-183.

Beis, D., Bartman, T., Jin, S-W., Scott, I.C., D'Amico, L.A., Ober, E.A., Verkade, H., Frantsve, J., Field, H.A., Wehman, A., Baier, H., Tallafuss, A., Bally-Culf, L., Chen, J-N., Stalnler, D.Y.R., and Jungblut, B. 2006. Genetic and cellular analyses of zebrafish atrioventricular cushion and valve development. Development and Disease 132(8): 4193-4204.

Bird, N.C., and P.M. Mabee. 2003. Developmental morphology of the axial skeleton of the zebrafish, *Danio rerio* (Ostariophysi: Cyprinidae). Developmental Dynamics 228:337–357.

Bradbury, J. 2004. Small fish, big science. PLoS Biology 2(5): 0568-0572.

Bretaud, S., Lee, S., and Guo, S. 2004. Sensitivity of zebrafish to environemental toxins implicated in Parkinson's disease. Neurotoxicology and Teratology 26(6): 857-864.

Budi, E.H., Patterson, L.B., and Parichy, D.M. 2008. Embryonic requirements for ErbB signaling in neural crest development and adult pigment pattern formation. Development 135: 2603-2614.

Clark, C.R., Taylor, J.D. and Tchen, T.T. 1987. Purification of black moor goldfish melanophores and responses to epinephrine. In Vitro Cellular & Developmental Biology 23(6): 417-421.

Connolly, M. H., and Hall, B.K. 2008. Embryonic heat shock reveals latent *hsp90* translation in zebrafish (*Danio rerio*). The International Journal of Developmental Biology 52: 71-79.

Connolly, M. 2008. Stress-induced variation in zebrafish (*Danio rerio*): The influence of heat shock on the development of the phenotpye. MSc. Thesis. Dalhousie University, Halifax, N.S.

Couly, G.F., Coltey, P.M., and Le Douarin, N.M., 1993. The triple origin of skull in higher vertebrates: a study in quail-chick chimeras. Development 117: 409–429

Couly, G., Creuzet, S., Bennaceur, S., Vincent, C., and Le Douarin, N.M. 2002. Interactions between Hox-negative cephalic neural crest cells and the foregut endoderm in patterning the facial skeleton in the vertebrate head. Development 129: 1061-1073.

Dave., G. 1985. The influence of pH on the toxicity of aluminum, cadmium, and iron to eggs and larvae of the zebrafish, *Brachydanio rerio*. Exotoxicology and Environmental Safety 10(2): 253-267.

Diogo, R., Hinits, Y., and Hughes, S.M. 2008. Development of mandibular, hyoid and hypobranchial muscles in the zebrafish: homologies and evolution of these muscles within bony fishes and tetrapods. BMC Developmental Biology 8: 24-45.

Donoghue, C.J., Graham, A., Kelsh, R.N. 2008. The origin and evolution of the neural crest. BioEssays 30:530- 541.

Eaton, R.C., and Farley, R.D. 1974. Growth and reduction of depensation of zebrafish, *Brachydanio rerio*, reared in the laboratory. Copeia 1974(1): 204-209.

Egan, R.J., Bergner, C.L., Hart, P.C., Cachat, J.M., Canavello, P.R., Elegante, M.F., Elkhayat, S.I., Bartels, B.K., Tien, A.K., Tien, D.H., Mohnot, S., Beeson, E., Glasgow, E., Amri, H., Zukowska, Z., and Kalueff, A.V. 2009. Understanding behavioural and physiological phenotypes of stress and anxiety in zebrafish. Behavioural Brain Research 205: 38-44.

Edsall, S.C., and Franz-Odendaal, T.A. 2010. A quick whole-mount staining protocol for bone deposition and resorption. Zebrafish 7(3): 275-280.

Evans, T.G., Yamamoto, Y., Jeffery, W.R., and Krone, P.H. 2005. Zebrafish *hsp70* is required for embryonic lens formation. Cell Stress & Chaperones 10(1): 66-78.

Ferreri, F., Nicolais, C., Boglione, C., and Bertolini, B. 2000. Skeletal characterization of wild and reared zebrafish: anomalies and meristic characters. Journal of Fish Biology 56: 1115-1128.

Franz-Odendaal, T.A., Ryan, K, and Hall, B.K. 2007. Developmental and morphological variation in the teleost craniofacial skeleton reveals an unusual mode of ossification. Journal of Experimental Zoology 308B: 709-721.

Gans, C., and Northcutt, R.G. 1983. Neural crest and the origin of vertebrates: A new head. Science 220(4594): 268-274.

Gillette-Ferguson, I., Ferguson, D.G., Poss, K.D., and Moorman, S.J. 2003. Changes in gravitational force induce alterations in gene expression that can be monitored in the live, developing zebrafish heart. Advanced Space Research 32(8): 1641-1646.

Goto, K., Okuyama, R., Sugiyama, H., Honda, M., Kobayashi, T., Uchara, K., Akema, T., Sugiura, T., Yamada, S., Ohira, Y., and Yoshioka, T. 2003. Effects of heat stress and mechanical stretch on protein expression in cultured skeletal muscle cells. European Journal of Physiology 447: 247-253.

Grenier, J., Teillet, M-A., Grifone, R., Kelly, R.G., Duprez, D. 2009. Relationship between neural crest cells and cranial mesoderm during head muscle development. PLoS ONE 4(2): e4381; doi:10.1371/journal.pone.0004381.

Gross, J.B., Hanken, J. 2008. Review of fate-mapping studies of osteogenic cranial neural crest in vertebrates. Developmental Biology 317: 389-400.

Gualandris-Parisot, L., Husson, D., Goulquier, F., Kan, P., Davet, J., Aimar, C., Dournon, C., and Duprat, A.M. 2001. *Pleurodeles waltl*, amphibian, urodele, is a suitable biological model for embryological and physiological space experiments on a vertebrate. Advances in Space Research 28(4): 569-578.

Hall, B.K. 1999. The Neural Crest in Development and Evolution. Springer-Verlag New York Inc., New York, NY.

Hall, B.K. 2005, Bones and Cartilage; Developmental and Evolutionary Skeletal Biology. Elsevier/Academic Press, London. pp 4-30; 230-231.

Hall, B.K. 2009. The Neural Crest and Neural Crest Cells in Vertebrate Development and Evolution. Springer Science+Business Media, New York, N.Y.

Hallare, A.B., Schirling, M., Kuckenbach, T., Köhler, H.-R., and Triebskorn, R. 2005. Combined effects of temperature and cadmium on developmental parameters and biomarker responses in zebrafish (*Danio rerio*) embryos. Journal of Thermal Biology 30: 7-17.

Hanken, J., and Hall, B.K. 1993. Mechanisms of skull diversity and evolution. The Skull, Volume 3: Functional and evolutionary mechanisms. (Edited by J. Hanken and B.K. Hall). University of Chicago Press, Chicago Ill. pp 2-5.

Harper, C., and Wolf, J.C. 2009. Morphologic effects of the stress response in fish. Institute for Laboratory Animal Research Journal 50(4): 387-396.

Hierck, B.P., Van der Heiden, K., Poelma, C., Westerweel, J., and Poelmann, R.E. 2008. Fluid shear stress and inner curvature remodelling of the embryonic heart. Choosing the right lane! Special Issue: Cardiac Development, The Scientific World Journal 8: 212-222.

Hikida, R.S., Gollnick, P.D., Dudley, G.A., Convertino, V.A., and Buchanan, P. 1989. Structural and metabolic characteristics of human skeletal muscle following 30 days of simulated microgravity. Aviation, Space, and Environmental Medicine 60(7): 664-670.

Inobe, M., Inobe, I., Adams, G.R., Baldwin, K.M., and Takeda, S. 2002. Effects of microgravity on myogenic factor expressions during postnatal development of rat skeletal muscle. Journal of Applied Ichthyology 9(1): 1936-1942.

Iwama, G.K., Afonson, L.O.B., Todgham, A., Ackerman, P., and Nakano, K. 2004. The Journal of Experimental Biology 207: 15-19.

Jiang, X., Iseki S., Maxson, R.E., Sucov, H.M., and Morriss-Kay, G.M. 2002. Tissue origins and interactions in the mammalian skull vault. Developmental Biology 241: 106-116.

Jiang, J.X., Siller-Jackson, A.J., and Burra, S. 2007. Roles of gap junctions and hemichannels in bone cell functions and in signal transmission of mechanical stress. Frontiers of Bioscience 12: 1450-1462.

Jones, E.A.V., le Noble, F., and Eichmann, A. 2006. What determines blood vessel structure? Genetic prespecification vs. hemodynamics. Physiology 21: 388-395.

Kelsh, R.N., Brand, M., Jiang, Y-J., Heisenberg, C-P., Lin, S., Haffter, P., Odenthal, J., Mullins, M.C., van Eeden, F.J.M., Furutani-Seiki, M., Granato, M., Hammerschmidt, M., Kane, D.A., Warga, R.M., Beuchle, D., Vogelsang, L., and Nüsslein-Volhard, C. 1996. Zebrafish pigmentation mutations and the processes of neural crest development. Development 123: 369-389.

Kelsh, R.N. 2004. Genetics and Evolution of Pigment Patterns in Fish. Pigment Cell Research 17: 326-336.

Kimmel, C.B., Ballard, W.W., Kimmel, S. R., Ullmann, B., and T.F. Schilling. 1995. Stages of embryonic development of the zebrafish. Developmental Dynamics 203:253-310.

Kimmel, C.B., DeLaurier, A., Ullmann, B., Dowd, J., and McFadden, M. 2010. Modes of developmental outgrowth and shaping of a craniofacial bone in zebrafish. PLoS ONE 5(3): e9475.

Klingenberg, C.P. 2011. MorphoJ: an integrated software package for geometric morphometrics. *Molecular Ecology Resources* **11:** 353-357.

Klymkowsky MW, Hanken J. 1991. Whole-mount staining of *Xenopus* and other vertebrates. Methods Cell Biol 36:419–441.

Knight, R.D., Javidan, Y., Nelson, S., Zhang, T., and Schilling, T. 2004. Skeletal and pigment cell defects in the *lockjaw* mutant reveal multiple roles for zebrafish *tfap2a* in neural crest development. Developmental Dynamics 229: 87-98.

Knight, R.D., Nair, S., Nelson, S.S., Afshar, A., Javidan, Y., Geisler, R., Rauch, G-J., and Schilling, T.F. 2003. *lockjaw* encodes a zebrafish *tfap2a*required for early neural crest development. Development 130: 5755-5768.

Knight, R.D., and Schilling, T.F. 2006. Cranial neural crest and development of the head skeleton. Neural Crest Induction and Differentiation. (Jean-Pierre Saint-Jeannet, ed.). Advances in Experimental Medicine and Biology 589: 120-133.

Koller, A., Sun, D., and Kaley, G. 1993. Role of shear stress and endothelial prostaglandins in flow- and viscosity-induced dilation of arterioles in vitro. Circulation Research 72: 1276-1284.

Köntges, G., and Lumsden, A. 1996. Rhombencephalic neural crest segmentation is preserved throughout craniofacial ontogeny. Development 122: 3229-3242.

Krone, P.H., Lele, Z., and Sass, J.B. 1997. Heat shock genes and the heat shock response in zebrafish embryos. Biochemistry and Cell Biology 75: 487-497.

Krone, P.H., Evans, T.G., and Blechinger, S.R. 2003. Heat shock gene expression and function during zebrafish embryogenesis. Cell & Developmental Biology 14: 267-274.

Kulesa, P.M., Bailey, C.M., Kasemeier-Kulesa, J.C., and McLennan, R. 2010. Cranial neural crest migration: New rules for an old road. Developmental Biology 344: 543-554.

Le Douarin, N.M., Creuzet, S., Couly, G., and Dupin, E. 2004. Neural crest cell plasticity and its limits. Development 131: 4637-4650.

Lele, Z., Hartson, S.D., Martin, C.C., Whitesell, L., Matts, R.L., and Krone, P.H. 1999. Disruption of zebrafish somite development by pharmacologic inhibition of Hsp90. Developmental Biology 210: 56-70.

Lindsey, B.W., Dumbarton, T.C., Moorman, S.J., Smith, F.M., and Croll, R.P. 2011. Effects of simulated microgravity on the development of the swimbladder and buoyancy control in larval zebrafish (*Danio rerio*). Journal of Experimental Zoology 315: 302-313.

Lister, J.A., Cooper, C., Nguyen, K., Modrell, M., Grant, K., and Raible, D.W. 2006. Zebrafish Foxd3 is required for development of a subset of neural crest derivatives. Developmental Biology 290: 92-104.

Logan, D.W., Burn, S.F., and Jackson, I.J. 2006. Regulation of pigmentation in zebrafish melanophores. Pigment Cell Research 19: 206-213.

Lumsden, A., Sprawson, N., and Graham, A. 1991. Segmental origin and migration of neural crest cells in the hindbrain region of the chick embryo. Development 113: 1281-1291.

Marí-Beffa, M., Santamaría, J.A., Murciano, C., Santos-Ruiz, L., Andrades, J.A., Guerado, E., and Becerra, J. 2007. Zebrafish fin in the Scientific World Journal 7: 1114-1127.

Marks, C., West, T.N., Bagatto, B., Moore, F.B-G. 2005. Developmental environment alters conditional aggression in zebrafish. Copeia 2005(4): 901-908.

Metscher, B.D. and Ahlberg, P.E. 1999. Zebrafish in context: Uses of a laboratory model in comparative studies. Developmental Biology 210: 1-14.

Meyer, A., Biermann, C.H., and Orti, Guillermo. 1993. The phylogenetic position of the zebrafish (*Danio rerio*), a model system in developmental biology: An invitation to the comparative method. Proceedings: Biological Sciences 252(1335): 231-236.

Moorman, S.J., Buress, C., Cordova, R., and Slater, J. 1999. Stimulus dependence of the development of the zebrafish (*Danio rerio*) vestibular system. Journal of Neurobiology 38: 247-258.

Moorman, S.J., Cordova, R., and Davies, S.A. 2002. A critical period for functional vestibular development in zebrafish. Developmental Dynamics 223:285-291.

Muller, M., Dalcq, J., Aceto, J., Larbuisson, A., Pasque, B., Nourizadeh-Lilladadi, R., Alestrom, P., and Martial, J.A. 2010. The function of the Egr1 transcription factor in cartilage formation and adaptation to microgravity in zebrafish, *Danio rerio*. Journal of Applied Ichthyology 26: 239-244.

Neff, A.W., Yokota, H., Chung, H-M., Wakahara, M., and Malacinski, G.M. 1998. Early amphibian (Anuran) morphogenesis is sensitive to novel gravitational fields. Developmental Biology 155: 270-274.

Nüsslein-Volhard, C., and Dahm, R. 2002. Zebrafish: a practical approach. Oxford University Press, Oxford, NY.

Parichy, D.M. 2003. Pigment patterns: fish in stripes and spots. Current Biology 13(24): R947- R950.

Parichy, D.M. 2006. Evolution of *Danio* pigment pattern development. Heredity 97: 200-210.

Parichy, D.M., Elizondo, M.R., Mills, M.G., Gordon, T.N, and Engeszer, R.E. 2009. Normal table of postembryonic zebrafish development: staging by externally visible anatomy of the living fish. Developmental Dynamics 238: 2975-3015.

Parichy, D.M., Turner, J.M., and Parker, N.B. 2003. Essential role for *puma* in development of postembryonic neural crest-derived cell lineages in zebrafish. Developmental Biology 256: 221-241.

Piotrowski, T., Schilling, T.F., Brand, M., Jiang, Y-J., Heisenberg, C-P., Beuchle, D., Grandel, H., van Eeden, F.J.M., Furutani-Seiki, M., Granato, M., Haffter, P., Hammerschmidt, M., Kane, D.A., Kelsh, R.N., Mullins, M.C., Odenthal, J., Warga, R.M., and Nüsslein-Volhard, C. 1996. Jaw and branchial arch mutants in zebrafish II: anterior arches and cartilage differentiation. Development 123: 345-356.

Pough, F.H., Janis, C.M., and J.B. Heiser. 2009. Vertebrate Life (8th Edition). Pearson Benjamin Cummings, San Francisco, CA.

Quarto, N., and Longaker, M.T. 2005. The zebrafish (*Danio rerio*): A model system for cranial suture patterning. Cells Tissues Organs 181: 109-118.

Quigley, I.K., Turner, J.M., Nuckels, R.J., Manuel, J.L., Budi, E.J., MacDonald, E.L. and Parichy, D.M. 2004. Pigment pattern evolution by differential deployment of neural crest and post-embryonic melanophore lineages in *Danio* fishes. Development 131(24): 6053- 6069.

Reich, K.M., Gay, C.V., and Frangos, J.A. 1990. Fluid shear stress as a mediator of osteoblast cyclic adenosine monophosphate production. Journal of Cellular Physiology 143: 100-104.

Renn, J., Seibt, D., Goerlich, R., Schartl, M., and Winkler, C. 2006. Simulated microgravity upregulates gene expression of the skeletal regulator Core binding Factor α1/Runx2 in Medaka fish larvae in vivo. Space Research 38: 1025-1031.

Renn, J., Winkler, C., Schartl, M., Fischer, R., and Goerlich, R. 2006. Zebrafish and medaka as models for bone research including implications regarding space-related issues. Protoplasma 229: 209-214.

Rodionov, V.I., Lim, S-S., Gelfand, V.I., and Borisy, G.G. 1994. Microtubule dynamics in fish melanophores. The Journal of Cell Biology 126: 1455- 1464.

Sahar, D.E., Longaker, M.T., and Quarto, N. 2005. *Sox9* neural crest determinant gene controls patterning and closure of the posterior frontal cranial suture. Developmental Biology 280: 344-361.

Sandell, L.L., and Trainor, P.A. 2006. Neural crest cell plasticity: Size matters. Neural Crest Induction and Differentiation (Jean-Pierre Saint-Jeannet, ed.). Advances in Experimental Medicine and Biology 589: 78-95.

Sanders, B.M. 1993. Stress proteins in aquatic organisms: an environmental perspective. Critical Reviews in Toxicology 23(1): 49-75.

Santacruz, H., Vriz, S., and Angelier, N. 1997. Molecular characterization of a heat shock cognate cDNA of zebrafish, *hsc70*, and developmental expression of the corresponding transcripts. Developmental Genetics 21: 223-233.

Santagati, F., and Rijli, F.M. 2003. Cranial neural crest and the building of the vertebrate head. Nature 4: 806-818.

Schilling, T.F., Piotrowski, T., Grandel, H., Brand, M., Heisenberg, C-P., Jiang, Y-J., Beuchle, D., Hammerschmidt, M., Kane, D.A., Mullins, M.C., van Eeden, F.J.M., Kelsh, R.N., Furutani-Seiki, M., Granato, M., Haffter, P., Odenthal, J., Warga, R.M., Trowe, T., and Nüsslein-Volhard, C. 1996. Jaw and branchial arch mutants in zebrafish I: branchial arches. Development 123: 329-344.

Schilling, T.F., Walker, C., and Kimmel, C.B. 1996. The *chinless* mutation and neural crest cell interactions in zebrafish jaw development. Development 122: 1417-1426.

Schilling, T.F., Prince, V., and Ingham, P.W. 2001. Plasticity in zebrafish *hox* expression in the hindbrain and cranial neural crest. Developmental Biology 231: 201-216.

Schliwa, M. 1984. Mechanisms of intracellular organelle transport. Cell and Muscle Motility: The Cytoskeleton. *Edited* by J.W. Shay. Plenum Press, New York, N.Y.

Schwartz, M.A., and DeSimone, D.W. 2008. Cell adhesion receptors in mechanotransduction. Current Opinion in Cell Biology 20: 551-556.

Serova, L.V., Denisova, L.A., Apanasenko, Z.I., Kuznetsova, M.A., and Mǎzerov, E.S. 1982. Reproduktivnaia funktsiia krys-samtsov posle poleta na biosputnike "Kosmos-1129". Kosmicheskaia Biologiia I Aviakosmicheskaia Meditsina 16(5): 62-65.

Shimada, N., Sokunbi, Gl, and Moorman, S.J. 2005. Changes in gravitational force affect gene expression in developing organ systems at different developmental times. BMC Developmental Biology 5:10.

Shimada, N., and Moorman, S.J. 2006. Changes in gravitational force cause changes in gene expression in the lens of developing zebrafish. Developmental Dynamics 235: 2686-2694.

Steenbergen, P.J., Richardson, M.K., and Champagne, D.L. 2010. The use of the zebrafish model in stress research. Progress in Neuro-Psychopharmacology and Biological Psychiatry (In Press; Available on-line: doi:10.1016/j.pnpbp.2010.10.010).

Tawk, M., Joulie, C., and Vriz, S. 2000. Zebrafish Hsp40 and Hsc70 genes are both induced during caudal fin regeneration. Mechanisms of Development 99: 183-186.

Thaler, C.D., and Haimo, L.T. 1992. Control of organelle transport in melanophores: Regulation of Ca^{2+} and cAMP levels. Cell Motility and the Cytoskeleton 22(3): 175-184.

Tian, B., Carlyle, W.C., Weigold, W.G., McDonald, K.M., Judd, D.L, Toher, C.A., Homans, D.C., Cohn, J.N. 1999. Localization of changes in β-actin expression in remodelled canine myocardium. Journal of Molecular Cell Cardiology 31: 751-760.

Tobin, J.L., Di Franco, M., Elchers, E., May-Simera, H., Garcia, M., Yan, J., Quinlan, R., Justice, M.J., Hennekam, R.C., Briscoe, J., Tada, M., Mayor, R., Burns, A.J., Lupski, J.R., Hammond, P., and Beales, P.L. 2008. Inhibition of neural crest migration underlies craniofacial dysmorphology and Hirschsprung's disease in Bardet-Biedl syndrome. Proceedings of the National Academy of Sciences 105(18):6714- 6719.

Trainor, P.A., Melton, K.R., and Manzanares, M. 2003. Origins and plasticity of neural crest cells and their roles in jaw and craniofacial evolution. International Journal of Developmental Biology 47: 541-553.

Vaglia, J.L., and Hall, B.K. 1999. Regulation of neural crest cell populations: occurrence, distribution and underlying mechanisms. International Journal of Developmental Biology 43: 95-110.

Vaglia, J.L., and Hall, B.K. 2000. Patterns of migration and regulation of trunk neural crest cells in Zebrafish (*Danio rerio*). International Journal of Developmental Biology 44: 867-881.

van Rijn, L.C. 1984. Sediment transport, Part I: Bed load transport. Journal of Hydraulic Engineering 110(10): 1431-1456.

Vascotto, S.G., Beckham, Y., and Kelly, G.M. 1997. The zebrafish's swim to fame as an experimental model in biology. The International Journal of Biochemistry and Cell Biology 75: 479-485.

Vasilyev, A., and Drummond, I.A. 2010. Fluid flow and guidance of collective cell migration. Cell Adhesion and Migration 4(3): 353-357.

Walker, M.B. and C.B. Kimmel. 2007. A two-color acid-free cartilage and bone stain for zebrafish larvae. Biotechnic & Histochemistry 82(1): 23-28.

Walker, M.B., Miller, C.T., Swartz, M.E., Eberhart, J.K., and Kimmel, C.B. 2007. phospholipase C, beta 3 is required for Endothelin1 regulation of pharyngeal arch patterning in zebrafish. Developmental Biology 304 (1): 194-207.

Webster, M., Sheets, H.D. 2010. A practical introduction to landmark-based geometric morphometrics. Quantitative Method in Paleobiology. Paleontological Society Papers, vol. 16. (Edited by J. Alroy and G. Hunt). Yale University Printing and Publishing Services, New Haven, CT. pp 163-188.

Witten, P.E., Hansen, A., and Hall, B.K. 2001. Features of mono- and multinucleated cells of the zebrafish *Danio rerio* and their contribution to skeletal development, remodelling and growth. Journal of Morphology 250: 197-207.

Witten, P.E., and Huysseune, A. 2009. A comparative view on mechanisms and functions of skeletal remodelling in teleost fish, with special emphasis on osteoclasts and their function. Biological Reviews 84: 315-346.

Yamaguchi, M., Yoshimoto, E., and Kondo, S. 2007. Pattern regulation in the stripe of zebrafish suggests an underlying dynamic and autonomous mechanism. Proceedings of the National Academy of Sciences 104(12): 4790- 4793.

Yamamoto, K., Sokabe, T., Watabe, T., Miyazono, K., Yamashita, J.K., Obi, S., Ohura, N., Matsushita, A., Kamiya, A., and Ando, J. 2005. Fluid shear stress induces differentiation of Flk-1-positive embryonic stem cells into vascular endothelial

cells in vitro. American Journal of Physiology and Heart and Circulatory Physiology 288(4): H1915-H1924.

Yelick, P.C. and Schilling, T.F. 2002. Molecular dissection of craniofacial development using zebrafish. Critical Reviews in Oral Biology & Medicine 13:308-322.

Yelick, P.C., and M.H. Connolly. 2010. A forward genetic screen for genes regulating mineralized tooth and bone formation in zebrafish (*Danio rerio*). Journal of Applied Ichthyology 26: 192-195.

Yu, H-H., and Moens, C.B. 2005. Semaphorin signaling guides cranial neural crest cell migration in zebrafish. Developmental Biology 280: 373-385.

Zuniga, E., Stellabotte, F., and Crump, J.G. 2010. Jagged-Notch signaling ensures dorsal skeletal identity in the vertebrate face. Development 137: 1843-1852.

Appendix 1: Methodology

1A. Bioreactor Set-up

1) Detach chamber from base; open all three ports on the end.
2) Fill chamber with tap water, swirl, and dump water.
3) Fill chamber with zebrafish system water, swirl, and dump water.
4) Pour zebrafish system water into chamber, but this time not to the top.
5) With a plastic pipette, pipette embryos into chamber through the largest port at required stages (e.g. 10, 12, 14 hpf).
6) Seal the largest port with cap.
7) Fill a large plastic syringe with zebrafish system water (make sure there are no bubbles in syringe).
8) Screw large plastic syringe to one of the two smaller ports and (GENTLY!) squeeze the water into the chamber to top it up (it is helpful to hold the chamber at this point and to gently tip it side to side while doing this to ensure all bubbles are forced out).
9) Close the two smaller ports; turn the chamber on its side- more bubbles may appear at this point, so repeat steps 7 and 8.
10) Once all bubbles are removed and all three ports are closed securely, reattach the chamber to the bioreactor base (secure round silver knob on left hand side with left hand to prevent motor from turning in wrong direction). Turn on when desired.

1B. Control Vessel Set-up

1) Rinse control vessel in first tap water and then zebrafish system water (as described above). Fill to nearly full with zebrafish system water.
2) Remove one port (there are only two) and pipette in the zebrafish embros. Screw port back in.

3) Top up vessel with plastic syringe as described above, except do not tip the control vessel; the control vessel ports do not seal shut as the vessel does not rotate.
4) Prop control vessel on edge of bioreactor base.

1C. Pigment Analysis Protocol

1) Separate clutch of embryos into two groups.
2) Stage embryos. Place one group into the bioreactor and place other group into the control vessel, as described above.
3) Turn on bioreactor for 96 hours starting at 10 hpf.
4) After 96 hours, remove embryos from bioreactor and control vessel. Randomly select six from each group and place them in their own individual well in a well plate. It is useful to keep one plate as SMG fish, and one plate as control fish. Place well plates in glass-front incubator set at 28.5 °C so that they are exposed to light-cycle.
5) Conduct the following steps for fish from each group, for a period of a week: 24 hours after removal from bioreactor, fish were anaesthetized and viewed under the microscope (Figure A1.1). Fish were anaesthetized in 0.01% MS-222 (ethyl 3-aminobenzoate methanesulfonic acid salt, 98%; Sigma-Aldrich, E10521), and photographed in 2.4% methyl-cellulose (Sigma-Aldrich, M0387). Methyl-cellulose is made by adding 2.4 ml methyl-cellulose to 100 ml zebrafish system water; agitate for 10 days at 4°C, store at 4°C; warm to room temperature before using).

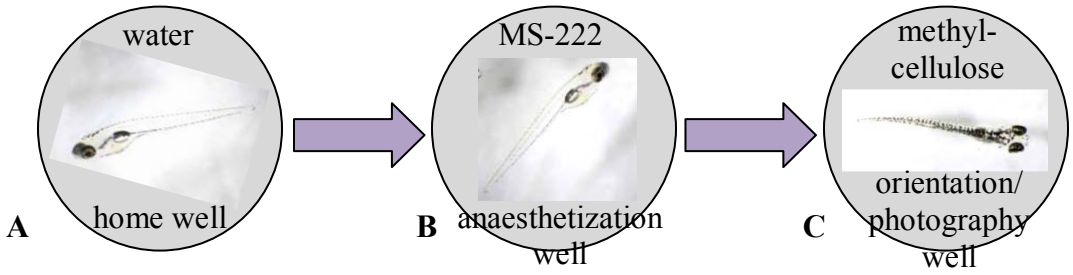

Figure A1.1: Schematic of the wells used to set up the embryos for image-taking. Embryos were moved from their home well (A), to a well containing 0.01% MS-222 (B). Once asleep, fish were moved to a third well (C) containing 2.4% methyl-cellulose, where they were orientated as desired.

6) Photograph the dorsal view of the entire fish; measure and record the SL of the fish.
7) Take a close-up of the dorsal view of the cranial skull; ensure fish is lying as straight as possible when you take this image.
8) If conducting a count, pipette 2-3 drops of a 1 mg/ml solution of epinephrine (Sigma-Aldrich, E1635) onto the dorsal side of the fish; wait 1-5 minutes for melanophores to contract (10 minutes on rare occasion), then take another picture.
9) Place fish in a well of zebrafish system water and transfer to fresh system water, until fish recovers.
10) Place fish back in "home" well.

1.D Cartilage Stain for larval zebrafish (adapted from Klymkowski and Hanken, 1991)

1) Fix fish in 10% Neutral Buffered Formalin (NBF; Fisher Scientific, 72210) overnight at room temperature, or in 4% PFA in 0.01M PBS (pH 7.4) overnight at 4°C.
2) Process fish to 70% ethanol (EtOH) for storage.
3) Move fish directly from 70% EtOH to Alcian blue solution (below) overnight at room temperature.
4) Rinse sample in 95% EtOH.
5) Move sample to Saturated Borax solution overnight at room temperature.
6) Digest tissue in a 2% borax/1% trypsin solution (in distilled water) 1-3 nights at room temperature.
7) Bleach fish in 5% hydrogen peroxide (use 3% stock solution) in 1% KOH overnight at room temperature.
8) Process to storage (100% glycerol) through glycerol/KOH series.

Solutions:

i) 0.01M PBS: 1 L solution,

8 g NaCl (Sigma-Aldrich, S3014)

1.15 g Na_2HPO_4 (EMD, SX0720-1)

0.2 g KCl (MP Biomedicals, 191427)

0.2 g KH_2PO_4 (Sigma-Aldrich, P5655)

Add 800 ml distilled water, pH solution to 7.4, top solution up to 1 L with distilled water.

ii) 4% PFA

Add 4% PFA (Sigma-Aldrich, P6148) to 0.01M PBS (above)

iii) Alcian Blue Solution: 100 ml

20 ml acetic acid (Fisher Scientific, A38212)

80 ml 100% alcohol

0.015 g Alcian Blue (Sigma-Aldrich, A3517)

iv) Saturated Borax solution:

Place desired volume of distilled water in beaker on stir plate- add stir bar, turn on stirrer.

Add spoons of Sodium Tetraborate Decahydrate (Sigma-Aldrich, B9876) until the powder no longer dissolves and the solution is saturated.

v) 2% Borax/1% Trypsin solution:

1g Trypsin (Fisher Scientific, T360-500)

2g Sodium Tetraborate Decahydrate

100 ml distilled water

vi) 1% KOH:

1g Potassium Hydroxide (Sigma-Aldrich, P1767) in 100 ml of distilled water.

vii) Glycerol/KOH series:

20 ml 100% glycerol + 80 ml 1% KOH

40 ml 100% glycerol + 60 ml 1% KOH

Store in 100% glycerol

1E. Bone Stain (Adapted from Franz-Odendaal et al., 2007)

1) Process specimens from 70% EtOH to distilled water (70% →50% →25% →H_2O; 1 hour in each).
2) Bleach specimens overnight at room temperature (bleach solution below).
3) Rinse in H_2O (add water and invert tubes 2-3 times).
4) Move samples into Saturated Borax for the day (room temperature).
5) Move samples to Alizarin Red Solution (below) overnight at room temperature.
6) Rinse samples in 1% KOH.
7) Move samples to 2% borax/1% trypsin solution (below) for 1-3 nights at room temperature.
8) Move samples through a glycerol/KOH series (below- one overnight in each).
9) Store samples in 100% glycerol.

Solutions:

i) 1% KOH (refer to 1.D. above)

ii) 2% Borax/1% Trypsin (refer to 1.D. above)

iii) Bleach solution:

5% Hydrogen peroxide (3% stock solution) in 1% KOH

iv) Alizarin Red solution:

1 mg/ml Alizarin Red (Sigma-Aldrich, A5533) in
1% KOH

v) Glycerol/KOH series:

20 ml 100% glycerol + 80 ml 1% KOH
40 ml 100% glycerol + 60 ml 1% KOH

Store in 100% glycerol

1F. Acid-Free Double Stain (Adapted from Walker and Kimmel, 2007)

1) Fix embryos in 4% PFA in 0.01M PBS (2 hrs room temperature with agitation, or overnight at 4°C) - store in 0.01M PBS.
2) Put samples directly into 50% ethanol for 10 minutes at room temperature with agitation.
3) Remove ethanol and add staining solution (see below) - agitate overnight at room temperature.
4) Rinse in distilled water (add water to tube with specimen and invert twice maximum).
5) Remove water and add bleach solution (below) to tubes for 20 minutes at room temperature, with lids open (no agitation).
6) **If fish are >20 dpf, add a step here: remove bleach and wash specimens in a 1% KOH solution for 1 hour at room temperature (agitation). The blue stain will stick to the outside of larger samples, obscuring the bone. This step does not completely solve the problem, but it helps. The remaining blue stain adhering to the specimens can be scraped off gently with forceps.
7) If fish are < 20 dpf, remove bleach and add 20% glycerol solution (made in 1% KOH) to tubes and agitate at room temperature for 30 min (can be left overnight).
8) Replace 20% glycerol solution with a 40% glycerol solution (made in 1% KOH), agitate at room temperature for 2 hours (can be left overnight).
9) Store in 100% Glycerol.

Solutions:

i) Staining Solution: 1 ml

990µl Part A+ 10 µl Part B (below)

ii) Part A: 100 ml

50 ml 0.4% (0.4g in 100 ml distilled water) Alcian Blue in 70% EtOH

70 ml 95% EtOH

25 ml 20mM $MgCl_2$ (Fischer Scientific, BP214)

(Final concentrations: 0.02% Alcian Blue, 20 mM $MgCl_2$, and 70% EtOH)

iii) Part B: 10 ml

0.05g Alizarin Red in 10 ml distilled water

iv) Bleaching Solution

Mix equal volumes 3% H_2O_2 and 2% KOH (2% KOH in distilled water) for a solution that has final concentrations of:

1.5% H_2O_2 and 1% KOH.

Appendix 2: Landmark Reference Points for Morphometric Analyses

2A. Pharyngeal Arch Landmarks

Ventral views of the cartilage-stained pharyngeal arches were assigned 46 landmarks (Figure A2.1) based on the following anatomical reference points. Nomenclature follows Cubbage and Mabee (1996).

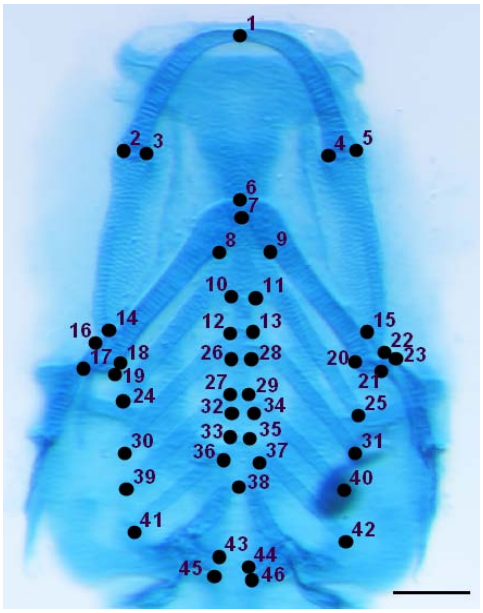

Figure A2.1: Ventral view of cartilage-stained pharyngeal arches with 46 landmarks. Scale bar is 100µm.

Landmark	Description
1	mandibular symphysis (joint joining left and right dentary bones)
2, 5	lateral edge of joint joining the mandible and the palatoquadrate
3, 4	medial edge of joint joining the mandible and the palatoquadrate
6	contact between the ventral hypohyals
7	contact between the dorsal hypohyals
8, 9	anterior contact between basibranchial 1 and the ceratohyals
10, 11	anterior contact between basibrancial 2 and ceratobranchial 1
12, 13	contact between posterior end of basibranchial 2 and anterior portion of ceratobranchial 3

14, 15	contact between the palatoquadrate, ceratohyal, and hyosymplectic
16, 22	anterior lateral edge where hyosymplectic contacts the palatoquadrate
17, 23	posterior lateral edge where hyosymplectic contacts the palatoquadrate
18, 20	anterior medial edge where hyosymplectic contacts the ceratohyal
19, 21	posterior medial edge where hyosymplectic contacts the ceratohyal
24, 25	lateral tips of 1st ceratobranchials
26, 28	contact between anterior-most point of basibranchial 3 and ceratobranchial 2
27, 29	contact between posterior-most point of basibranchial 3 and ceratobranchial 3
30, 31	lateral tips of 2nd ceratobranchials
32, 34	contact between anterior-most point of basibranchial 4 and ceratobranchial 3
33, 35	contact between posterior-most point of basibranchial 4 and ceratobranchial 4
36, 37	contact between posterior medial edge of ceratobranchial 4 and anterior medial edge of ceratobranchial 5
38	contact between the 5th ceratobranchials
39, 40	lateral tips of 3rd ceratobranchials
41, 42	lateral tips of 4th ceratobranchials
43, 44	medial tips of anterior-most teeth on ceratobranchial 5
45, 46	medial tips of posterior-most teeth on ceratobrancial 5

2B. Dorsal Skull Landmarks

The dorsal view of the adult zebrafish skull was initially assigned 15 landmarks incorporating the premaxilla, the vomer, the frontals and parietals (Figure A2.2 A). This was subsequently reduced to 9 landmarks surrounding the frontals in order to pin-point the region with the most variation (Figure A2.2 B). Landmarks appearing in parantheses in the list below represent the landmark's new assigned number in the revised analysis of

the reduced data set (as in Figure A2.2 B). Nomenclature follows Cubbage and Mabee (1996) and Quarto and Longaker (2005).

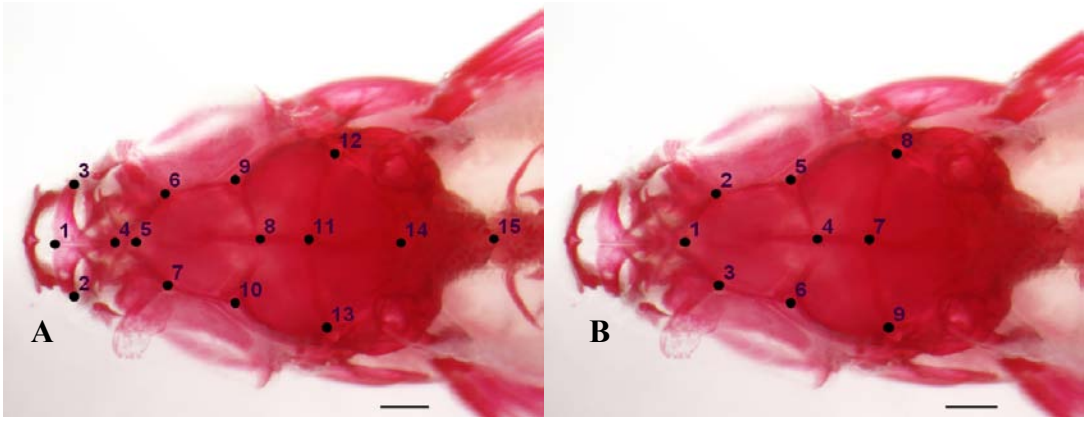

Figure A2.2 Dorsal view of bone-stained adult zebrafish skulls with 15 landmarks (A) and 9 landmarks (B) for morphometric analysis. Scale bars are 500 µm.

Landmark	Description
1	anterior-most point of the contact between two premaxilla halves
2, 3	lateral edges of premaxilla
4	anterior-most point of the kinethmoid
5 (1)	posterior-most point of the kinethmoid, anterior-most edge of the anterior frontals
6 (2), 7 (3)	posterior point where the lateral ethmoids make contact with the anterior half of the frontals
8 (4)	contact between the overlapping frontals and the interfrontal suture
9 (5), 10 (6)	lateral edges of overlapping frontals
11 (7)	contact between the interfrontal and coronal sutures
12 (8), 13 (9)	lateral edges of coronal suture
14	posterior-most end of parietal bones (where sagittal suture contacts lamboid suture)
15	posterior-most end of the basioccipital

2C. Operculum Landmarks

Right lateral opercula were assigned five landmarks in both the adult and the 35 dpf specimens (Figure 2A.3). Landmarks were assigned to anatomical reference points described by Albertson and Yelick (2007) and Kimmel et al. (2010). Nomenclature follows Kimmel et al. (2010).

Figure A2.3 Lateral view of a ight lateral adult bone-stained operculum with 5 landmarks. The same five landmarks were applied to juvenile opercula (35 dpf). Scale bar is 500 µm.

Landmark	Description
1	joint socket
2	joint apex
3	posterior-dorsal apex
4	posterior-most point of curve
5	ventral apex

Appendix 3: Stress Analyses Charts and Statistics

3A. Data Tables

The number of precaudal, caudal, and total vertebrae was counted (Tables A3.1-A3.4). Non-parametric statistical analyses were conducted on the caudal and total number of vertebrae (as described below). These charts represent all adult fish used in the study.

Table A3.1: Number of vertebrae of fish exposed to 12 hours of SMG starting at 10 hpf and fish exposed to 12 hours of vibrations starting at 10 hpf. DOB, date of birth; DOD date of death; SL, standard length.

Fish I.D.	Age (dpf)	"Treatment"	Precaudal #	Caudal #	Total Vert #	SL (mm)
AB-7 (a)	120	12hr SMG at 10 hpf	10	15	25	17
AB-7 (b)	120	12hr SMG at 10 hpf	10	14	25	14
AB-7 (c)	120	12hr SMG at 10 hpf	12	13	25	16.5
AB-7	120	12 hr C+V at 10 hpf	9	14	23	19

Table A3.2: Number of vertebrae of fish exposed to 24 hours of SMG starting at 12 hpf and fish exposed to 24 hours of vibrations (C+V) starting at 12 hpf.

Fish I.D.	Age (dpf)	"Treatment"	Precaudal #	Caudal #	Total Vert #	SL (mm)
AB-10 (a)	120	24hr SMG at 12hpf	10	15	25	15
AB-10 (b)	120	24hr SMG at 12hpf	10	15	25	15
AB-10 (c)	120	24hr SMG at 12hpf	10	15	25	14.5
AB-10 (d)	120	24hr SMG at 12hpf	10	17	27	15
AB-10 (e)	120	24hr SMG at 12hpf	10	16	26	18
AB Tupper (a)	120	24hr SMG at 12hpf	10	15	25	16.5
AB Tupper (b)	120	24hr SMG at 12hpf	10	16	26	14
AB Tupper (c)	120	24hr SMG at 12hpf	10	15	25	14
AB Tupper (d)	120	24hr SMG at 12hpf	10	16	26	18
AB Tupper (e)	120	24hr SMG at 12hpf	10	17	27	14
AB Tupper (f)	120	24hr SMG at 12hpf	10	15	25	14
Ab31	120	24hr SMG at 12hpf	10	15	25	19
AB-10 (a)	120	24hr C+V at 12 hpf	10	15	25	15
AB Tupper (e)	120	24hr C+V at 12 hpf	10	16	26	18
AB Tupper (f)	120	24hr C+V at 12 hpf	10	16	26	15
AB31 (a)	120	24hr C+V at 12 hpf	10	15	25	19
AB31 (b)	120	24hr C+V at 12 hpf	10	15	25	16
AB31 c	120	24hr C+V at 12 hpf	10	15	25	17

Table A3.3 Number of vertebrae of fish exposed to 96 hours of SMG starting at 10 hpf, and fish exposed to 96 hours of vibrations starting at 10 hpf.

Fish I.D.	Age (dpf)	"Treatment"	Precaudal #	Caudal #	Total Vert #	SL (mm)
ABAQ	120	96hr SMG at 10hpf	12	16	28	20
AB-21	120	96hr SMG at 10hpf	10	15	25	18
AB-22	120	96hr SMG at 10hpf	10	14	24	21
H2036.8xAB (a)	120	96hr SMG at 10hpf	10	16	26	19
H2036.8xAB (b)	120	96hr SMG at 10hpf	10	15	25	20
H2036.8xAB (c)	120	96hr SMG at 10hpf	10	14	24	22
AB-22 (a)	120	96hr C+V at 10 hpf	10	15	25	18
AB-22 (b)	120	96hr C+V at 10 hpf	10	15	25	19
AB-21 (a)	120	96hr C+V at 10 hpf	10	16	26	18
AB-21 (b)	120	96hr C+V at 10 hpf	10	16	26	17
AB-21 (c)	120	96hr C+V at 10 hpf	10	15	25	18
ABAQ	120	96hr C+V at 10 hpf	10	16	26	19
H2036.8xAB	120	96hr C+V at 10 hpf	10	15	25	21
AB-34 (a)	120	96hr C+V at 10 hpf	10	15	25	18
AB-34 (b)	120	96hr C+V at 10 hpf	9	16	25	17
AB-34 (c)	120	96hr C+V at 10 hpf	10	15	25	18
AB-34 (d)	120	96hr C+V at 10 hpf	10	15	25	17
AB-34 (e)	120	96hr C+V at 10 hpf	9	16	25	18

Table A3.4: Vertebrae number in fish raised under normal conditions.

Fish ID	Clutch ID	Age (dpf)	Precaudal #	Caudal #	Total vert #	SL (mm)
CNV-A	H2036.8xAB	120	10	15	25	19
CNV-B	H2036.8xAB	120	10	15	25	19
CNV-D	AB-12	120	10	16	26	20
CNV-E	AB-12	120	10	16	26	17
CNV-F	AB-12	120	10	15	25	22
CNV-G	AB-12	120	11	16	27	20
CNV-H	AB-15	120	10	16	26	22
CNV-I	AB-15	120	10	16	26	20
CNV-J	AB-15	120	10	15	25	20
CNV-K	H2036.8xH2120.5	120	10	15	25	21
CNV-L	AB-20	120	10	15	25	22
CNV-M	AB-24	120	10	15	25	21
CNV-N	AB-24	120	10	15	25	17
CNV-O	AB-24	120	10	15	25	19
CNV-P	Sox10GFPCrelox	120	10	15	25	20

3B. Statistical Analyses

Non-parametric statistical analysis was conducted on the caudal and total number of vertebrae using Minitab (version 15.0). Outputs are below for different pairwise comparisons.

3B. 1 Caudal Vertebrae:

a) 96 hour SMG at 10 hpf vs. CNV:

```
Kruskal-Wallis Test on Caudal vert

C2             N  Median  Ave Rank      Z
1(CNV)        15   15.00      11.7   0.78
2(SMG)         6   15.00       9.3  -0.78
Overall       21              11.0

H = 0.61  DF = 1  P = 0.436
H = 0.78  DF = 1  P = 0.377  (adjusted for ties)
```

Mann-Whitney Test and CI

```
              N  Median
Caudal vert  15  15.000
C4            6  15.000


Point estimate for ETA1-ETA2 is -0.000
95.3 Percent CI for ETA1-ETA2 is (-1.000,1.000)
W = 175.0
Test of ETA1 = ETA2 vs ETA1 not = ETA2 is significant at 0.4596
The test is significant at 0.4015 (adjusted for ties)
```

96 hour C+V at 10 hpf vs. CNV:

```
Kruskal-Wallis Test on caudal vert

C2             N  Median  Ave Rank      Z
1(CNV)        15   15.00      13.5  -0.37
3(C+V)        12   15.00      14.6   0.37
Overall       27              14.0

H = 0.13  DF = 1  P = 0.714
H = 0.19  DF = 1  P = 0.662  (adjusted for ties)
```

Mann-Whitney Test and CI

```
              N  Median
caudal vert  15  15.000
C4           12  15.000


Point estimate for ETA1-ETA2 is -0.000
```

```
95.2 Percent CI for ETA1-ETA2 is (-1.000,-0.000)
W = 202.5
Test of ETA1 = ETA2 vs ETA1 not = ETA2 is significant at 0.7327
The test is significant at 0.6832 (adjusted for ties)
```

b) 96 hour SMG at 10 hpf vs. 96 hour C+V at 10 hpf:

```
Kruskal-Wallis Test on caudal vert

C2             N  Median  Ave Rank      Z
2(SMG)         6   15.00       7.8  -0.94
3(C+V)        12   15.00      10.3   0.94
Overall       18               9.5

H = 0.88  DF = 1  P = 0.349
H = 1.07  DF = 1  P = 0.300  (adjusted for ties)
```

Mann-Whitney Test and CI

```
              N  Median
caudal vert  12  15.000
C4            6  15.000


Point estimate for ETA1-ETA2 is 0.000
95.6 Percent CI for ETA1-ETA2 is (0.000,1.000)
W = 124.0
Test of ETA1 = ETA2 vs ETA1 not = ETA2 is significant at 0.3736
The test is significant at 0.3250 (adjusted for ties)
```

c) 24 hour SMG at 12 hpf vs. CNV:

```
Kruskal-Wallis Test on Caudal vert

C2             N  Median  Ave Rank      Z
1(CNV)        15   15.00      13.2  -0.61
4(SMG)        12   15.00      15.0   0.61
Overall       27              14.0

H = 0.37  DF = 1  P = 0.542
H = 0.51  DF = 1  P = 0.474  (adjusted for ties)
```

Mann-Whitney Test and CI

```
              N  Median
Caudal vert  15  15.000
C4           12  15.000


Point estimate for ETA1-ETA2 is -0.000
95.2 Percent CI for ETA1-ETA2 is (-1.000,0.000)
W = 197.5
Test of ETA1 = ETA2 vs ETA1 not = ETA2 is significant at 0.5582
The test is significant at 0.4916 (adjusted for ties)
```

d) 24 hour C+V at 12 hpf vs. CNV:

```
Kruskal-Wallis Test on caudal vert

C2             N  Median  Ave Rank     Z
1(CNV)        15   15.00      11.0  0.00
5(C+V)         6   15.00      11.0  0.00
Overall       21              11.0

H = 0.00  DF = 1  P = 1.000
H = 0.00  DF = 1  P = 1.000  (adjusted for ties)
```

Mann-Whitney Test and CI

```
              N  Median
caudal vert  15  15.000
C4            6  15.000


Point estimate for ETA1-ETA2 is 0.000
95.3 Percent CI for ETA1-ETA2 is (-1.000,1.000)
W = 165.0
Test of ETA1 = ETA2 vs ETA1 not = ETA2 is significant at 1.0000
The test is significant at 1.0000 (adjusted for ties)
```

e) 24 hour SMG at 12 hpf vs. 24 hour C+V at 12 hpf:

```
Kruskal-Wallis Test on caudal vert

                      Ave
C2             N  Median  Rank      Z
4(SMG)        12   15.00   9.9   0.47
5(C+V)         6   15.00   8.7  -0.47
Overall       18           9.5

H = 0.22  DF = 1  P = 0.640
H = 0.29  DF = 1  P = 0.589  (adjusted for ties)
```

Mann-Whitney Test and CI

```
              N  Median
caudal vert   6  15.000
C4           12  15.000


Point estimate for ETA1-ETA2 is -0.000
95.6 Percent CI for ETA1-ETA2 is (-1.000,0.000)
W = 52.0
Test of ETA1 = ETA2 vs ETA1 not = ETA2 is significant at 0.6734
The test is significant at 0.6268 (adjusted for ties)
```

f) 12 hour SMG at 10 hpf vs. CNV:

```
Kruskal-Wallis Test on Caudal vert

C2             N  Median  Ave Rank      Z
1(CNV)        15   15.00      10.7   2.07
6(SMG)         3   14.00       3.7  -2.07
Overall       18               9.5

H = 4.30  DF = 1  P = 0.038
```

```
H = 5.71  DF = 1  P = 0.017  (adjusted for ties)

* NOTE * One or more small samples
```

Mann-Whitney Test and CI

```
              N  Median
Caudal vert  15  15.000
C4            3  14.000


Point estimate for ETA1-ETA2 is 1.000
95.6 Percent CI for ETA1-ETA2 is (0.000,1.999)
W = 160.0
Test of ETA1 = ETA2 vs ETA1 not = ETA2 is significant at 0.0440
The test is significant at 0.0202 (adjusted for ties)
```

3B.2 Total Vertebrae

a) 96 hour SMG at 10 hpf vs. CNV:

```
Kruskal-Wallis Test on total vert

C2             N  Median  Ave Rank      Z
1(CNV)        15   25.00      11.5   0.62
2(SMG)         6   25.00       9.7  -0.62
Overall       21              11.0

H = 0.39  DF = 1  P = 0.533
H = 0.48  DF = 1  P = 0.486  (adjusted for ties)
```

Mann-Whitney Test and CI

```
             N  Median
total vert  15  25.000
C4           6  25.000


Point estimate for ETA1-ETA2 is 0.000
95.3 Percent CI for ETA1-ETA2 is (-1.000,1.000)
W = 173.0
Test of ETA1 = ETA2 vs ETA1 not = ETA2 is significant at 0.5593
The test is significant at 0.5141 (adjusted for ties)
```

b) 96 hour C+V at 10 hpf vs. CNV:

```
Kruskal-Wallis Test on total vert

C2             N  Median  Ave Rank      Z
1(CNV)        15   25.00      14.6   0.44
3(C+V)        12   25.00      13.3  -0.44
Overall       27              14.0

H = 0.19  DF = 1  P = 0.661
H = 0.30  DF = 1  P = 0.582  (adjusted for ties)
```

Mann-Whitney Test and CI

```
             N  Median
total vert  15  25.000
C4          12  25.000


Point estimate for ETA1-ETA2 is 0.000
95.2 Percent CI for ETA1-ETA2 is (-0.000,0.000)
W = 219.0
Test of ETA1 = ETA2 vs ETA1 not = ETA2 is significant at 0.6783
The test is significant at 0.6027 (adjusted for ties)
```

c) 96 hour SMG at 10 hpf vs. 96 hour C+V at 10 hpf:

```
Kruskal-Wallis Test on total vert

                      Ave
C2             N  Median  Rank      Z
2(SMG)         6   25.00   8.8  -0.42
3(C+V)        12   25.00   9.9   0.42
Overall       18           9.5

H = 0.18  DF = 1  P = 0.673
H = 0.23  DF = 1  P = 0.629  (adjusted for ties)
```

Mann-Whitney Test and CI

```
             N  Median
total vert  12  25.000
C4           6  25.000


Point estimate for ETA1-ETA2 is -0.000
95.6 Percent CI for ETA1-ETA2 is (-1.000,1.001)
W = 118.5
Test of ETA1 = ETA2 vs ETA1 not = ETA2 is significant at 0.7079
The test is significant at 0.6677 (adjusted for ties)
```

d) 24 hour SMG at 12 hpf vs. CNV:

```
Kruskal-Wallis Test on total vert

C2             N  Median  Ave Rank      Z
1(CNV)        15   25.00      13.3  -0.49
4(SMG)        12   25.00      14.8   0.49
Overall       27              14.0

H = 0.24  DF = 1  P = 0.626
H = 0.32  DF = 1  P = 0.569  (adjusted for ties)
```

Mann-Whitney Test and CI

```
             N  Median
total vert  15  25.000
C4          12  25.000
```

```
Point estimate for ETA1-ETA2 is 0.000
95.2 Percent CI for ETA1-ETA2 is (-1.000,0.000)
W = 200.0
Test of ETA1 = ETA2 vs ETA1 not = ETA2 is significant at 0.6430
The test is significant at 0.5881 (adjusted for ties)
```

e) 24 hour C+V at 12 hpf vs. CNV:

```
Kruskal-Wallis Test on total vert

C2             N  Median  Ave Rank      Z
1(CNV)        15   25.00      11.1   0.08
5(C+V)         6   25.00      10.8  -0.08
Overall       21              11.0

H = 0.01  DF = 1  P = 0.938
H = 0.01  DF = 1  P = 0.925  (adjusted for ties)
```

Mann-Whitney Test and CI

```
             N  Median
total vert  15  25.000
C4           6  25.000


Point estimate for ETA1-ETA2 is -0.000
95.3 Percent CI for ETA1-ETA2 is (-1.000,1.000)
W = 166.0
Test of ETA1 = ETA2 vs ETA1 not = ETA2 is significant at 0.9690
The test is significant at 0.9624 (adjusted for ties)
```

f) 24 hour SMG at 12 hpf vs. 24 hour C+V at 12 hpf:

```
Kruskal-Wallis Test on total vert

                      Ave
C2             N  Median  Rank      Z
4(SMG)        12   25.00   9.9   0.47
5(C+V)         6   25.00   8.7  -0.47
Overall       18           9.5

H = 0.22  DF = 1  P = 0.640
H = 0.29  DF = 1  P = 0.589  (adjusted for ties)
```

Mann-Whitney Test and CI

```
             N  Median
total vert   6  25.000
C4          12  25.000


Point estimate for ETA1-ETA2 is -0.000
95.6 Percent CI for ETA1-ETA2 is (-1.000,0.000)
W = 52.0
Test of ETA1 = ETA2 vs ETA1 not = ETA2 is significant at 0.6734
The test is significant at 0.6268 (adjusted for ties)
```

g) 12 hour SMG at 10 hpf vs. CNV:

```
Kruskal-Wallis Test on Total Vert

C2             N  Median  Ave Rank      Z
1(CNV)        15   25.00      10.0   0.89
6(SMG)         3   25.00       7.0  -0.89
Overall       18                9.5

H = 0.79  DF = 1  P = 0.374
H = 1.29  DF = 1  P = 0.257  (adjusted for ties)

* NOTE * One or more small samples
```

Appendix 4: Pigment Analyses

4A. Melanophore Coverage

Pigment analysis was conducted by measuring the percentage of the dorsal surface area covered with melanophores. The average percentages of the dorsal head covered by melanophores for all four experiments are combined into table A4.1. The SL, total surface area of the dorsal head, the surface area covered by melanophores, and the percentage covered by melanophores were recorded for both the C+V and SMG groups (Tables A4.2a-g and A4.3a-g). Empty cells in the charts indicate that no measurement is available for that day because the fish died.

Table A4.1: Average percentage of the dorsal view of the skull covered by melanophores, combining all four experiments. "C+Vs" refers to the 96h C+V at 10 hpf group; "SMGs" refers to the 96h SMG at 10 hpf group; "Day" refers to the day post-removal from exposure.

Day	**1**	**2**	**3**	**4**	**5**	**6**	**7**
C+Vs	17.55	15.80	14.31	12.99	11.77	11.83	9.89
SMGs	21.32	16.73	13.76	11.21	10.88	11.59	11.21

Tables A4.2 A-G Percentage of the dorsal head covered by melanophores, in fish from the 96h C+V at 10hpf group, 1st run, over the course of a week.

A

Control Fish Day 1 of measurements (5dpf)				
Fish Label	Standard Length	total surface size of dorsal head (mm²)	area covered by pigment (mm²)	percentage of head covered with pigment
Control A	2.0	128.07	59.79	46.68
Control B	3.8	199.08	21.59	10.84
Control C	3.9	134.79	21.03	15.6
Control D	3.8	130.57	30.07	23.03
Control E	3.7	191.7	24.47	12.77
Control F	3.6	206.93	26.92	13.00
avg				20.32 (± 13.6)

B

Control Fish Day 2 of measurements (6dpf)				
Fish Label	Standard Length	total surface size of dorsal head (mm²)	area covered by pigment (mm²)	percentage of head covered with pigment
Control A	3.6	225.27	30.67	13.61
Control B	3.9	239.70	38.35	16.01
Control C	3.8	163.45	22.40	13.7
Control D	3.7	272.97	38.08	13.95
Control E	4.0	172.96	37.56	21.72
Control F	3.7	177.22	27.81	15.69
avg				15.78 (± 3.09)

C

Control Fish Day 3 of measurements (7dpf)				
Fish Label	Standard Length	total surface size of dorsal head (mm²)	area covered by pigment (mm²)	percentage of head covered with pigment
Control A	3.9	230.86	31.21	13.52
Control B	3.9	227.31	33.50	14.74
Control C	3.8	229.01	28.51	12.45
Control D	3.5	207.34	36.63	15.25
Control E	3.8	212.76	40.50	19.04
Control F	3.6	234.42	22.65	9.66
avg				14.11 (± 3.13)

D

Control Fish Day 4 of measurements (8dpf)				
Fish Label	Standard Length	total surface size of dorsal head (mm²)	area covered by pigment (mm²)	percentage of head covered with pigment
Control A	4.2	240.04	25.25	10.52
Control B	3.9	208.64	24.12	11.56
Control C	3.9	219.74	31.89	14.51
Control D	3.7	212.75	29.73	13.97
Control E	3.9	225.59	25.15	11.15
Control F	3.7	219.96	26.69	12.13
avg				12.31 (± 1.61)

E

Control Fish Day 5 of measurements (9dpf)				
Fish Label	Standard Length	total surface size of dorsal head (mm²)	area covered by pigment (mm²)	percentage of head covered with pigment
Control A	4.2	242.08	25.18	10.4
Control B	3.9	213.73	28.50	13.33
Control C	4.0	221.43	19.58	8.84
Control D	3.9	194.08	15.84	8.16
Control E	3.9	211.71	18.99	8.97
Control F	3.9	202.92	16.37	8.07
avg				9.63 (± 1.99)

F

Control Fish Day 6 of measurements (10dpf)				
Fish Label	Standard Length	total surface size of dorsal head (mm²)	area covered by pigment (mm²)	percentage of head covered with pigment
Control A	4.2	234.12	24.19	10.33
Control B	3.9	222.48	16.44	7.39
Control C	4	228.21	20.79	9.11
Control D	3.9	228.78	18.90	8.26
Control E	4.0	223.50	18.20	8.42
Control F	3.9	206.68	16.79	8.13
avg				8.61 (± 1.01)

G

Control Fish Day 7 of measurements (11dpf)				
Fish Label	Standard Length	total surface size of dorsal head (mm²)	area covered by pigment (mm²)	percentage of head covered with pigment
Control A	4.2	227.12	19.88	8.75
Control B	3.9	222.64	17.29	7.77
Control C	4.1	240.69	20.53	8.53
Control D	3.9	206.30	15.93	7.71
Control E	4.0	245.07	16.54	6.75
Control F	3.9	210.07	17.41	8.29
avg				7.97 (± 0.72)

Tables A4.3A-G Percentage of dorsal skull covered with melanophores in fish from 96h SMG at 10 hpf; 1st run, over seven days.

A

SMG Fish Day 1 of measurements (5dpf)				
Fish Label	SL (mm)	total surface size of dorsal head (mm²)	area covered by pigment (mm²)	percentage of head covered with pigment
Control A	3.6	226.18	54.99	24.31
Control B	3.7	191.00	38.37	20.10
Control C	3.7	322.09	38.16	11.85
Control D	3.8	291.96	18.77	6.43
Control E	3.6	256.56	58.69	22.88
Control F	3.8	202.31	50.4	24.91
avg				18.41 (± 7.57)

B

SMG Fish Day 2 of measurements (6dpf)				
Fish Label	Standard Length	total surface size of dorsal head (mm²)	area covered by pigment (mm²)	percentage of head covered with pigment
Control A	3.8	218.08	31.11	14.23
Control B	3.7	221.08	28.29	12.8
Control C	3.8	289.93	16.67	5.75
Control D	3.7	241.52	21.14	8.75
Control E	3.7	188.69	39.6	21
Control F	3.8	183.86	31.81	17.3
avg				13.31 (± 5.55)

C

SMG Fish Day 3 of measurements (7dpf)				
Fish Label	Standard Length	total surface size of dorsal head (mm²)	area covered by pigment (mm²)	percentage of head covered with pigment
Control A	3.8	209.49	19.06	9.11
Control B	3.7	234.07	22.56	9.64
Control C				
Control D	3.7	222.79	23.29	10.46
Control E	3.7	209.75	31.26	14.9
Control F	3.7	223.83	28.14	12.57
avg				11.34 (± 2.39)

D

SMG Fish Day 4 of measurements (8dpf)				
Fish Label	Standard Length	total surface size of dorsal head (mm²)	area covered by pigment (mm²)	percentage of head covered with pigment
Control A	3.8	210.86	17.22	8.17
Control B	3.8	214.17	20.02	9.35
Control C				
Control D	3.8	214.49	18.7	8.56
Control E	3.8	207.54	22.75	10.96
Control F	3.8	218.46	37.83	17.32
avg				10.87 (± 3.76)

E

SMG Fish Day 5 of measurements (9dpf)				
Fish Label	Standard Length	total surface size of dorsal head (mm²)	area covered by pigment (mm²)	percentage of head covered with pigment
Control A	3.8	204.42	11.67	5.71
Control B	3.9	207.11	12.63	6.1
Control C				
Control D	3.8	203.45	11.53	5.67
Control E	3.9	221.72	21.08	9.51
Control F	3.8	249.83	20.98	8.4
avg				7.08 (± 1.77)

F

SMG Fish Day 6 of measurements (10dpf)				
Fish Label	Standard Length	total surface size of dorsal head (mm²)	area covered by pigment (mm²)	percentage of head covered with pigment
Control A	3.8	212.82	15.03	7.06
Control B	3.9	216.27	17.69	8.18
Control C				
Control D	3.9	223.10	16.91	7.58
Control E	3.9	219.40	20.50	9.34
Control F				
avg				8.04 (± 0.86)

G

SMG Fish Day 7 of measurements (11dpf)				
Fish Label	Standard Length	total surface size of dorsal head (mm²)	area covered by pigment (mm²)	percentage of head covered with pigment
Control A	3.8	215.49	13.08	6.11
Control B	4.0	214.23	14.40	6.72
Control C				
Control D	3.9	225.06	14.86	6.6
Control E				
Control F				
avg				6.48 (± 0.32)

Tables A4.4 A-G Measure of the percentage of the dorsal skull covered in melanophores, fish exposed to 96 hours of vibrations starting at 10 hpf; 2nd run.

A

Control Fish Day 1 of measurements (5dpf)				
Fish Label	Standard Length	total surface size of dorsal head (mm²)	area covered by pigment (mm²)	percentage of head covered with pigment
Control A	3.8	246.34	66.50	26.99
Control B	3.8	241.32	20.09	8.32
Control C	3.9	252.54	28.46	11.28
Control D	3.6	219.15	23.97	10.94
Control E	3.9	258.83	19.67	7.60
Control F	3.7	230.71	18.05	7.82
avg				12.16 (± 7.44)

B

Control Fish Day 2 of measurements (6dpf)				
Fish Label	Standard Length	total surface size of dorsal head (mm²)	area covered by pigment (mm²)	percentage of head covered with pigment
Control A	3.8	227.13	30.17	13.28
Control B	3.8	227.61	11.33	4.98
Control C	3.9	257.52	57.05	22.16
Control D	3.7	216.63	18.62	8.60
Control E	3.9	251.58	17.65	7.02
Control F	3.7	220.24	12.04	5.46
avg				10.25 (± 6.56)

C

Control Fish Day 3 of measurements (7dpf)				
Fish Label	Standard Length	total surface size of dorsal head (mm²)	area covered by pigment (mm²)	percentage of head covered with pigment
Control A	3.8	222.27	48.46	21.8
Control B	3.8	221.02	12.25	5.54
Control C	3.9	248.69	35.21	14.17
Control D	3.8	203.96	19.87	9.74
Control E	3.9	253.81	17.28	6.81
Control F	3.7	213.44	10.44	4.89
avg				10.49 (± 6.50)

D

Control Fish Day 4 of measurements (8dpf)				
Fish Label	Standard Length	total surface size of dorsal head (mm²)	area covered by pigment (mm²)	percentage of head covered with pigment
Control A	3.8	218.67	24.28	11.10
Control B	3.4	212.01	10.05	4.74
Control C	3.9	241.15	18.93	7.85
Control D	3.8	210.35	17.57	8.35
Control E	3.9	240.90	18.95	7.86
Control F	3.7	213.03	11.44	5.37
avg				7.55 (± 2.28)

E

Control Fish Day 5 of measurements (9dpf)				
Fish Label	Standard Length	total surface size of dorsal head (mm²)	area covered by pigment (mm²)	percentage of head covered with pigment
Control A	3.8	216.82	32.70	15.08
Control B				
Control C	3.9	224.26	18.62	8.30
Control D	3.8	192.06	17.43	9.08
Control E	3.9	249.87	14.43	5.77
Control F	3.7	204.83	10.24	5.00
avg				8.65 (± 3.98)

F

Control Fish Day 6 of measurements (10dpf)				
Fish Label	Standard Length	total surface size of dorsal head (mm²)	area covered by pigment (mm²)	percentage of head covered with pigment
Control A				
Control B				
Control C	3.9	241.28	27.54	11.41
Control D	3.8	183.27	23.69	12.93
Control E	3.9	242.62	11.60	4.78
Control F	3.7	213.74	11.55	5.40
avg				8.63 (± 4.14)

G

Control Fish Day 7 of measurements (11dpf)				
Fish Label	Standard Length	total surface size of dorsal head (mm²)	area covered by pigment (mm²)	percentage of head covered with pigment
Control A				
Control B				
Control C				
Control D				
Control E	3.9	235.04	13.39	5.69
Control F	3.7	204.34	92.10	4.51
avg				5.10 (± 0.83)

Tables A4.5 A-G Measure of the percentage of the dorsal skull covered in melanophores, fish exposed to 96 hours SMG starting at 10 hpf; 2nd run.

A

SMG Fish Day 1 of measurements (5dpf)				
Fish Label	Standard Length	total surface size of dorsal head (mm²)	area covered by pigment (mm²)	percentage of head covered with pigment
SMG A	3.9	250.23	47.18	18.85
SMG B	3.7	238.34	18.99	7.97
SMG C	3.6	228.60	25.49	11.15
SMG D	3.7	263.47	30.64	11.63
SMG E	3.9	231.06	33.52	14.51
SMG F	3.9	252.57	46.74	18.51
avg				13.77 (± 4.33)

B

SMG Fish Day 2 of measurements (6dpf)				
Fish Label	Standard Length	total surface size of dorsal head (mm²)	area covered by pigment (mm²)	percentage of head covered with pigment
SMG A	3.9	216.73	27.95	12.89
SMG B	3.7	218.95	11.89	5.43
SMG C	3.6	228.52	12.88	5.64
SMG D	3.8	251.44	19.42	7.72
SMG E	3.9	225.63	31.81	14.10
SMG F	3.9	246.14	39.97	16.24
avg				10.34 (± 4.66)

C

SMG Fish Day 3 of measurements (7dpf)				
Fish Label	Standard Length	total surface size of dorsal head (mm²)	area covered by pigment (mm²)	percentage of head covered with pigment
SMG A	3.9	233.44	24.18	10.36
SMG B	3.8	224.71	10.82	4.82
SMG C	3.6	218.38	12.53	5.74
SMG D	3.8	250.95	14.19	5.66
SMG E	3.9	234.51	22.16	9.45
SMG F	3.9	243.19	27.72	11.40
avg				7.90 (± 2.82)

D

SMG Fish Day 4 of measurements (8dpf)				
Fish Label	Standard Length	total surface size of dorsal head (mm²)	area covered by pigment (mm²)	percentage of head covered with pigment
SMG A	3.9	227.49	14.76	6.48
SMG B	3.8	226.63	10.93	4.82
SMG C	3.6	221.12	12.05	5.45
SMG D	3.9	246.22	12.78	5.19
SMG E	3.9	231.08	21.92	9.49
SMG F	3.9	224.41	24.13	10.75
avg				7.03 (± 2.49)

E

SMG Fish Day 5 of measurements (9dpf)				
Fish Label	Standard Length	total surface size of dorsal head (mm²)	area covered by pigment (mm²)	percentage of head covered with pigment
SMG A	3.9	211.89	24.75	11.68
SMG B	3.8	221.03	11.21	5.07
SMG C	3.6	207.71	12.23	5.88
SMG D	3.8	234.92	13.07	5.57
SMG E	3.9	226.40	21.23	9.38
SMG F	3.9	223.73	21.74	9.72
avg				7.88 (± 2.73)

F

SMG Fish Day 6 of measurements (10dpf)				
Fish Label	Standard Length	total surface size of dorsal head (mm²)	area covered by pigment (mm²)	percentage of head covered with pigment
SMG A	3.9	213.03	19.91	9.35
SMG B	3.8	219.99	14.17	6.44
SMG C	3.6	200.66	13.57	6.71
SMG D	3.9	241.82	13.77	5.69
SMG E	3.9	228.04	22.43	9.83
SMG F	4.0	231.25	21.70	9.38
avg				7.90 (± 1.81)

G

SMG Fish Day 7 of measurements (11dpf)				
Fish Label	Standard Length	total surface size of dorsal head (mm²)	area covered by pigment (mm²)	percentage of head covered with pigment
SMG A				
SMG B	3.8	182.70	14.11	7.72
SMG C	3.6	213.81	13.73	6.42
SMG D	3.9	235.67	12.41	5.27
SMG E	3.9	218.72	18.22	8.33
SMG F	4.0	212.15	19.33	9.11
avg				7.37 (± 1.53)

Tables A4.6 A-G Measure of the percentage of the dorsal skull covered in melanophores, fish exposed to 96 hours of vibrations starting at 10 hpf; 3rd run.

A

Control Fish Day 1 of measurements (5dpf)				
Fish Label	Standard Length	total surface size of dorsal head (mm²)	area covered by pigment (mm²)	percentage of head covered with pigment
Control A	3.8	241.58	24.58	10.17
Control B	3.5	206.26	23.10	11.20
Control C	3.9	240.68	64.58	26.83
Control D	3.8	236.35	38.39	16.24
Control E	3.6	225.17	78.27	34.76
Control F	3.7	226.63	68.93	30.42
avg				21.60 (± 10.45)

B

Control Fish Day 2 of measurements (6dpf)				
Fish Label	Standard Length	total surface size of dorsal head (mm²)	area covered by pigment (mm²)	percentage of head covered with pigment
Control A	3.8	243.68	51.51	21.14
Control B				
Control C	3.9	238.48	52.68	22.09
Control D	3.9	232.04	18.57	8.00
Control E	3.7	214.49	63.44	29.58
Control F	3.8	238.25	61.58	25.85
avg				21.33 (± 8.17)

C

Control Fish Day 3 of measurements (7dpf)				
Fish Label	Standard Length	total surface size of dorsal head (mm²)	area covered by pigment (mm²)	percentage of head covered with pigment
Control A	3.8	223.89	49.33	22.03
Control B				
Control C	3.9	231.99	31.84	13.72
Control D	3.9	238.82	34.67	14.52
Control E	3.7	223.81	28.68	12.81
Control F	3.8	229.68	48.83	21.26
avg				16.87 (± 4.41)

D

Control Fish Day 4 of measurements (8dpf)				
Fish Label	Standard Length	total surface size of dorsal head (mm²)	area covered by pigment (mm²)	percentage of head covered with pigment
Control A	3.8	219.94	24.74	11.25
Control B				
Control C	4.0	229.73	29.42	12.81
Control D	4.0	224.60	35.54	15.82
Control E	3.7	199.12	43.79	21.99
Control F	3.9	223.55	43.74	19.57
avg				16.29 (± 4.50)

E

Control Fish Day 5 of measurements (9dpf)				
Fish Label	Standard Length	total surface size of dorsal head (mm²)	area covered by pigment (mm²)	percentage of head covered with pigment
Control A	3.8	220.36	32.24	14.63
Control B				
Control C	4	221.60	26.85	12.12
Control D	4	231.18	27.47	11.88
Control E	3.8	191.89	44.52	23.20
Control F				
avg				15.46 (± 5.31)

F

Control Fish Day 6 of measurements (10dpf)				
Fish Label	Standard Length	total surface size of dorsal head (mm²)	area covered by pigment (mm²)	percentage of head covered with pigment
Control A	3.8	214.55	25.85	12.05
Control B				
Control C	4	219.23	31.69	14.46
Control D	4	217.59	31.95	14.68
Control E	3.8	190.82	57.50	30.13
Control F				
avg				17.83 (± 8.29)

G

Control Fish Day 7 of measurements (11dpf)				
Fish Label	Standard Length	total surface size of dorsal head (mm²)	area covered by pigment (mm²)	percentage of head covered with pigment
Control A				
Control B				
Control C	4.0	216942.4	19191.98	8.846578631
Control D	4.0	201773.2	18423.92	9.131004514
Control E				
Control F				
avg				8.99 (± 0.20)

Tables A4.7 A-G Measure of the percentage of the dorsal skull covered in melanophores, fish exposed to 96 hours SMG starting at 10 hpf; 3rd run.

A

SMG Fish Day 1 of measurements (5dpf)				
Fish Label	Standard Length	total surface size of dorsal head (mm²)	area covered by pigment (mm²)	percentage of head covered with pigment
SMG A	3.6	209.17	27.24	13.02
SMG B	3.5	221.48	72.09	32.55
SMG C	3.7	231.84	59.34	25.60
SMG D	3.8	225.78	34.04	15.08
SMG E	3.7	224.12	62.68	27.97
SMG F	3.6	222.33	48.40	21.77
avg				22.66 (± 7.56)

B

SMG Fish Day 2 of measurements (6dpf)				
Fish Label	Standard Length	total surface size of dorsal head (mm²)	area covered by pigment (mm²)	percentage of head covered with pigment
SMG A	3.7	202.95	35.97	17.72
SMG B	3.6	205.53	54.68	26.60
SMG C	3.7	222.17	55.88	25.15
SMG D	3.9	219.34	14.99	6.83
SMG E	3.8	233.01	40.82	17.52
SMG F	3.7	214.11	49.69	23.21
avg				19.51 (± 7.26)

C

SMG Fish Day 3 of measurements (7dpf)				
Fish Label	Standard Length	total surface size of dorsal head (mm²)	area covered by pigment (mm²)	percentage of head covered with pigment
SMG A	3.6	197.74	26.38	13.34
SMG B				
SMG C	3.7	212.14	51.87	24.45
SMG D	3.9	223.78	52.97	23.67
SMG E	3.8	221.22	39.46	17.84
SMG F	3.8	219.51	43.87	19.99
avg				19.86 (± 4.53)

D

SMG Fish Day 4 of measurements (8dpf)				
Fish Label	Standard Length	total surface size of dorsal head (mm²)	area covered by pigment (mm²)	percentage of head covered with pigment
SMG A				
SMG B				
SMG C	3.6	208.31	19.44	9.33
SMG D	3.9	229.79	32.41	14.10
SMG E	3.8	202.87	29.96	14.77
SMG F	3.8	207.06	18.66	9.01
avg				11.80 (± 3.05)

E

SMG Fish Day 5 of measurements (9dpf)				
Fish Label	Standard Length	total surface size of dorsal head (mm²)	area covered by pigment (mm²)	percentage of head covered with pigment
SMG A				
SMG B				
SMG C	3.7	212903.3	22440.53	10.54
SMG D	3.9	208255.2	22278.46	10.70
SMG E	3.8	206808.2	20574.17	9.95
SMG F	3.8	192055.1	37886.42	19.73
avg				12.73 (± 4.68)

F

SMG Fish Day 6 of measurements (10dpf)				
Fish Label	Standard Length	total surface size of dorsal head (mm²)	area covered by pigment (mm²)	percentage of head covered with pigment
SMG A				
SMG B				
SMG C	3.7	205.32	18.59	9.05
SMG D	3.9	214.46	28.63	13.35
SMG E	3.9	191.24	27.67	14.47
SMG F	3.8	184.08	20.70	11.25
avg				12.03 (± 2.39)

G

SMG Fish Day 7 of measurements (11dpf)				
Fish Label	Standard Length	total surface size of dorsal head (mm²)	area covered by pigment (mm²)	percentage of head covered with pigment
SMG A				
SMG B				
SMG C				
SMG D	3.9	207648.8	26827.47	12.92
SMG E	3.9	194057.6	26140.5	13.47
SMG F	3.6	232511.8	30622.03	13.17
avg				13.19 (± 0.27)

Table A4.8 A-G Measure of the percentage of the dorsal skull covered in melanophores, fish exposed to 96 hours of vibrations starting at 10 hpf; 4th run.

A

Control Fish Day 1 of measurements (5dpf)				
Fish Label	Standard Length	total surface size of dorsal head (mm²)	area covered by pigment (mm²)	percentage of head covered with pigment
Control A	3.6	214.34	23.97	11.18
Control B	3.6	199.96	25.68	12.84
Control C	3.7	216.26	49.88	23.06
Control D	3.8	229.19	44.27	19.32
Control E	3.7	212.99	47.01	22.07
Control F	3.8	211.33	41.06	19.43
avg				17.98 (± 4.88)

B

Control Fish Day 2 of measurements (6dpf)				
Fish Label	Standard Length	total surface size of dorsal head (mm²)	area covered by pigment (mm²)	percentage of head covered with pigment
Control A	3.7	222.63	13.97	6.27
Control B	3.7	208.39	41.56	19.94
Control C	3.8	205.58	42.63	20.74
Control D	3.8	211.53	22.86	10.81
Control E	3.7	199.82	33.43	16.73
Control F	3.8	210.74	56.69	26.90
avg				16.90 (± 7.40)

C

Control Fish Day 3 of measurements (7dpf)				
Fish Label	Standard Length	total surface size of dorsal head (mm²)	area covered by pigment (mm²)	percentage of head covered with pigment
Control A	3.8	217.66	12.43	5.71
Control B	3.8	208.44	34.53	16.57
Control C	3.8	205.27	51.26	24.97
Control D	3.8	220.81	16.83	7.62
Control E	3.7	212.73	35.95	16.90
Control F	3.8	209.41	59.66	28.49
avg				16.71 (± 9.06)

D

Control Fish Day 4 of measurements (8dpf)				
Fish Label	Standard Length	total surface size of dorsal head (mm²)	area covered by pigment (mm²)	percentage of head covered with pigment
Control A	3.8	199.37	18.71	9.38
Control B	3.8	209.05	37.50	17.94
Control C	3.8	205.16	58.66	28.59
Control D	3.9	224.53	25.01	11.14
Control E	3.8	222.63	28.98	13.02
Control F	3.9	230.49	55.62	24.13
avg				17.37 (± 7.66)

E

Control Fish Day 5 of measurements (9dpf)				
Fish Label	Standard Length	total surface size of dorsal head (mm²)	area covered by pigment (mm²)	percentage of head covered with pigment
Control A	3.9	183.52	11.11	6.05
Control B	3.9	198.03	24.43	12.34
Control C	3.9	192.98	37.62	19.49
Control D	3.9	193.68	10.23	5.28
Control E	3.9	182.33	28.14	15.43
Control F	4.0	211.68	58.35	27.57
avg				14.36 (± 8.46)

F

Control Fish Day 6 of measurements (10dpf)				
Fish Label	Standard Length	total surface size of dorsal head (mm²)	area covered by pigment (mm²)	percentage of head covered with pigment
Control A	3.9	186.16	11.63	6.25
Control B	4.0	200.93	12.74	6.34
Control C	3.9	201.23	32.39	16.10
Control D	3.9	202.54	16.33	8.06
Control E	4.0	202.43	39.38	19.45
Control F	4.0	205.41	48.24	23.48
avg				13.28 (± 7.41)

G

Control Fish Day 7 of measurements (11dpf)				
Fish Label	Standard Length	total surface size of dorsal head (mm²)	area covered by pigment (mm²)	percentage of head covered with pigment
Control A	3.9	184.03	17.08	9.28
Control B	4.0	192.82	36.04	18.69
Control C	3.9	200.02	45.12	22.56
Control D	4.0	189.39	33.30	17.58
Control E	4.0	200.82	40.67	20.25
Control F	4.0	197.95	50.91	25.72
avg				19.01 (± 5.59)

Tables A4.9 A-G Measure of the percentage of the dorsal skull covered in melanophores, fish exposed to 96 hours SMG at 10 hpf; 4th run.

A

SMG Fish Day 1 of measurements (5dpf)				
Fish Label	Standard Length	total surface size of dorsal head (mm²)	area covered by pigment (mm²)	percentage of head covered with pigment
SMG A	3.5	178.35	61.77	34.63
SMG B	3.7	207.73	50.74	24.43
SMG C	3.8	203.35	62.76	30.86
SMG D	3.6	226.67	52.42	23.13
SMG E	3.5	208.25	74.68	35.86
SMG F	3.6	214.59	72.25	33.67
avg				30.43 (± 5.42)

B

SMG Fish Day 2 of measurements (6dpf)				
Fish Label	Standard Length	total surface size of dorsal head (mm²)	area covered by pigment (mm²)	percentage of head covered with pigment
SMG A	3.7	162.74	39.01	23.97
SMG B	3.8	205.34	26.74	13.02
SMG C	3.8	207.65	64.24	30.94
SMG D	3.8	224.35	51.00	22.73
SMG E	3.7	201.26	46.61	23.16
SMG F	3.8	194.09	55.72	28.71
avg				23.75 (± 6.21)

C

SMG Fish Day 3 of measurements (7dpf)				
Fish Label	Standard Length	total surface size of dorsal head (mm²)	area covered by pigment (mm²)	percentage of head covered with pigment
SMG A	3.7	171.55	22.57	13.16
SMG B	3.8	197.53	22.58	11.43
SMG C	3.8	213.08	54.43	25.54
SMG D	3.9	211.79	25.81	12.19
SMG E	3.8	202.42	19.89	9.83
SMG F	3.8	208.21	48.67	23.38
avg				15.92 (± 6.74)

D

SMG Fish Day 4 of measurements (8dpf)				
Fish Label	Standard Length	total surface size of dorsal head (mm²)	area covered by pigment (mm²)	percentage of head covered with pigment
SMG A	3.7	176.02	19.07	10.83
SMG B	3.9	193.82	36.85	19.01
SMG C	3.9	200.98	39.56	19.68
SMG D	3.9	208.87	25.80	12.35
SMG E	3.8	191.96	26.76	13.94
SMG F	3.8	197.68	29.60	14.97
avg				15.13 (± 3.56)

E

SMG Fish Day 5 of measurements (9dpf)				
Fish Label	Standard Length	total surface size of dorsal head (mm²)	area covered by pigment (mm²)	percentage of head covered with pigment
SMG A				
SMG B	3.9	180.01	11.28	6.27
SMG C				
SMG D	3.9	206.43	42.78	20.72
SMG E	3.9	189.56	45.59	24.05
SMG F	3.9	191.68	23.54	12.28
avg				15.83 (± 8.07)

F

SMG Fish Day 6 of measurements (10dpf)				
Fish Label	Standard Length	total surface size of dorsal head (mm²)	area covered by pigment (mm²)	percentage of head covered with pigment
SMG A				
SMG B	3.9	179.69	17.24	9.59
SMG C				
SMG D	3.9	195.07	55.50	28.45
SMG E	3.9	178.01	41.65	23.40
SMG F	3.9	189.76	23.00	12.12
avg				18.39 (± 9.00)

G

SMG Fish Day 7 of measurements (11dpf)				
Fish Label	Standard Length	total surface size of dorsal head (mm²)	area covered by pigment (mm²)	percentage of head covered with pigment
SMG A				
SMG B	3.9	194.52	13.81	7.10
SMG C				
SMG D	3.9	198.15	62.39	31.49
SMG E	3.9	177.74	26.28	14.79
SMG F				
avg				17.79 (± 12.47)

Pigment Count

In addition to measuring the percentage of the dorsal surface area covered with melanophores, melanophores in the dorsal region were counted during the last two runs (tables below).

Table A4.10: Average number of melanophores in the dorsal view of the head for both SMG and C+V, over a period of seven days. "Day" refers to the day post-removal from exposure.

Average Number of Melanophores in Dorsal View of the Head							
Day	1	2	3	4	5	6	7
C+V	49.75	50.32	57.12	62.40	63.42	65.38	62.25
SMGs	40.58	45.25	52.47	57.54	59.88	62.00	67.29

Table A4.11 Number of melanophores in the dorsal surface region of fish exposed to 96 hours of vibrations starting at 10 hpf over the course of a week; 3rd run.

CONTROL FISH Melanophore Count Run 3							
	Day 1	Day 2	Day 3	Day 4	Day 5	Day 6	Day 7
Fish A	68	57	57	64	67	72	
Fish B	48						
Fish C	49	51	53	53	56	76	66
Fish D	51	56	50	52	51	65	74
Fish E	59	54	67	80	84	82	
Fish F	46	46	50	45			
AVG	**53.5** (±8.41)	**52.8** (±4.44)	**55.4** (±7.09)	**58.8** (±13.66)	**64.5** (±14.62)	**73.75** (±7.14)	**70** (±5.66)

Table A4.12 Number of melanophores in the dorsal surface region of fish exposed to 96 hours of vibrations starting at 10 hpf over the course of a week; 4th run.

CONTROL FISH Melanophore Count Run 4							
	Day 1	Day 2	Day 3	Day 4	Day 5	Day 6	Day 7
Fish A	49	54	63	78	74	65	65
Fish B	47	41	51	64	58	54	56
Fish C	48	45	58	61	72	68	57
Fish D	45	42	57	65	58	53	52
Fish E	48	55	69	70	61	57	55
Fish F	39	50	55	58	51	45	42
AVG	**46.00** (±3.69)	**47.83** (±6.05)	**58.83** (±6.34)	**66.00** (±7.13)	**62.33** (±8.91)	**57.00** (±8.41)	**54.50** (±7.50)

Table A4.13 Number of melanophores in the dorsal surface region of fish exposed to 96 hours SMG starting at 10 hpf over the course of a week; 3rd run.

SMG FISH Melanophore Count Run 3							
	Day 1	Day 2	Day 3	Day 4	Day 5	Day 6	Day 7
Fish A	26	32	38				
Fish B	43	40					
Fish C	40	36	40	43	63	66	78
Fish D	30	57	47	38	44	64	65
Fish E	46	43	43	40	54	65	74
Fish F	40	36	40	60	66	68	72
AVG	**37.5** (±7.79)	**40.66** (±8.85)	**41.6** (±3.51)	**45.25** (±10.05)	**56.75** (±9.91)	**65.75** (±1.71)	**72.25** (±5.44)

Table A4.14 Number of melanophores in the dorsal surface region of fish exposed to 96 hours SMG starting at 10 hpf over the course of a week; 4th run.

SMG FISH Melanophore Count Run 4							
	Day 1	Day 2	Day 3	Day 4	Day 5	Day 6	Day 7
Fish A	44	52	63	70			
Fish B	42	49	58	61	60	60	62
Fish C	43	54	56	67			
Fish D	41	45	74	76	67	61	63
Fish E	50	52	68	74	62	57	62
Fish F	42	47	61	71	63	55	
AVG	**43.67** (±3.27)	**49.83** (±3.43)	**63.33** (±6.68)	**69.83** (±5.34)	**63.00** (±2.94)	**58.25** (±2.75)	**62.33** (±0.58)

Pigment Statistics

Melanophore Coverage

Statistical analysis was conducted on the average percentages of the head covered with melanophores; a one-way ANOVA was used to determine if a significant difference existed between the averages of each group. Linear regression was performed to determine if the trend lines could be broken down into three different sections (three different slopes). The Minitab outputs are as follows:

One-Way ANOVA (Melanophore Coverage):

One-way ANOVA: C1, C2 (C1= Controls; C2= SMG)

```
Source  DF     SS    MS     F      P
Factor   1    0.5   0.5  0.04  0.841
Error   12  133.4  11.1
Total   13  133.9

S = 3.334   R-Sq = 0.35%   R-Sq(adj) = 0.00%


                          Individual 95% CIs For Mean Based on
                          Pooled StDev
Level  N    Mean  StDev  ---------+---------+---------+---------+
C1     7  13.448  2.629  (------------------*-----------------)
C2     7  13.812  3.914     (------------------*-----------------)
                          ---------+---------+---------+---------+
                                12.0      13.5      15.0      16.5

Pooled StDev = 3.334
```

Linear Regression (Melanophore Coverage):

Regression Analysis: log(y) versus Day number, Day345*Day-2, ...

```
The regression equation is
log(y) = 2.89 - 0.111 Day number - 0.0041 Day345*Day-2 + 0.139 Day67*Day-5
         + 0.143 SMG or Control - 0.0454 SMG*Day


Predictor           Coef  SE Coef      T      P
Constant          2.8933   0.1110  26.06  0.000
Day number      -0.11078  0.04829  -2.29  0.023
Day345*Day-2    -0.00413  0.05745  -0.07  0.943
Day67*Day-5       0.1390   0.1458   0.95  0.341
SMG or Control    0.1428   0.1210   1.18  0.239
SMG*Day         -0.04541  0.02874  -1.58  0.115


S = 0.477580   R-Sq = 16.0%   R-Sq(adj) = 14.5%


Analysis of Variance

Source           DF       SS      MS      F      P
Regression        5  12.4018  2.4804  10.87  0.000
Residual Error  286  65.2317  0.2281
Total           291  77.6335


Source          DF   Seq SS
Day number       1  10.5790
Day345*Day-2     1   0.9872
Day67*Day-5      1   0.2142
SMG or Control   1   0.0521
SMG*Day          1   0.5694


Unusual Observations

        Day
Obs  number  log(y)     Fit  SE Fit  Residual  St Resid
  1    1.00  3.8433  2.7826  0.0744    1.0608      2.25R
 28    1.00  1.8610  2.8799  0.0741   -1.0190     -2.16R
 56    2.00  1.6054  2.6718  0.0583   -1.0663     -2.25R
 60    2.00  1.6974  2.6718  0.0583   -0.9743     -2.06R
 74    2.00  1.7492  2.7238  0.0581   -0.9746     -2.06R
 79    2.00  1.6919  2.7238  0.0581   -1.0318     -2.18R
 80    2.00  1.7299  2.7238  0.0581   -0.9939     -2.10R
107    3.00  1.5872  2.5569  0.0436   -0.9697     -2.04R
125    3.00  1.5728  2.5634  0.0441   -0.9907     -2.08R
205    5.00  3.3167  2.3270  0.0687    0.9897      2.09R
238    6.00  3.4055  2.3676  0.0810    1.0379      2.21R
260    6.00  3.3481  2.2380  0.0832    1.1102      2.36R
291    7.00  3.4497  2.2208  0.1028    1.2289      2.63R

R denotes an observation with a large standardized residual.
```

Pigment Statistics

Melanophore Number

One-way ANOVA was conducted on the average number of melanophores present in each group over a period of a week.

One-Way ANOVA (Melanophore #):

One-way ANOVA: C1, C2 (C1= Controls; C2= SMG)

```
Source  DF     SS    MS     F      P
Factor   1   46.9  46.9  0.72  0.414
Error   12  785.6  65.5
Total   13  832.5

S = 8.091   R-Sq = 5.63%   R-Sq(adj) = 0.00%


                         Individual 95% CIs For Mean Based on
                         Pooled StDev
Level  N    Mean  StDev  ---+---------+---------+---------+------
C1     7  58.661  6.403         (------------*-------------)
C2     7  55.001  9.484  (------------*------------)
                         ---+---------+---------+---------+------
                         50.0      55.0      60.0      65.0

Pooled StDev = 8.091
```

Appendix 5: Acid-Free Double-Stained Juvenile Fish

Table A5.1 lists all the zebrafish that were stained with the acid-free double-stain for bone and cartilage.

Table A5.1: Chart of all (n=125) juvenile zebrafish (4, 10, 35 dpf) stained with the acid-free double whole-mount stain for bone and cartilage.

Fish ID	DOB	DOD	AGE (dpf)	SL (mm)	Treatment	C+V/SMG/CNV
AB18A	8.12.10	8.16.10	4	3.5	none	CNV
AB18B	8.12.10	8.16.10	4	3.4	none	CNV
AB18C	8.12.10	8.16.10	4	3.4	none	CNV
AB18D	8.12.10	8.16.10	4	3.7	none	CNV
AB18E	8.12.10	8.16.10	4	3.4	none	CNV
AB18F	8.12.10	8.16.10	4	3.5	none	CNV
AB18G	8.12.10	8.16.10	4	3.1	none	CNV
AB18H	8.12.10	8.16.10	4	3.3	none	CNV
AB18I	8.12.10	8.16.10	4	3.4	none	CNV
Sox10A	3.10.11	3.20.11	10	3.4	none	CNV
Sox10B	3.10.11	3.20.11	10	3.6	none	CNV
Sox10C	3.10.11	3.20.11	10	3.4	none	CNV
Sox10D	3.10.11	3.20.11	10	3.5	none	CNV
Sox10E	3.10.11	3.20.11	10	3.4	none	CNV
Sox10F	3.10.11	3.20.11	10	3.3	none	CNV
Sox10G	3.10.11	3.20.11	10	3.5	none	CNV
Sox10H	3.10.11	3.20.11	10	3.2	none	CNV
Sox10I	3.10.11	3.20.11	10	3.4	none	CNV
AB39A	3.24.11	4.28.11	35	4.8	none	CNV
AB39B	3.24.11	4.28.11	35	8.6	none	CNV
AB39C	3.24.11	4.28.11	35	9.6	none	CNV
Sox10GFPA	4.13.11	5.18.11	35	10.0	none	CNV
Sox10GFPB	4.13.11	5.18.11	35	8.1	none	CNV
sox10A	5.12.11	5.16.11	4	3.4	12hat10hpf	C+V
sox10B	5.12.11	5.16.11	4	3.1	12hat10hpf	C+V
sox10C	5.12.11	5.16.11	4	3.1	12hat10hpf	C+V
sox10D	5.12.11	5.16.11	4	3.4	12hat10hpf	C+V
sox10A	5.12.11	5.22.11	10	3.3	12hat10hpf	C+V
sox10B	5.12.11	5.22.11	10	3.6	12hat10hpf	C+V
sox10C	5.12.11	5.22.11	10	3.8	12hat10hpf	C+V
sox10D	5.12.11	5.22.11	10	3.7	12hat10hpf	C+V
sox10E	5.12.11	5.22.11	10	4.0	12hat10hpf	C+V
sox10A	5.12.11	5.16.11	4	3.3	12hat10hpf	SMG
sox10B	5.12.11	5.16.11	4	3.4	12hat10hpf	SMG
sox10C	5.12.11	5.16.11	4	3.2	12hat10hpf	SMG
sox10D	5.12.11	5.16.11	4	3.4	12hat10hpf	SMG
sox10E	5.12.11	5.16.11	4	3.5	12hat10hpf	SMG
sox10F	5.12.11	5.16.11	4	3.4	12hat10hpf	SMG
sox10G	5.12.11	5.16.11	4	2.8	12hat10hpf	SMG
sox10H	5.12.11	5.16.11	4	3.2	12hat10hpf	SMG
sox10A	5.12.11	5.22.11	10	3.5	12hat10hpf	SMG
sox10B	5.12.11	5.22.11	10	3.6	12hat10hpf	SMG

sox10C	5.12.11	5.22.11	10	3.8	12hat10hpf	SMG
sox10D	5.12.11	5.22.11	10	3.7	12hat10hpf	SMG
sox10E	5.12.11	5.22.11	10	3.9	12hat10hpf	SMG
sox10F	5.12.11	5.22.11	10	3.7	12hat10hpf	SMG
sox10G	5.12.11	5.22.11	10	3.7	12hat10hpf	SMG
sox10H	5.12.11	5.22.11	10	3.8	12hat10hpf	SMG
AB34A	2.25.11	3.1.11	4	3.2	96hat10hpf	C+V
AB34B	2.25.11	3.1.11	4	3.1	96hat10hpf	C+V
AB34C	2.25.11	3.1.11	4	3.2	96hat10hpf	C+V
Sox10A	11.5.10	11.9.10	4	2.9	96hat10hpf	C+V
Sox10B	11.5.10	11.9.10	4	3.3	96hat10hpf	C+V
Sox10C	11.5.10	11.9.10	4	3.3	96hat10hpf	C+V
Sox10D	11.5.10	11.9.10	4	3.3	96hat10hpf	C+V
Sox10E	11.5.10	11.9.10	4	3.4	96hat10hpf	C+V
Sox10F	11.5.10	11.9.10	4	3.5	96hat10hpf	C+V
Sox10A	4.1.11	5.6.11	10	3.6	96hat10hpf	C+V
Sox10B	4.1.11	5.6.11	10	3.5	96hat10hpf	C+V
Sox10C	4.1.11	5.6.11	10	3.2	96hat10hpf	C+V
Sox10D	4.1.11	5.6.11	10	3.3	96hat10hpf	C+V
AB40A	3.25.11	4.29.11	35	8.6	96hat10hpf	C+V
AB40B	3.25.11	4.29.11	35	7.0	96hat10hpf	C+V
AB40C	3.25.11	4.29.11	35	7.3	96hat10hpf	C+V
AB40D	3.25.11	4.29.11	35	8.3	96hat10hpf	C+V
AB40E	3.25.11	4.29.11	35	8.5	96hat10hpf	C+V
AB40F	3.25.11	4.29.11	35	6.7	96hat10hpf	C+V
AB40G	3.25.11	4.29.11	35	7.1	96hat10hpf	C+V
Sox10GFPCreA	4.20.11	5.25.11	35	8.4	96hat10hpf	C+V
Sox10GFPCreB	4.20.11	5.25.11	35	6.7	96hat10hpf	C+V
Sox10A	4.1.11	5.6.11	35	8.1	96hat10hpf	C+V
Sox10B	4.1.11	5.18.11	>35*	8.5	96hat10hpf	C+V
AB34A	2.25.11	3.1.11	4	3.3	96hat10hpf	SMG
AB34B	2.25.11	3.1.11	4	3.2	96hat10hpf	SMG
AB34C	2.25.11	3.1.11	4	3.2	96hat10hpf	SMG
Sox10A	11.5.10	11.9.10	4	3.3	96hat10hpf	SMG
Sox10B	11.5.10	11.9.10	4	3.2	96hat10hpf	SMG
Sox10C	11.5.10	11.9.10	4	3.5	96hat10hpf	SMG
Sox10D	11.5.10	11.9.10	4	3.2	96hat10hpf	SMG
Sox10E	11.5.10	11.9.10	4	3.4	96hat10hpf	SMG
Sox10F	11.5.10	11.9.10	4	3.3	96hat10hpf	SMG
Sox10G	11.5.10	11.9.10	4	3.6	96hat10hpf	SMG
Sox10H	11.5.10	11.9.10	4	3.2	96hat10hpf	SMG
Sox10I	11.5.10	11.9.10	4	3.3	96hat10hpf	SMG
Sox10J	11.5.10	11.9.10	4	3.4	96hat10hpf	SMG
AB40A	3.25.11	4.29.11	35	5.4	96hat10hpf	SMG
AB40B	3.25.11	4.29.11	35	7.5	96hat10hpf	SMG
AB40C	3.25.11	4.29.11	35	7.3	96hat10hpf	SMG
sox10A	4.20.11	5.25.11	35	11..5	96hat10hpf	SMG
sox10B	4.20.11	5.25.11	35	8.0	96hat10hpf	SMG
sox10A	4.13.11	4.23.11	10	3.4	24hat12hpf	C+V
sox10B	4.13.11	4.23.11	10	3.2	24hat12hpf	C+V
sox10C	4.13.11	4.23.11	10	3.2	24hat12hpf	C+V

sox10D	4.13.11	4.23.11	10	3.4	24hat12hpf	C+V
sox10E	4.13.11	4.23.11	10	3.4	24hat12hpf	C+V
AB41A	4.6.11	5.11.11	35	9.2	24hat12hpf	C+V
AB41B	4.6.11	5.11.11	35	7.3	24hat12hpf	C+V
AB41C	4.6.11	5.11.11	35	5.0	24hat12hpf	C+V
AB41D	4.6.11	5.11.11	35	5.4	24hat12hpf	C+V
AB41E	4.6.11	5.11.11	35	6.7	24hat12hpf	C+V
AB41F	4.6.11	5.11.11	35	6.0	24hat12hpf	C+V
AB41G	4.6.11	5.11.11	35	5.8	24hat12hpf	C+V
AB41H	4.6.11	5.11.11	35	8.5	24hat12hpf	C+V
AB41I	4.6.11	5.11.11	35	7.8	24hat12hpf	C+V
Sox10GFPCreA	4.13.11	5.18.11	35	9.0	24hat12hpf	C+V
Sox10GFPCreB	4.13.11	5.18.11	35	10.0	24hat12hpf	C+V
Sox10GFPCreC	4.13.11	5.18.11	35	8.8	24hat12hpf	C+V
AB36A	3.2.11	4.6.11	35	7.0	24hat12hpf	C+V
AB36B	3.2.11	4.6.11	35	5.5	24hat12hpf	C+V
AB36C	3.2.11	4.6.11	35	5.0	24hat12hpf	C+V
sox10A	4.13.11	4.23.11	10	3.3	24hat12hpf	SMG
sox10B	4.13.11	4.23.11	10	3.4	24hat12hpf	SMG
sox10C	4.13.11	4.23.11	10	3.1	24hat12hpf	SMG
sox10D	4.13.11	4.23.11	10	3.0	24hat12hpf	SMG
sox10E	4.13.11	4.23.11	10	3.3	24hat12hpf	SMG
AB36	3.2.11	4.6.11	35	7.0	24hat12hpf	SMG
AB41A	4.6.11	5.11.11	35	11.6	24hat12hpf	SMG
AB41B	4.6.11	5.11.11	35	8.5	24hat12hpf	SMG
AB41C	4.6.11	5.11.11	35	10.0	24hat12hpf	SMG
AB41D	4.6.11	5.11.11	35	8.0	24hat12hpf	SMG
AB41E	4.6.11	5.11.11	35	8.0	24hat12hpf	SMG
AB41F	4.6.11	5.11.11	35	6.3	24hat12hpf	SMG
Sox10GFPCreA	4.13.11	5.18.11	35	6.0	24hat12hpf	SMG
Sox10GFPCreB	4.13.11	5.18.11	35	7.5	24hat12hpf	SMG
Sox10GFPCreC	4.13.11	5.18.11	35	10.4	24hat12hpf	SMG

* At 35 dpf, this individual was too small (< 5 mm SL) due to the presence of a much larger sibling in the same cup. Therefore, the specimen was raised beyond 35 dpf.